

This article was downloaded by:

On: 23 January 2011

Access details: *Access Details: Free Access*

Publisher *Taylor & Francis*

Informa Ltd Registered in England and Wales Registered Number: 1072954 Registered office: Mortimer House, 37-41 Mortimer Street, London W1T 3JH, UK



Journal of Coordination Chemistry

Publication details, including instructions for authors and subscription information:

<http://www.informaworld.com/smpp/title~content=t713455674>

Optical Resolution and Asymmetric Syntheses by use of Adsorption on Clay Minerals

Akihiko Yamagishi^a

^a Department of Chemistry, College of Arts and Sciences, The University of Tokyo, Komaba Meguro, Tokyo, Japan

To cite this Article Yamagishi, Akihiko(1987) 'Optical Resolution and Asymmetric Syntheses by use of Adsorption on Clay Minerals', Journal of Coordination Chemistry, 16: 2, 131 – 211

To link to this Article: DOI: 10.1080/00958978708081202

URL: <http://dx.doi.org/10.1080/00958978708081202>

PLEASE SCROLL DOWN FOR ARTICLE

Full terms and conditions of use: <http://www.informaworld.com/terms-and-conditions-of-access.pdf>

This article may be used for research, teaching and private study purposes. Any substantial or systematic reproduction, re-distribution, re-selling, loan or sub-licensing, systematic supply or distribution in any form to anyone is expressly forbidden.

The publisher does not give any warranty express or implied or make any representation that the contents will be complete or accurate or up to date. The accuracy of any instructions, formulae and drug doses should be independently verified with primary sources. The publisher shall not be liable for any loss, actions, claims, proceedings, demand or costs or damages whatsoever or howsoever caused arising directly or indirectly in connection with or arising out of the use of this material.

OPTICAL RESOLUTION AND ASYMMETRIC SYNTHESSES BY USE OF ADSORPTION ON CLAY MINERALS

AKIHIKO YAMAGISHI

Department of Chemistry, College of Arts and Sciences, The University of Tokyo, Komaba Meguro, Tokyo 153, Japan

(Received December 28, 1985; in final form September 10, 1986)

The interactions of metal complexes with layer clay minerals are reviewed with a special attention to the aggregate behaviours of bound species. Experimental evidences have been presented for the formation of stereoregular adsorbate layers from a solution of a racemic metal complex. The opposite enantiomers of a complex are adsorbed in an alternative way in the interlayer space of a clay mineral. The causes for such stereoregularity have been discussed from the viewpoint of stereochemical interactions between adsorbed molecules. The phenomena are extended to the development of the novel methods of optical resolution and asymmetric syntheses by use of clay minerals. In these methods, an adduct of a clay and a chelate is used as a chiral adsorbent. Chirality has been recognized or induced due to the stacking interactions of an adsorbed molecule with a pre-adsorbed optically active chelate. The methods are further extended to the electrochemical syntheses of an optically active molecule by use of an electrode modified with a film of a clay-chelate adduct.

Keywords: clay minerals, asymmetric syntheses, stereoregular complexes, adsorption

1. INTRODUCTION

This article reviews the interactions of a metal ion or a metal complex ion with layer clay minerals. Layer clay minerals adsorb these ionic species in their interlamellar spaces.¹ In such a region, a bound species interacts with the surface of a clay due to various forces such as electrostatic, electronic and steric forces. As a result, a bound molecule tends to be adsorbed with a definite orientation with respect to a clay surface.

Another remarkable feature on these systems is that a bound molecule interacts with its neighboring molecules in steric manners. These intermolecular interactions often lead to the formation of an adsorbate aggregate with ordered structures. The present article is focussed on the structures and properties of such an interlayer aggregate formed when a metal complex is adsorbed by a clay mineral. Experimental evidences have been presented to reveal the existence of an aggregate of metal complex and also to understand the causes of the aggregate formation.

A greater part of the content is devoted to describing the methods of optical resolution and asymmetric syntheses by use of an ion-exchange adduct of a clay and a metal chelate. The methods were recently initiated by the present author on the basis of the stereoregular adsorption of an optically active metal complex by a clay mineral.

The initial impact for the method was given by the finding that the racemic mixture of a certain kind of tris(chelated) complex was adsorbed by two times more than the pure enantiomer of the same chelate. The results indicated that the racemic mixture is adsorbed by a clay mineral as a unit of a racemic pair. As a result, it forms a

bi-dimensional racemic pair in the interlamellar space of a clay. It implies that an enantiomer of the adsorbed chelate is surrounded by its opposite enantiomers in that region. Such strict regularity is caused by the stereochemical stacking interactions between neighboring molecules. The finding was extended to the discrimination of the chirality of a molecule by an ion-exchange adduct of a clay and an optically active chelate due to the stereoselective stacking between the molecule and a preadsorbed chelate on the surface of a clay.

This review begins with the description of the general properties of clay minerals as an ion adsorbent. The next section reviews the spectroscopic studies on the adsorption of a metal complex ion by a clay mineral. The interaction of a metal complex with a clay is interpreted in terms of the basic concepts of coordination chemistry. The fourth section deals with the aggregation phenomena of metal complexes bound with a clay mineral. Evidences are presented for the intermolecular interactions among bound species. The fifth section describes the occurrence of stereoregular adsorption of a tris(chelated) or bis(chelated) metal complex in the interlayer space of a clay. A certain kind of optically active metal chelate forms a racemic adsorbate layer in the interlamellar space of a clay. Opposite enantiomers of such a chelate are stacked stereoselectively. The finding provided a basis for the development of the methods of optical resolution and asymmetric syntheses by utilizing a clay-chelate adduct as a chiral adsorbent. The results on the liquid column chromatography on such an adduct are described in the sixth section. The seventh section presents the synthetic results using the same adduct as a chiral template. The final section discusses the significance of the above finding in conjunction with the origin and amplification of optical activity in the living systems. A postulate has been presented for the possible role of a clay mineral in producing optically active compounds during the chemical evolution.

2. THE STRUCTURES AND PROPERTIES OF CLAY MINERALS AS ADSORBENTS

A term "clay" denotes a particle-like component in a soil, ranging in size from 0.1 to 1 μm .² A clay consists of plate-like microcrystallines named clay minerals.³ According to the X-ray diffraction investigations, a clay mineral takes a layer structure. A single layer is composed of silica and alumina sheets that are combined face-to-face with each other.⁴ Table I shows three major classes of clay minerals that are classified on the basis of the ratio of silica to alumina included in one layer.⁵ Among various types of clay minerals, this review is mainly concerned with a 2:1 type mineral, especially a species called montmorillonite, because of its remarkably high swelling and adsorbing properties. For this kind of mineral, one alumina sheet called an octahedral sheet is sandwiched between two silica sheets called tetrahedral sheets (Fig. 1). Another type of species which often appear in this article is kaolinite belonging to a 1:1 type mineral. A unit layer of kaolinite consists of one alumina sheet combined with one silica sheet. Accordingly the layer has two different surfaces, half siloxane and half hydroxylated alumina.

Table II shows a typical example of elemental compositions of montmorillonite which is produced in Japan.⁶ It is noted that the ratio of Si to Al is about 2, coinciding with the structure in Figure 1. There are, however, appreciable amounts of other metal elements included in the table. Ti^{IV} , Fe^{III} and Mn^{II} are considered to be present by the isomorphous replacements of either Si^{IV} in a tetrahedral sheet or Al^{III} in an octahedral sheet.⁷ The replacement of a trivalent atom, Al^{III} , with a divalent atom

TABLE I
Classification of phyllosilicates related to clay minerals^a

Layer type	Group (x = charge per formula unit) [†]	Sub-group	Species*
1:1	Serpentine-kaolin (x ~ 0)	Serpentines Kaolins	Chrysotile, antigorite, lizardite, amesite Kaolinite, dickite, nacrite
2:1	Talc-pyrophyllite (x ~ 0)	Tales Pyrophyllites	Talc, willemseite Pyrophyllite
	Smectite (x ~ 0.2-0.6)	Saponites	Saponite, hectorite, saucornite
	Vermiculite (x ~ 0.6-0.9)	Montmorillonites Trioctahedral vermiculites	Montmorillonite, beidellite, nontronite Trioctahedral vermiculite
	Mica (x ~ 1.0)	Dioctahedral micas	Dioctahedral vermiculite
	Brittle mica (x ~ 2.0)	Trioctahedral micas Trioctahedral brittle micas	Philoposite, biotite, lepidolite Muscovite, paragonite
	Chlorite (x variable)	Trioctahedral chlorites Di, trioctahedral chlorites	Clintonite, anandite Margarite
2:1 inverted ribbons	Sepiolite-palygorskite (x variable)	Sepiolites Palygorskites	Cincochlore, chamosite, nimite Donbassite Cookeite, sudoite Sepiolite, loughlinitite Palygorskite

* Only a few examples are given.

[†] x refers to an O₁₀(OH)₂ formula unit for smectite, vermiculite, mica and brittle mica.

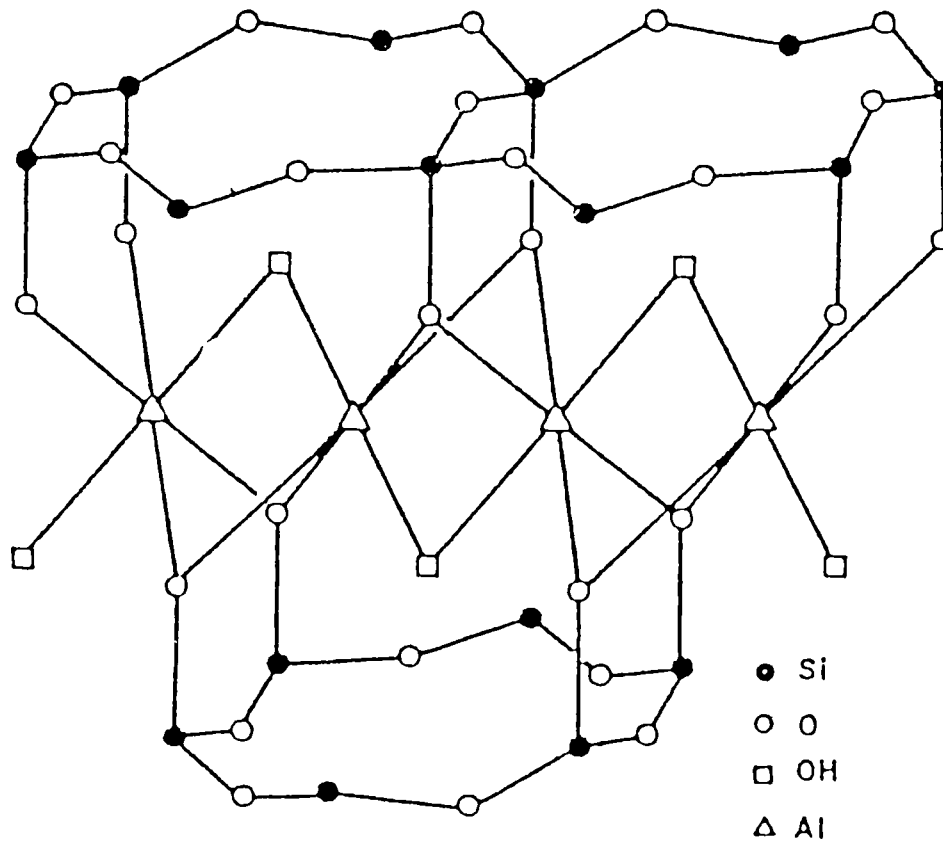


FIGURE 1 Crystal structure of prototype of three-layer silica-alumina clay.²

TABLE II
Chemical composition of sodium montmorillonite produced in Japan⁶

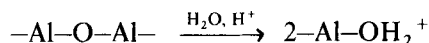
element	chemical composition (%)	atomic ratio
SiO ₂	57.96	0.9646
TiO ₂	trace	
Al ₂ O ₃	21.87	0.4290
Fe ₂ O ₃	1.92	0.0240
MnO	trace	
MgO	3.44	0.0853
CaO	0.54	0.0096
Na ₂ O	2.98	0.0962
K ₂ O	0.14	0.028
H ₂ O [†]	5.71	
H ₂ O	5.04	
Total	99.60	

causes the deficiency of a positive charge in that octahedron. Thus these substitutions result in the permanent negative charge of a unit layer. Alkali and alkaline earth metals in the table, Na^I , K^I , Mg^{II} and Ca^{II} , are adsorbed between the layers in order to compensate such a negative charge.⁷ These metal ions are dissociated from a clay, when a clay is dispersed in water. As a result, a clay stays in a solution as a negatively charged colloidal particle.² In other types of clay minerals, the isomorphous substitution by a metal ion with lower valence takes place in a tetrahedral silicate sheet. For example, in vermiculite belonging to a 2:1 type mineral, about 25% of silicon in a silicate sheet is replaced with aluminium.⁸ For such substitutions, negative charges exist more close to an external surface, resulting in stronger attraction toward cations in the interlayer spaces. Thus vermiculite is less swelling in water than montmorillonite.

There have been a great deal of studies accumulated on the adsorption of organic and inorganic molecules by a clay. The results were compiled in several review articles and monographs.^{2,9,10} Summarizing the experimental results, a clay is concluded to adsorb a molecule in the following modes of interactions:

i) Cation-exchange mechanism: Because of the presence of the permanent negative charge of a layer, a clay ordinarily possesses the cation-exchange capacity (CEC). CEC ranges from 80-100 meq per 100 g for montmorillonite and vermiculite and 1-10 meq per 100 g for kaolinite.² As a result, cationic molecules are adsorbed by being replaced with the exchangeable cations in the interlayer spaces. In this interaction mode, cationic molecules are located in a narrow flat region between the layers.

ii) Anion exchange mechanism: A clay also possesses anion-exchange capacity (AEC). The amount of AEC is estimated to be 20 and 2 meq per 100 g of montmorillonite and kaolinite, respectively.² The structural origin for AEC is not certain yet. However, it is suspected that the breaking of an alumina bond at the edge of a microcrystalline such as



is responsible for the positive charge of a layer.² In coinciding with this mechanism, there is an electron micrographic evidence that negatively charged gold sol is adsorbed exclusively on the edge of a clay crystal.^{11,12}

iii) Ion-dipole interaction. The negative charge of a layer is capable of polarizing a molecule in the interlamellar space. Accordingly a polar neutral molecule is adsorbed by a clay due to the ion-dipole interaction with a clay layer. A number of neutral organic molecules are considered to be adsorbed in this mechanism. This mechanism is also important in the adsorption of a simple metal ion. For example, the adsorption strength of an alkali metal ion by montmorillonite surface varies in the order of $\text{Li}^I < \text{Na}^I < \text{K}^I < \text{Rb}^I < \text{Cs}^I$. These metal ions might be bound due to the ion-dipole interaction, because the observed order coincides with the polarizability of a hydrated metal ion.¹³

iv) Hydrogen-bonding interaction. For 1:1 type clay minerals such as kaolinite, hydroxyl groups are present on the alumina side of a layer. Accordingly a molecule having an electronegative group such as a carbonyl group is adsorbed by forming a hydrogen bond with a clay surface. Invertedly the oxygen atoms in a silica side are possible to form a hydrogen bond with a molecule containing OH, NH and/or NH_2 groups. This mechanism is important in the adsorption of an organic molecule such as amino acids, alcohol, amides and nitriles.⁹

v) Coordination mechanism: A metal ion in an interlayer space may provide a coordination site for an intercalated molecule. Such coordination is noted as a predominant factor in adsorbing neutral organic molecules such as alcohols, glycols, nitriles and amids. Typical examples are seen in the adsorption of acrylonitrile on a montmorillonite surface in which acrylonitrile is coordinated with a metal ion to form a square planar complex in an interlamellar space.¹⁴

The above modes of interactions lead to the following sorptive features characteristic of clay minerals. These are rarely observed in other types of adsorbing materials.

i) Uniform electric field: negative charge centers in a clay such as montmorillonite are present in the octahedral alumina sheets (Fig. 1). Accordingly an adsorbate on a layer surface is located about 5 Å above such negative charges, experiencing rather uniform electric field. The situations are quite different from the binding of an ionic molecule to an ion-exchange resin such as poly(styrene sulfonate) in which an adsorbed ion is attracted by the electric field localized on a negatively charged sulfonate group.

ii) Orientational control: a molecule intercalated between the layers of a clay is under the spacial restriction by the upper and lower silicate or alumina sheets. As a result, an adsorbed molecule takes a definite orientation with respect to the surface of a clay. This kind of orientational control is rarely seen in other non-crystalline organic adsorbents.

iii) High density: when a molecule is adsorbed by a clay such as montmorillonite to the saturation of CEC, the adsorbate occupies a surface area of about 100 Å per molecule.¹⁵ Accordingly it is possible that a bulky molecule whose size is larger than 10 Å interacts with its neighboring molecules due to various kinds of intermolecular forces. Such situations hardly occur in the case of other ion-exchanging materials, in which a surface charge density is not so high as to allow adsorbates to interact intermolecularly.

One consequence of these circumstances is that adsorbed molecules are organized to form a molecular aggregate with ordered structure. A known example for such a phenomenon is the adsorption of an amine cation with a long alkyl group by montmorillonite or vermiculite. Figure 2 shows the variation in the distance between the neighboring layers when montmorillonite adsorbs an alkyl ammonium cation with an alkyl chain of various length.¹⁶ The distance, termed as basal spacing, corresponds to $d(001)$ of a clay crystalline. $d(001)$ is measured from the X-ray diffraction pattern on a powder or film sample of such a complex of clay-intercalated molecule.⁵ The height of an interlayer space is estimated by subtracting the thickness of a layer (9.6 Å for a montmorillonite layer¹⁷) from the observed basal spacing. It is seen that the basal spacing jumps from 13.5 Å to 17.5 Å at the chain length of 11.

The results are rationalized by assuming that an amine cation forms a monolayer aggregate when it has an alkyl chain shorter than 10. In such an aggregate, the alkyl chain is laid in parallel with a surface of a layer. To the contrary, an amine cation with an alkyl chain longer than 12 forms a double layer because one molecule is too bulky to be accommodated as a monolayer. It is emphasized that the observed abrupt change of the aggregate structure is possible only because the adsorbed molecules interact with one another and behave as a single unit in an interlayer space. When the distribution of permanent negative charges in a clay layer is not uniform, the change of a basal spacing occurs less abruptly.¹⁸ The transition from a monolayer to a double layer of an adsorbed amine cation takes place gradually over some range of the chain length because of the heterogeneity in the distribution of adsorbates.

Figure 2 is concerned with the adsorption of a molecule of a variable size by a

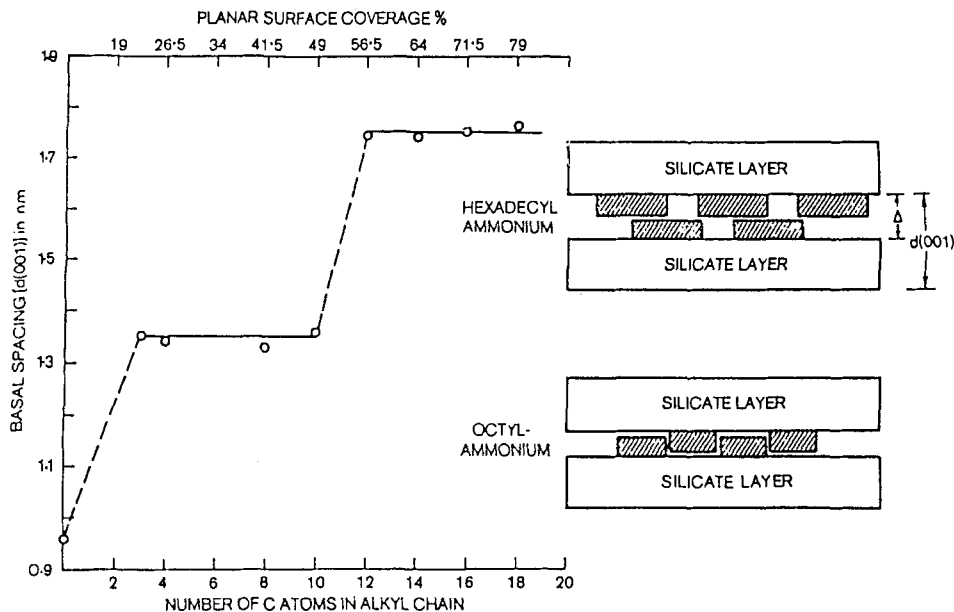


FIGURE 2 Variation in basal spacing with a number of carbon atoms in an alkyl chain in the complexes of montmorillonite with primary *n*-alkylammonium ions.¹⁶

clay with a constant site density. The similar phenomenon is studied from a different approach when a molecule of a constant size is adsorbed by a clay with variable site density. For example, a dodecyl ammonium cation is intercalated by montmorillonite with various magnitudes of CEC.¹⁹ As drawn in Figure 3 (left), for a clay with low CEC, the ammonium cations are adsorbed with their alkyl chains in parallel with the clay surface. For a clay with intermediate CEC, the alkyl chain inclines at some angle with respect to the surface. The chain stands up more steeply from a surface for a clay with higher CEC.

These conclusions are obtained from the dependence of an observed basal spacing of a clay-ammonium cation adduct on the CEC of a used clay. In these cases, too, ammonium cations in an aggregate behave as one unit in the interlayer space. Interestingly, when the above clay-ammonium cation complexes get contact with an alcohol with a long chain, they are swollen until they all exhibit the same value of the basal spacing. Most likely the alcohols and the ammine cations are arranged in a double layer as depicted in Figure 3 (right). In this case, the neutral alcohols are inserted between the adsorbed ammonium cations with their alkyl chains all perpendicular to the surface. Since alcohols are neutral, this insertion process does not depend on the charge density of a clay layer. In other words, the correlative interactions between adsorbates depend very much on their molecular properties.

In an example below, the X-ray diffraction measurements ascertain two-dimensional regularity in an adsorbate layer. Lysine is adsorbed by a single crystal of vermiculite from an aqueous solution as a mono-cationic species.²⁰ From the polarized infrared spectra, the lysine molecule is concluded to take an orientation as shown in Figure 4. X-ray diffraction measurements confirm that there exists a superlattice on a *ab*-plane of vermiculite layer. It is suspected that the bound molecules are arranged on a silicate

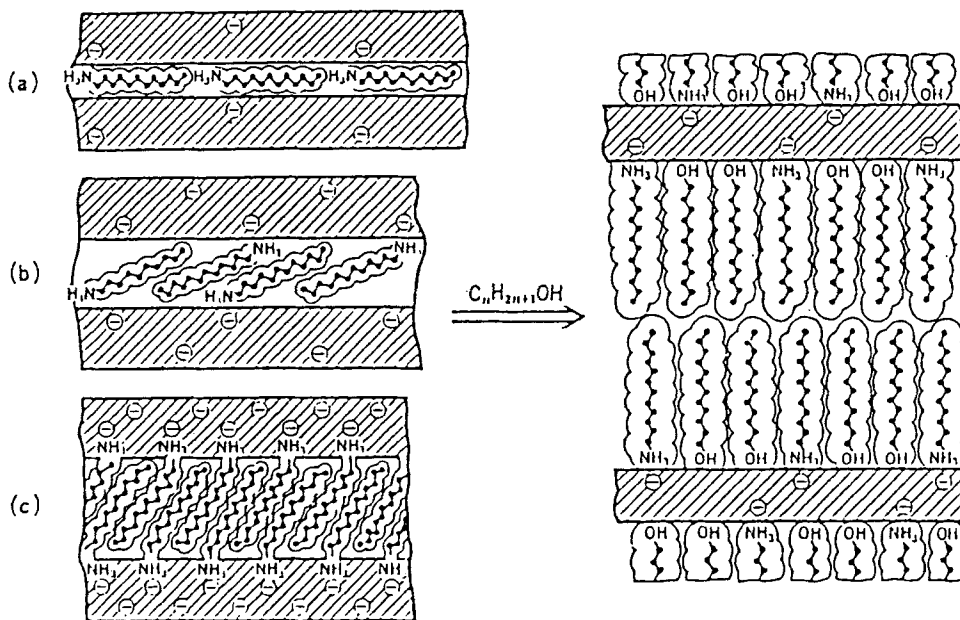


FIGURE 3 Structures of the *n*-alkylammonium complexes of montmorillonites with different CEC (schematized from ref. 19).¹⁴ The complexes show the same basal spacing when they are immersed in *n*-dodecanol (right).

sheet of a clay with a hexagonal symmetry as shown in Figure 5. It is believed that the dimensions and bonding capabilities of lysine molecules match well the geometrical arrangement of the hexagonally arranged oxygen atoms which form the surface of the silicate sheet. In fact, no such superlattice is observed in the vermiculite complexes containing other amino acids such as ornithine, histidine, and arginine. It is instructive to see the proposed configuration in Figure 5 from the view point of controlling the chemical reaction stereoregularly. The adsorbed lysine molecules would be changed into a stereoregular polypeptide if they are polymerized under the configurational regularity as shown in Figure 5. In this sense, the layer structure of a clay is possible to present a new type of reaction medium for chemical reactions.

3. INTERCALATION OF METAL COMPLEX IONS IN LAYER CLAY MINERALS

This section reviews the adsorption of transition metal ions and transition metal complex ions by a 2:1 or 1:1 layer clay mineral.^{2,9,10} Various kinds of spectroscopic techniques have been employed so far to investigate the structures of metal complex ions intercalated in the interlayer space of a clay. In the following, several representative examples are presented.

The stereochemistry of hydrated Cu^{II} ions in the interlamellar spaces of microcrystalline layer silicates has been studied by the esr technique.²¹ The anisotropic components of the *g* factors in the esr spectra due to Cu^{II} ions in an oriented film sample are measured at room temperature. In such a film, the (001) planes of the clay microcrystallines are orientated in parallel with the film surface. The coordination structure of a

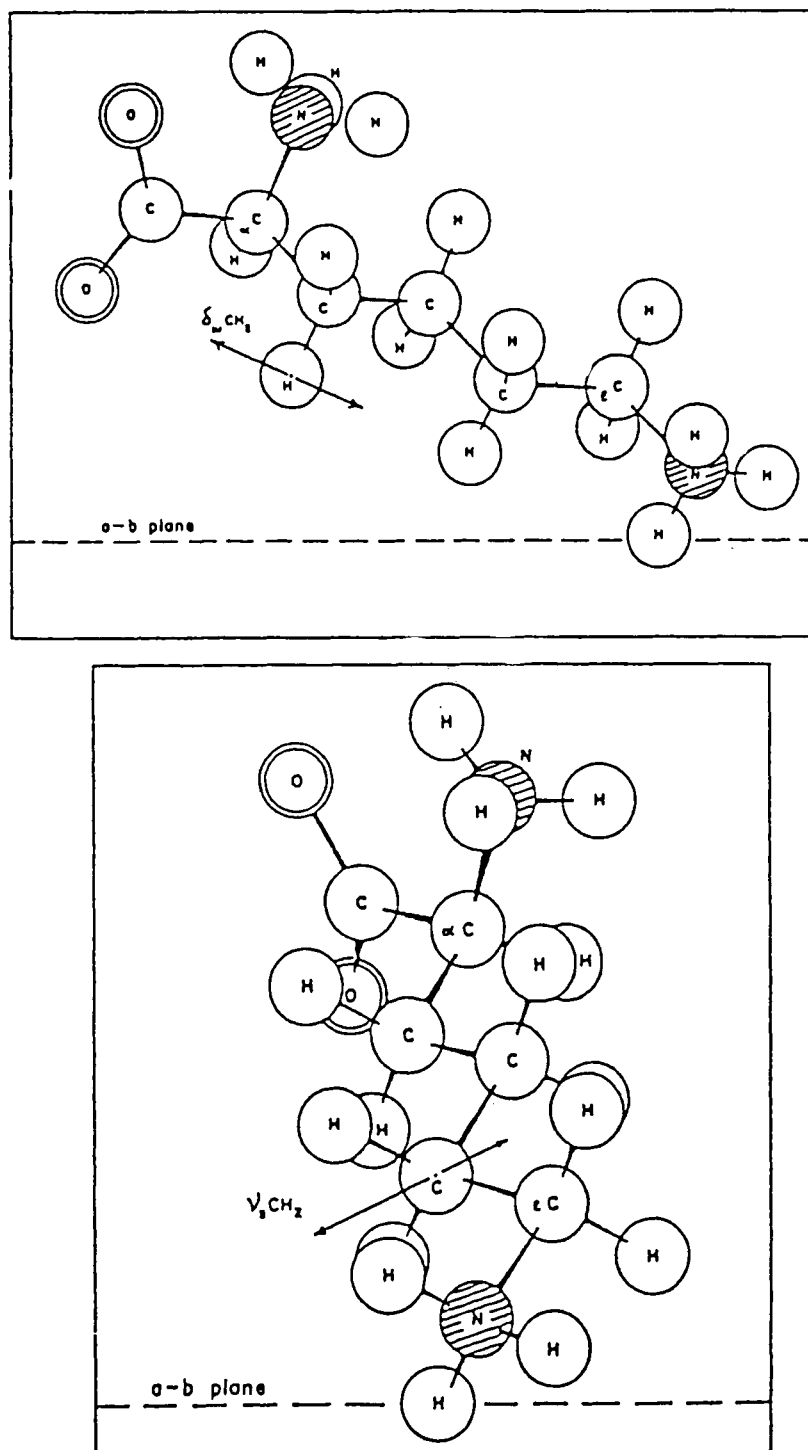


FIGURE 4 Structure of a lysine molecule in the interlamellar region of vermiculite; normal to (a) the CH_2 wagging and (b) the symmetric stretching transition moment direction.²⁰

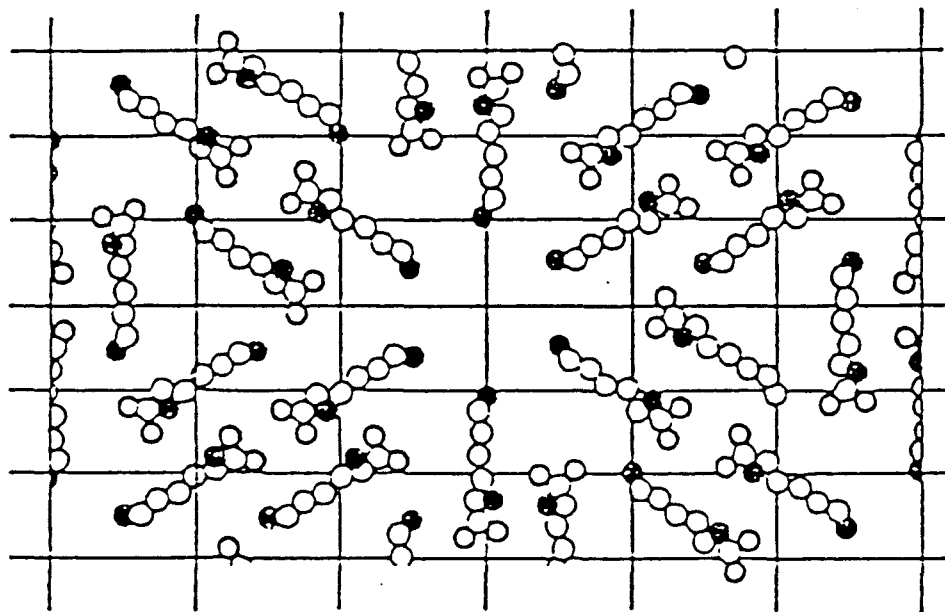


FIGURE 5 Proposed configuration for hydrogen-bonded pairs of lysine molecules on the surface of a silicate sheet. Amino groups are represented by the filled circles.²⁰

Cu^{II} ion depends very much on the hydration level of a clay. When a monolayer of water occupies the interlamellar regions, the esr signals are consistent with the conclusions that the ion has axial symmetry and that the symmetry axis is perpendicular to a silicate layer. The Cu^{II} ion is most likely coordinated to four water molecules in the xy plane and two silicate oxygen atoms along the z axis as shown in Figure 6A. Under the conditions that two layers of water occupy the interlamellar region, the esr spectrum is lacking of any orientational dependence of the film with respect to a magnetic field. It indicates that the ion is in an axially elongated tetragonal field of six water molecules and that the symmetry axis is inclined with respect to the silicate layers at an angle of about 45° (Fig. 6B). When several layers of water molecules occupy the interlamellar regions, a hexaquo-coordinated Cu^{II} ion is formed and tumbles rapidly, giving rise to a single, isotropic esr signal just like a Cu^{II} ion in a homogeneous solution. These results indicate that a metal ion experiences a wide variety of coordination structures simply by changing the hydration level in the interlayer region. If it were tried to realize the same variation of coordination structure in a homogeneous phase, it would need to prepare several extreme conditions.

It is natural to expect that a metal ion which is in the very low hydration level as in Figure 6A would exhibit a strong coordinating tendency toward an organic molecule. The interaction of aromatic molecules such as benzene and its alkylated derivatives with montmorillonite is studied along this line.²² When Cu^{II} ion-exchanged montmorillonite is placed in benzene vapour for 24 hours, the deeply colored complexes are formed. When the complexes are characterized by infrared spectroscopy, two types of adsorbed species of benzene (denoted as types I and II) are found besides those physically adsorbed. The infrared spectrum of type I (green form) has absorption bands shifted not very much from those of physically adsorbed benzene or liquid benzene, whereas type II (red form), which is formed under a dry

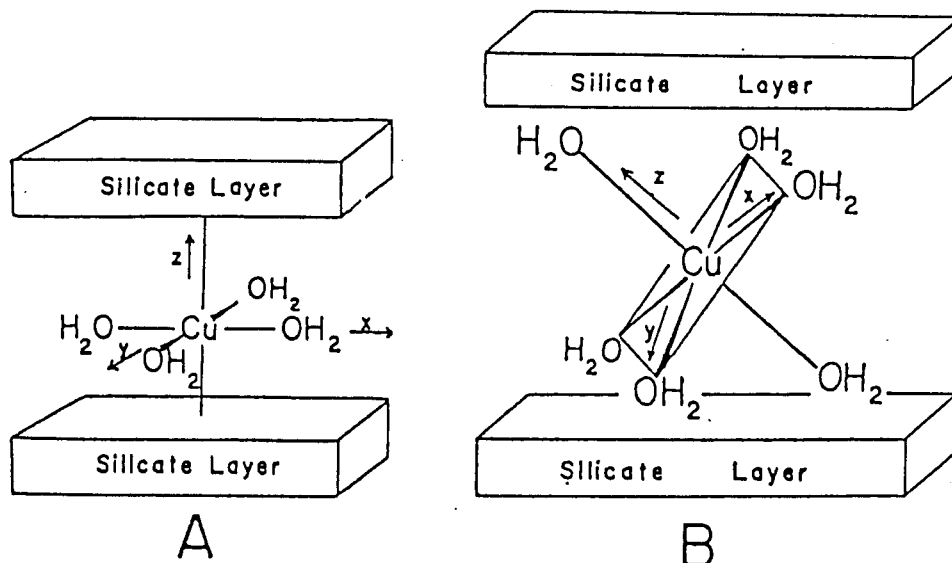


FIGURE 6 Schematic representation of the stereochemistry of hydrated Cu(II) under conditions where (A) one layer and (B) two layers of water occupy the interlamellar regions.²¹

atmosphere, shows broad absorption bands quite different from the spectrum of liquid benzene. Although infrared spectra alone do not offer sufficient information to clarify the structure of type II species, at least the strong chemical modification of a benzene molecule has been confirmed in type II species. ESR studies show that an organic free radical is formed and that the Cu^{II} ion is reduced to the Cu^I ion when type II species is formed. Based on the loss of aromaticity in this complex, a "sigma-type complex" is proposed in which sigma bonding is formed between the metal ion and benzene.²³

More recently resonance Raman spectroscopy has been applied to identify the above benzene complexes with Cu^{II} montmorillonite.²⁴ According to this method, the objective species is selectively excited in resonance with the excitation source. Thus the interference from other species such as physically adsorbed molecules and the vibrations due to adsorbate montmorillonite is completely eliminated. As a result, the dark red complex previously named as type II complex has been identified to be the poly(*p*-phenylene) cation (Fig. 7). The cation is reversibly reduced to poly(*p*-phenylene) in the presence of water vapour. The latter compound was previously named type I complex. It is now denied, therefore, that a benzene molecule is sigma-bonded to dehydrated Cu^I ion.

The interactions of tris(ethylenediamine)Cu^{II} ([Cu(en)₃]²⁺) with montmorillonite are investigated by X-ray diffraction, infrared and esr spectroscopies.²⁵ Addition of 0.1 M (M = mol dm⁻³) of [Cu(en)₃]²⁺ to a clay suspension causes instantaneous flocculation of the clay, indicating that clay particles are aggregated by being bridged with this complex. The pH is increased concomitantly from neutral pH to about 13. It implies that some parts of coordinated ethylenediamine molecules are dissociated to a solution to make the solution alkaline. As a result, the Cu^{II} ion in the interlayer region would be a uni- or bis-chelated complex. The *d*(001) spacing for a series of samples is recorded after mounting the various amount of the chelate at a constant

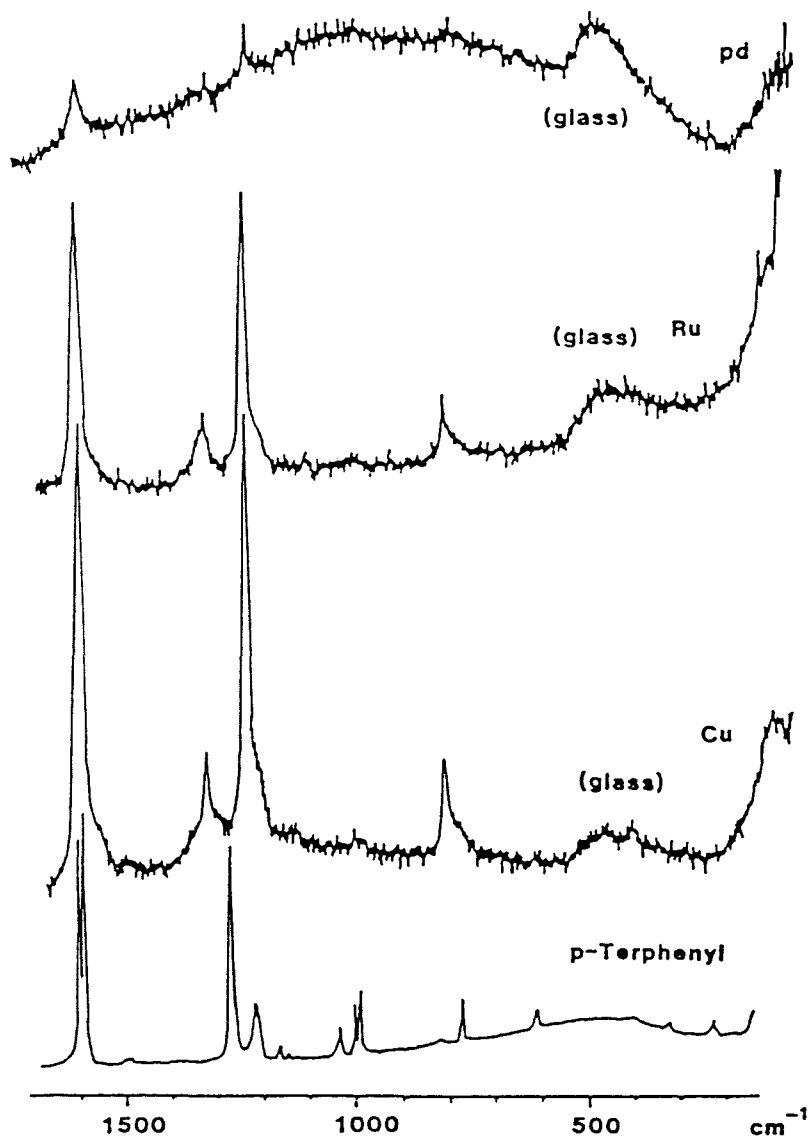


FIGURE 7 Resonance Raman spectra of benzene adsorbed on Pd(II), Ru(III) and Cu(II) montmorillonites (type II, excitation by Ar 514.4 nm line) and Raman spectrum of solid *p*-terphenyl.²⁴

humidity. The spacing is found to be constant at 12.6 Å for the adsorption range of 30% to 100% of the CEC of a clay. The $d(001)$ spacing is the sum of the theoretical thickness of the clay layer (9.6 Å) and the thickness of the molecules lying between the clay layers. It is found that a tris-chelated complex, $[\text{Cu}(\text{en})_3]^{2+}$, whose thickness is estimated to be about 6 Å, is too large to fit in the interlamellar space with the height of about 3 Å. This agrees with the above view of the dissociation of ethylenediamine ligands from a bound chelate. Infrared spectra of the oriented film show that the Cu-N bonds are in parallel with the film surface. Thus the complex ion in a clay is planar and most probably a square planar bis-ethylenediamine complex.

The esr signals of the same sample are found to be anisotropic and two g values obtained for parallel and perpendicular orientaton (2.053 and 2.120, respectively) suggest that the d_{z^2} orbital of the complex points toward the clay surface. Such a conformation would be stabilized by the additional coordination of oxygen atoms in a silicate surface with a Cu^{II} atom. Summarizing the above spectroscopic results, the most reasonable bound structure of the complex is shown in Figure 8. This example shows that a labile metal complex undergoes the change in its coordination structure when it is intercalated by a clay.

The interaction of $[\text{Cr}(\text{NH}_3)_6]^{3+}$ and $[\text{Cr}(\text{en})_3]^{3+}$ on chlorite, illite and kaolinite has been studied by X-ray photoelectron spectroscopy (XPS).²⁶ The adsorption of the Cr complexes with clays begins when the pH of a solution is maintained above 3. During the 7-day interaction time, the pH of the suspension increases to alkaline region as already seen in the case of $[\text{Cu}(\text{en})_3]^{2+}$.²⁵ $[\text{Cr}(\text{en})_3]^{3+}$ is found to be adsorbed by the clays about two times more than $[\text{Cr}(\text{NH}_3)_6]^{3+}$. The observed pH changes appear to be associated with a clay-catalyzed hydrolysis of the chromium-amine complexes. XPS binding energy data for adsorbed chromium complexes indicate that the dominant species are aquated chromium complexes. Nitrogen/chromium atom ratios, calculated from the XPS peak intensities, are less than 6:1 for complexes adsorbed on the clays, suggesting that the complexes are initially adsorbed but subsequently hydrolyzed to produce aqua-chromium surface species such as $[\text{Cr}(\text{NH}_3)_n(\text{H}_2\text{O})_{6-n}]^{3+}$ and $[\text{Cr}(\text{en})_n(\text{H}_2\text{O})_{6-2n}]^{3+}$ with $n = 2 - 4$. The results imply that even a substitution-inert complex of chromium(III) undergoes the elimination of a coordinated ligand when it is intercalated in a clay.

The adsorption of porphyrin compounds are studied for kaolinite and Ca-montmorillonite.²⁷ Prophyryns have been detected in variety of geologic environments and their adsorption states are interested in order to understand the diagenesis of minerals. These molecules are planar so that they are expected to be intercalated between the clay layers. In fact, porphyrins investigated (Table III) are adsorbed very

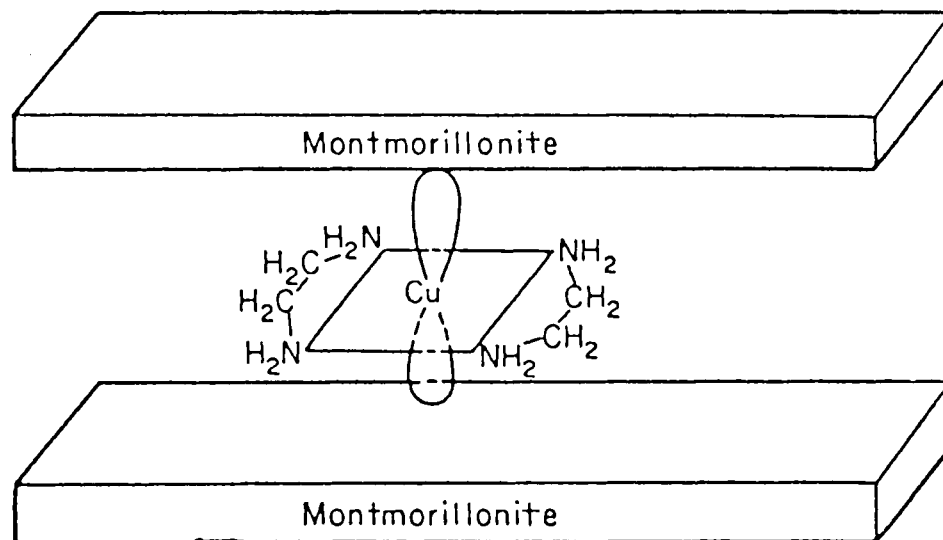


FIGURE 8 Proposed structure of $[\text{Cu}(\text{en})_2]^{2+}$ intercalated in montmorillonite.²⁵

TABLE III
Analysis of adsorption experiments at pH 9²⁷

Clay	Porphyrin	$V_1 + V_{II}$	V_{II}	K_{II}
Kaolinite	Hematoporphyrin	6.627 ± 0.115	0.808 ± 0.146	1.069 ± 0.053
	Protoporphyrin	6.179 ± 0.860	0.717 ± 0.353	1.216 ± 0.581
	Hemin	14.885 ± 3.952	0.828 ± 0.423	1.448 ± 0.686
Kaolinite-PO ₄	Hematoporphyrin	2.018 ± 0.143	0.915 ± 0.087	1.181 ± 0.030
	Protoporphyrin	1.965 ± 0.258	0.755 ± 0.217	0.402 ± 0.047
	Hemin	3.762 ± 0.280	0.866 ± 0.311	1.261 ± 0.221
Montmorillonite	Hematoporphyrin	20.695 ± 2.629	0.727 ± 0.211	0.376 ± 0.018
	Protoporphyrin	23.482 ± 4.808	0.824 ± 0.124	0.227 ± 0.004
	Hemin	40.456 ± 7.647	0.638 ± 0.275	0.779 ± 0.239
Montmorillonite-PO ₄	Hematoporphyrin	4.062 ± 0.825	1.131 ± 0.412	1.472 ± 0.399
	Protoporphyrin	3.487 ± 0.313	0.651 ± 0.154	0.411 ± 0.025
	Hemin	8.047 ± 0.840	0.718 ± 0.186	0.414 ± 0.216

strongly by the clays as shown by the isotherms at pH 9 (Fig. 9). The results are analyzed in terms of two parallel Langmuir-type adsorptions denoted by reactions (I) and (II). Table III lists the numerical results in which V_1 and V_{II} are the number of sites capable of adsorbing porphyrin in regions of first (I) and second (II) stages, respectively. K_{II} is the adsorption constant of porphyrin in the stage II. At pH 9, porphyrin is negatively charged due to the ionization of its carboxylic acid substituents; hematoporphyrin and protoporphyrin have a negative -2 charge, while hamatin has a charge of -1 . It is reasonable, therefore, that the sum of $N_1 + V_{II}$ is of the same order of the anion exchange capacity (AEC) of the clays, although the maximum adsorption is always larger for hemin than hematoporphyrin and protoporphyrin. AEC has been estimated to be 10 meq and 30 mew for 100 gram of kaolinite and montmorillonite, respectively.²⁶ It is of interest in what part of a clay particle a porphyrin molecule is located. If it is intercalated between the layers, the molecule would be adsorbed with its porphyrin plane in parallel with a clay surface. If it is adsorbed at the edge of a crystalline, the molecule would be orientated in various directions with respect to the surface. There has been no spectroscopic evidence for the orientation of the porphyrine plane, although the preliminary experiments by electric dichroism measurements support the former possibility.²⁹

As for the application of the electric dichroism method for a clay system, interesting results have been obtained on the system of sepiolite-cationic dye complex.³⁰ Although the system includes no metal complex, the work is introduced here to show the applicability of the method to the clay suspension systems. Sepiolite also belongs to a 2:1 silica-fused alumina mineral like montmorillonite except that it does not take a plate-like structure but is of a rod-type structure (Table I). In solution, a sepiolite crystalline takes a dimension of about $4 \text{ \AA} \times 10 \text{ \AA} \times \text{few microns}$. It possesses CEC of the order of 20 meq per 100 gram. Under the high electric field pulse, a clay particle is orientated with its long axis in the direction of the field. If a bound dye cation is in a definite direction with respect to the long axis, the cation exhibits the dichroism in its electronic absorption spectrum under the electric field. The magnitude of such dichroism is measured to determine the direction of the transition moment due to a bound dye with respect to the long axis of a clay crystalline. As a result, a

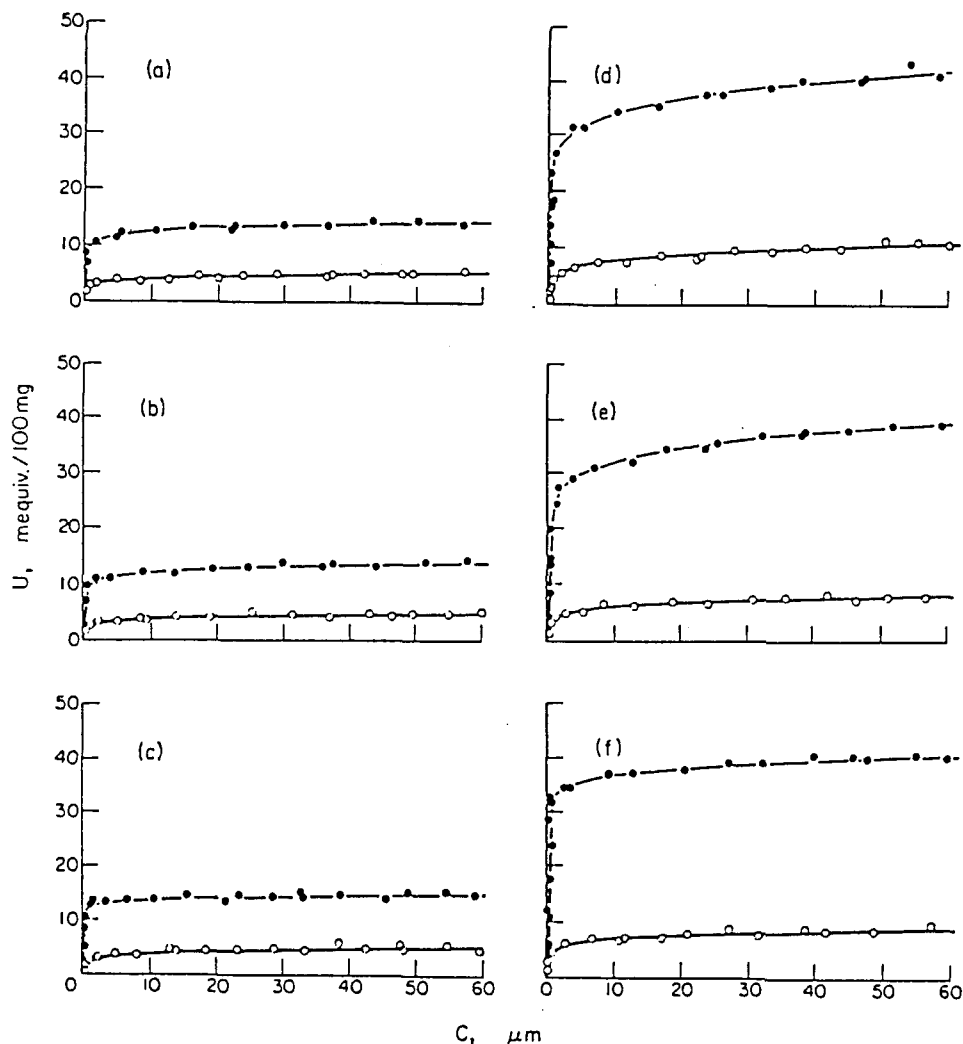


FIGURE 9 Adsorption of porphyrins by kaolinite and montmorillonite at pH 9.²⁷ (a) Hematoporphyrin-kaolinite; (b) protoporphyrin-kaolinite; (c) hematin-kaolinite; (d) hematoporphyrin-montmorillonite; (e) protoporphyrin-montmorillonite; (f) hematin-montmorillonite. An open circle and a filled circle denote phosphate-treated and untreated clays, respectively.

dye cation, Acridine Orange cation, is concluded to be bound to a clay particle with its long molecular axis in almost parallel with the long axis of a clay crystal.

Luminescence from a metal complex also provides a valuable information on the bound structures in a clay. The adsorption of tris(2,2'-bipyridine)ruthenium(II) ($[\text{Ru}(\text{bpy})_3]^{2+}$) is investigated by electronic absorption, luminescence and XPS spectroscopies.³¹ The electronic spectra of $[\text{Ru}(\text{bpy})_3]^{2+}$ adsorbed on montmorillonite and kaolinite are shown in Figures 10a and b, respectively. The absorption spectrum of $[\text{Ru}(\text{bpy})_3]^{2+}$ consists of two bands; the one around 280 nm is assigned to an intraligand $\pi - \pi^*$ transition and the one around 450 nm to a metal-to-ligand $d - \pi^*$ charge-transfer transition. On adsorption by montmorillonite, the intraligand absorp-

tion decreases in intensity with the concomitant splitting to two peaks. The charge-transfer absorption is red-shifted to 472 nm. These spectral changes are attributed to the distortion of bipyridine ligands from planarity and also the destabilization of the ground electronic state of $[\text{Ru}(\text{bpy})_3]^{2+}$ in the intercalated state. This interpretation is in conjunction with the XPS data which show that the adsorbed ruthenium has a spatial 3+ valence due to the electron flow from a ruthenium atom to the nitrogen atoms in the ligands. In comparison to montmorillonite, kaolinite gives less pronounced effects on the electronic spectrum when it adsorbs $[\text{Ru}(\text{bpy})_3]^{2+}$. No splitting takes place in the intraligand excitation region and the charge-transfer absorption band is shifted to 465 nm. The results suggest that for kaolinite the complex does not penetrate the interlayer space but is localized on the external surface of a crystal. Phosphorescence emission spectra of $[\text{Ru}(\text{bpy})_3]^{2+}$ at 77 K in an ethylene glycol/water glass are measured in the presence of montmorillonite or kaolinite. The emission spectrum is more drastically changed when the complex is adsorbed by montmorillonite than when it is adsorbed by kaolinite. The degree of polarization, p , of the phosphorescence is compared among no clay, montmorillonite and kaolinite systems. p at 298 and 77 K is obtained to be 0, 0.20 (no clay); 0.10, 0.15 (montmorillonite); 0.11, 0.11 (kaolinite), respectively. In no clay system, the chelate, which is freely rotating in a medium at 298 K, is restricted to move at 77 K. In the montmorillonite system, the chelate which is a little restricted at 298 K acquires rotation freedom even at 77 K. In the kaolinite system, these features are similar to those in the montmorillonite system but less prominent. These results support the conclusions as to the sites of the adsorbed complex. That is, the main adsorption site is in an interlamellar region and on the external surface of a crystal for montmorillonite and kaolinite, respectively.

The similar experiments are performed for six kinds of 2:1 type clay minerals as listed in Table IV.³² The shift of the peak on phosphorescence emission due to a bound $[\text{Ru}(\text{bpy})_3]^{2+}$ is plotted as a function of negative charge density of a clay sample. As a result, the variation of the emission maximum is linearly correlated with the negative charge density. The observed correlation is rationalized in terms of the location of a bound chelate in a clay crystalline. On a clay with low surface charge density, the chelate penetrates the layers because such a clay swells easily in an aqueous suspension. The intercalated chelate would suffer torsional distortion between the upper and lower layers, which leads to the large shift of the emission maximum. Oppositely, on a clay with high surface charge density, the chelate does not penetrate the layers since the clays are hard to be expanded under the attack of water molecules. In this case the chelate is adsorbed on an external surface, being in a less strained situation. Accordingly the shift in the emission maximum would be small.

The interaction of a nucleotide and a divalent metal ion is investigated in the presence of a clay thermodynamically and theoretically.³³ The study has been motivated to clarify the role of a clay mineral in the prebiotic organic syntheses. Most naturally occurring clays do not readily adsorb important biomonomers such as amino acids and nucleotides. However, when a clay is converted to a homoionic clay by replacement with divalent transition-metal ions, the clay is revealed to bind the above biomonomers. It is rationalized that a stable complex is formed between a nucleotide and a metal ion in an interlamellar space of a clay. Table V summarizes the results for a clay containing Zn^{II} , Cu^{II} , Ni^{II} , Co^{II} and Mg^{II} , when a nucleotide is added to a clay suspension as a dibasic form. In the table, a denotes the number of moles of nucleotides adsorbed at saturation or the number of exchangeable cationic site in a clay. K_{clay} and K_{aq} are the equilibrium constants of a 1:1 complex formation between a dibasic form of nucleotide and a metal cation in the presence or in the absence of a clay, respectively. Among the investigated metal ions, Zn^{II} is the most effective in forming a stable complex with a nucleotide in a clay. It is also noted that

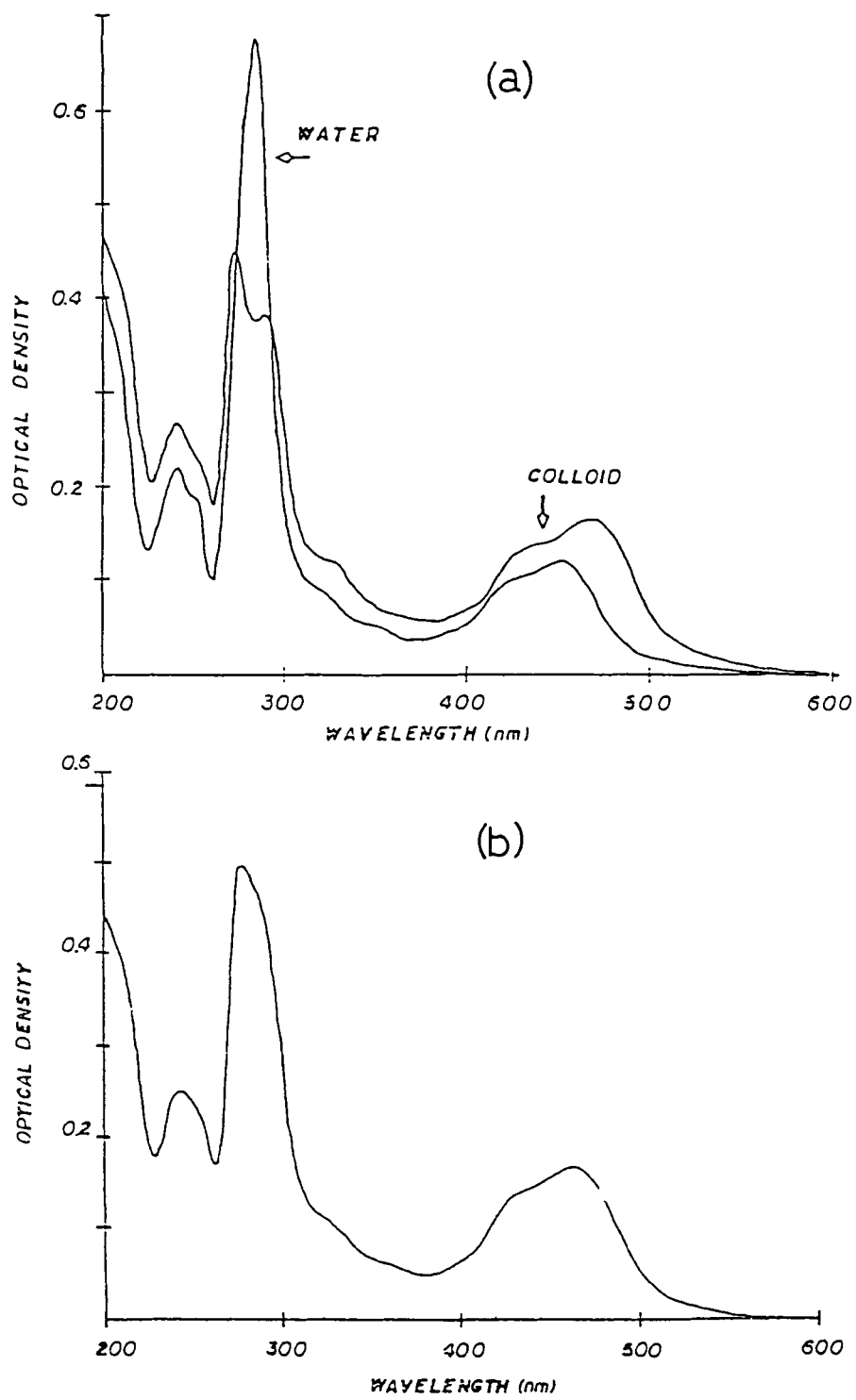


FIGURE 10 (a) Absorption spectrum of $[\text{Ru}(\text{bpy})_3]^{2+}$ in water and adsorbed on a montmorillonite colloid and (b) absorption spectrum of $[\text{Ru}(\text{bpy})_3]^{2+}$ adsorbed on a kaolinite colloid.³¹

TABLE IV
Properties of the Clay Minerals³²

clay	Fe ₂ O ₃ , %	FeO, %	CEC mequiv/ 100 g	mean charge density, e ⁻ per Si ₄ Al ₂ O ₁₀ (OH) ₂	surface area, m ² /g
Barasym SSM-100 (BS)	0.053		36	0.387	134
Hectorite (H)	0.19	0.17	44	0.245	63
Otay (O)	1.87	0.13	117	0.359	148
Camp Berteau (CB)	3.45	0.05	83	0.339	86
Moosburg	4.15	0.17	90	0.314	127
Wyoming Bentonite	5.18	0.06	65	0.270	32

the stability of a complex varies significantly for different nucleotides with the same metal (Zn^{II}) and for different metals with the same nucleotide (5'-AMP). The enthalpies of formation of hydrated metal ions in the interlamellar region are calculated for Zn^{II} and Mg^{II} (Table VI). The INDO-type semiempirical molecular orbital method is applied for this calculation. It is predicted that the hexaaquo complex

TABLE V
Measured affinity constants and fractional cation site availability for
nucleotide adsorption on homoionic bentonite clays³³

A. Metal cation specificity for adsorption of 5'-AMP			
clay cation	a_s^a	$\log K_{\text{clay}}^b$	$\log K_{\text{aq}}$
Zn ²⁺	0.80	3.18	2.72
Cu ²⁺	0.24	3.12	3.18
Ni ²⁺	0.004	3.16	2.84
Co ²⁺	0.003	2.82	2.56
Mg ²⁺	0.005	2.44	1.97
B. 5'-Nucleotide specificity for Zn ²⁺ -exchanged clays			
nucleotide	a_s^a	$\log K_{\text{clay}}^b$	$\log K_{\text{aq}}$
5'-AMP	0.80	3.18	2.7
5'-IMP	0.41	2.36	2.6
5'-GMP	0.78	2.20	
C. Nucleotide isomer specificity for Zn ²⁺ -exchanged clays			
nucleotide	a_s^a	$\log K_{\text{clay}}^b$	
5'-AMP	0.80	3.18	
2'-AMP	0.53	3.05	
3'-AMP	0.55	2.91	

^a a_s = number of moles of nucleotide adsorbed at saturation \equiv number of exchangeable cationic sites in clay. ^b With assumption of a 1:1 cation-nucleotide complex.

TABLE VI
Calculated energies of model clay-cation-hydrated complexes³³

	E , au	ΔE , kcal/mol	$R(M-OH_2)^d$ $\Delta(\Delta E)^e$	\AA
$Zn \cdot 6H_2O \cdot \text{clay}$	-449.2126	-1112.87 ^a	0	1.97
$Mg \cdot 6H_2O \cdot \text{clay}$	-449.0726	-1024.93 ^a	88	1.85
$[Zn \cdot 6H_2O]^{2+}$	-110.1347	-828.6 ^b	284.2	1.87
$[Mg \cdot 6H_2O]^{2+}$	-110.5359	-1080.37 ^b	32.5	1.67
$3H_2O \cdot \text{clay}$	-339.0320			
H_2O	-18.1357			

^aEnergy of complex formation calculated from $M^{2+} + 3H_2O + \text{clay} \cdot 3H_2O \rightarrow [M \cdot \text{clay} \cdot 6H_2O]^{2+}$.
^bEnergy of hydration calculated from $M^{2+} + 6H_2O \rightarrow [M \cdot 6H_2O]^{2+}$. ^c $\Delta(\Delta E)$ = stabilization energy of complex relative to that of $Zn \cdot 6H_2O \cdot \text{clay}$. ^dOptimized metal- OH_2 distance.

of Zn^{II} is stabilized by interaction with the clay, while the hexaaquo complex of Mg^{II} is destabilized in the clay. With the same approach, the possible geometry of a 1:1 nucleotide-metal(II) ion complex is calculated and the optimized form of such a complex is placed in the interlamellar space of a clay (Fig. 11). If the complex is bound to a clay surface as shown in the figure, the molecular planes of the base residue and glucose group in a nucleotide take a parallel and vertical orientation with respect to a clay surface, respectively. Such situations would be favorable for a nucleotide to be polymerized to a polynucleotide with stereoregularity. In this sense, a clay which contains Zn^{II} ions in its exchangeable sites is possible to act as a stereospecific template in polymerization of nucleotides.

Summarizing the contents of this section, a metal complex ion is replaced with an exchangeable cation in a clay and mostly penetrates the space between the layers.

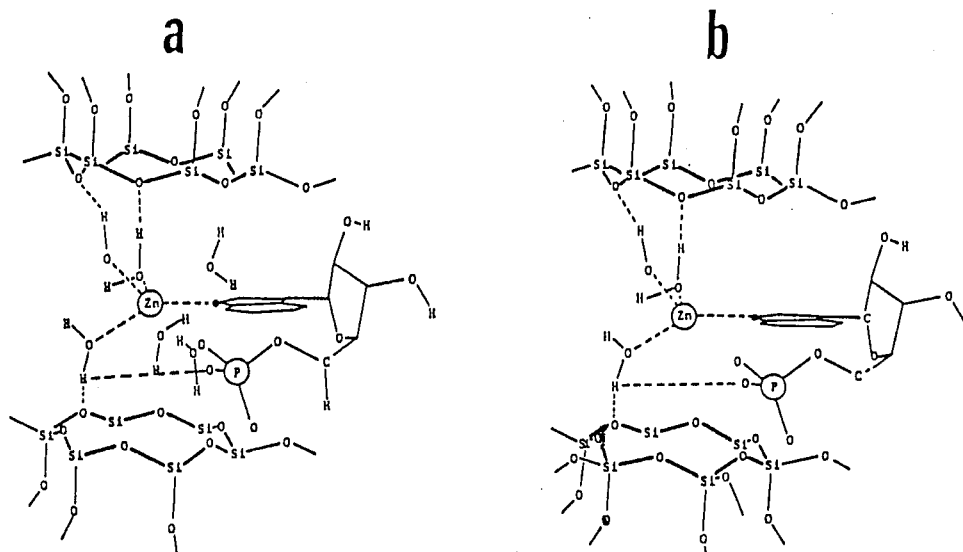


FIGURE 11 Computer graphic representation of 5'-AMP complexing to the metal cation in the interlamellar space of the clay.³³ (a) Complex with a fully hydrated clay and (b) complex with three interfering water molecules.

Inside the interlayer space, the complex undergoes the structural deformation which has been confirmed with various spectroscopies. As an extreme case, the complex is chemically changed into a less bulky form such as the change from an octahedral configuration to a square planar configuration. In that case, it occurs frequently that an empty site around a central metal ion is coordinated by the oxygen atom in a silicate or an alumina sheet of a clay. For the class of a clay which does not expand in a suspended state, an exchanged metal complex is adsorbed on an external surface of a crystalline. Under such circumstances, the bound complex suffers less structural deformation than in an intercalated state.

4. AGGREGATED STATES OF ADSORBED MOLECULES IN INTERLAMELLAR REGIONS

In the previous section, the spectroscopic evidences are presented for the structure of an intercalated metal complex ion. The structure of a bound metal complex as an isolated species is determined by interaction with a clay in steric, electric and electronic manners. Another point of interest lies in the problem how a bound species interacts with each other. Such an interaction is crucially important in understanding the structure of bound molecules as an interlamellar aggregate.

The existence of an intermolecular force between bound molecules is already pointed out in the case of organic cationic molecules such as amine cations with long alkyl chains (Figs. 2, 3). For the adsorption of metal complexes, the similar kind of interaction has been first observed in the case of the adsorption of tris(1,10-phenanthroline)metal(II) ($[M(\text{phen})_3]^{2+}$). Figure 12 shows the adsorption isotherm of $[\text{Fe}(\text{phen})_3]^{2+}$ and $[\text{Cu}(\text{phen})_3]^{2+}$ on sodium hectorite in a suspended condition.³⁴ Both of the phenanthroline complexes exhibit a marked affinity towards the mineral surface. They are adsorbed almost quantitatively until the adsorbed amount reaches about 130 meq per 100 g of a clay. This amount is about 1.6 times of CEC (84.2 meq per 100 g). After this stage, the amount of the adsorbed chelate increases gradually to the saturated level of 170 meq per 100 g. It should be noted that this saturated amount is almost two times excess of the CEC of the used hectorite. The figure includes the adsorption isotherm of cetylpyridinium bromide. This molecule is also adsorbed beyond the CEC of a clay. There is, however, no saturating tendency observed for the binding of cetylpyridinium bromide. Besides when the clay-adsorbate complexes are washed with water several times, half of the phenanthroline complexes are removed, while the adsorbed cetylpyridinium ions are very stable against washing. The results suggest that there exists a distinct difference in binding strength between one CEC equivalent of adsorbed $[\text{Fe}(\text{phen})_3]^{2+}$ and two CEC equivalents of $[\text{Fe}(\text{phen})_2]^{2+}$. Such distinction does not exist in the adsorption of cetylpyridinium ions.

The adsorption of $[\text{Fe}(\text{phen})_3]^{2+}$ in excess of CEC is apparently caused by the interaction between external $[\text{Fe}(\text{phen})_3]^{2+}$ ions and intercalated $[\text{Fe}(\text{phen})_3]^{2+}$ ions. In order to test the selectivity of the intermolecular forces, other cations are added to a suspension of hectorite in which one CEC equivalent of $[\text{Fe}(\text{phen})_3]^{2+}$ is exchanged.³⁴ No $[\text{Fe}(\text{phen})_3]^{2+}$ is released from the clay when MgCl_2 or tetrapropylammonium bromide is added to the suspension. To this contrary, when $[\text{Ni}(\text{phen})_3]^{2+}$ is added, about one equivalent of $[\text{Ni}(\text{phen})_3]^{2+}$ is adsorbed by the clay with the release or only 0.2 equivalent of $[\text{Fe}(\text{phen})_3]^{2+}$. The results imply that $[\text{Ni}(\text{phen})_3]^{2+}$ is attracted toward bound $[\text{Fe}(\text{phen})_3]^{2+}$ by the same forces which are responsible for the adsorption of $[\text{Fe}(\text{phen})_3]^{2+}$ beyond CEC.

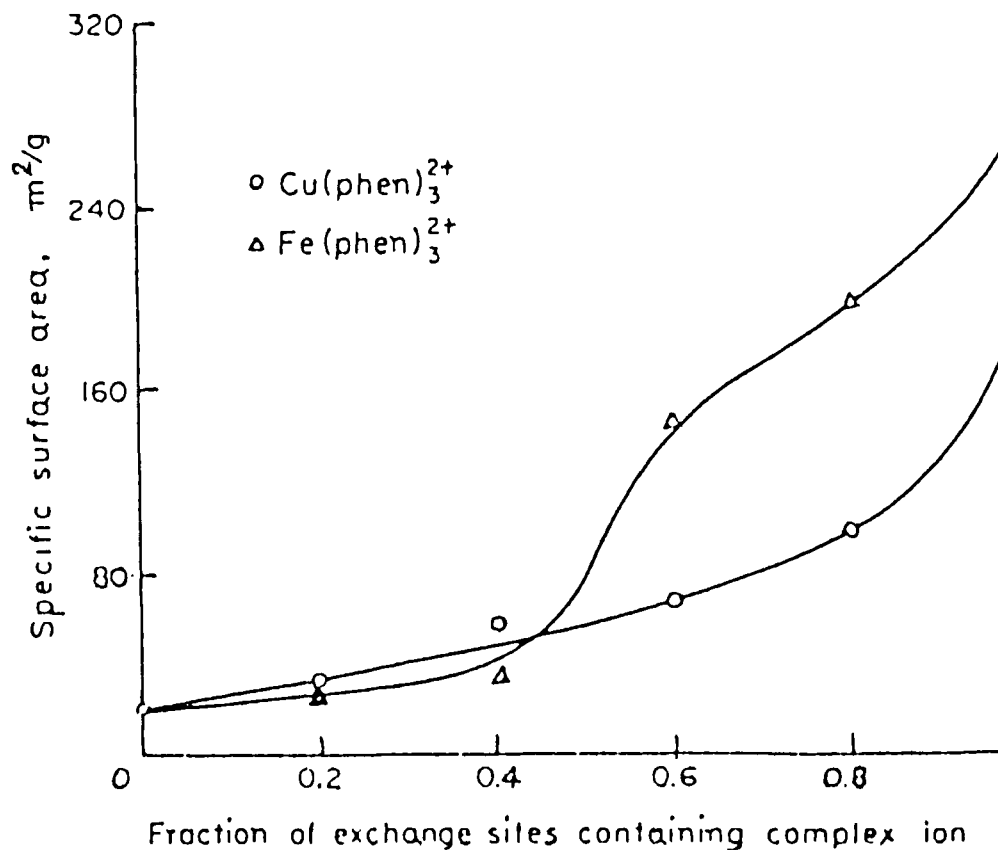


FIGURE 12 Adsorption isotherms of $[\text{Fe}(\text{phen})_3]\text{Br}_2$ (a filled circle) and $[\text{Cu}(\text{phen})_3]\text{SO}_4$ (an open circle) on sodium hectorite and cetylpyridinium (a filled circle on a dotted curve) on sodium montmorillonite.³⁴

Table VII lists the X-ray diffraction results on the films of sodium hectorite containing fractional amount of $[\text{M}(\text{phen})_3]^{2+}$.³⁴ The $d(001)$ of the film increases from 13.6 Å at no loading of the chelate to 17.5 Å at one CEC equivalent of chelate loading. The height of the space between the layers is calculated to be 7.9 Å by subtracting the thickness of a layer (9.6 Å) from the observed value of $d(001)$. The value is almost equal to the height of $[\text{M}(\text{phen})_3]^{2+}$ along its three-fold symmetry axis. Thus the chelate is concluded to be adsorbed in the interlamellar space under this configuration. Surprisingly enough two different basal spacings are observed at 16.4 Å and 13.2 Å in the region of intermediate loading. It means that the sample is a mixture of clay-chelate adducts with different basal spacings. The results are best understood by the assumption that the chelates favor the adsorption in a given interlayer before adsorption occurs in succeeding interlayers. Otherwise if the adsorption is completely random with respect to the layers, the uniform increase of the basal spacing would be observed with the increase of chelate loading. In summarizing the above results, it is concluded that there exists an intermolecular force between the bound $[\text{M}(\text{phen})_3]^{2+}$ ions which attract the molecules as close as possible in the same interlayer space. Such a force has saturating tendency at the loading of two times excess of CEC.

TABLE VII
X-ray basal spacings of Na(I) hectorite exchanged at various levels with $[\text{Fe}(\text{phen})_3]^{2+}$
and $[\text{Cu}(\text{phen})_3]^{2+}$ ³⁴

Ion in complex	S*	Air dry (Å)	100°C (Å)	150°C (Å)
Fe(II)	0.01	13.6	11.8	11.8
	0.2	15.8, (13.2)	16.0, (12.4)	12.4, 16.0
	0.4	16.4, 13.2	(16.7), 12.3	(17.0), 11.8
	0.6	(16.7), 13.2	17.5	(17.2), 11.8
	0.8	17.4	17.4	17.0
	1.0	17.4	17.4	17.2
Cu(II)	0.0	13.6	11.8	11.8
	0.2	12.6	12.4	11.8
	0.4	14.7	14.7	13.6
	0.6	15.8	15.5	15.5
	0.8	16.4	16.1	16.0
	1.0	17.5	17.5	17.1

* S denotes fraction of exchange sites occupied by complex ion.

The adsorption beyond CEC is observed for other kinds of metal complexes and clays. Fe^{II} , Co^{II} or Ni^{II} complexes with 2,2'-bipyridyl (byp) or 1,10-phenanthroline (phen) are adsorbed by colloiddally dispersed sodium hectorite, sodium montmorillonite, and *n*-butylammonium vermiculite.³⁵ As given in Table VIII, these complexes are all adsorbed in more than two times excess of CEC when they are added in large excess of a clay. The basal spacing is determined by X-ray diffraction measurements on a powdered sample containing various amounts of chelates in the temperature range from 60°C to 550°C. It is concluded that, when a clay contains metal complexes in more than CEC, the $d(001)$ attains as high as 28 Å. At 60°C, such clay-chelate complexes collapse at elevated temperatures to result in the lowering of the basal

TABLE VIII
Adsorption of complex salt by Na^+ -saturated hectorite, Na^+ -saturated Upton montmorillonite, and *n*-butylammonium-saturated vermiculite in a 0.2% clay suspension.³⁵

Clay	Complex salt	CEC-equivalents of complex salt added to clay			
		0.5	1.0	2.0	5.0
Na^+ -Hectorite	$[\text{Fe}(\text{phen})_3]\text{SO}_4$	0.50	1.00	1.98	2.77
	$[\text{Fe}(\text{byp})_3]\text{SO}_4$	0.50	1.00	1.90	2.68
	$[\text{Ni}(\text{phen})_3]\text{SO}_4$	0.50	1.00	1.99	2.78
	$[\text{Co}(\text{phen})_3]\text{SO}_4$	0.50	1.00	1.98	2.76
Na^+ -Upton Montmorillonite	$[\text{Fe}(\text{phen})_3]\text{SO}_4$	0.50	1.00	1.98	2.54
	$[\text{Fe}(\text{byp})_3]\text{SO}_4$	0.50	1.00	1.94	2.47
<i>n</i> -butyl- NH_3^+ -Vermiculite	$[\text{Fe}(\text{phen})_3]\text{SO}_4$	0.50	1.00	1.82	1.99
	$[\text{Ni}(\text{phen})_3]\text{SO}_4$	0.50	1.00	1.88	2.08
	$[\text{Co}(\text{phen})_3]\text{SO}_4$	0.50	0.98	1.85	2.06

spacing to 16.7 Å. At 60°C the bound metal complexes which are loaded in two times excess of CEC are suspected to form a double layer. Since the external anions are included to compensate the positive charge of the clay-chelate adduct under such high loading, the anions will also contribute to the large value of the basal spacing.

Nitrogen gas is introduced to the above clay-chelate complex to measure the area for physical adsorption.³³ From the results in Table IX, it is seen that an appreciable area is still open to the adsorption of N₂ in a clay containing one CEC equivalent of a chelate, while an area for the adsorption of N₂ is reduced to less than one half in a clay containing two CEC equivalents of a chelate. The results indicate that in the one CEC equivalent samples, voids could exist between adsorbed complexes within the interlayer. However, at the higher loadings these interstitial voids are filled with intercalated complexes.

The evidences for the adsorption exceeding the CEC of a clay is obtained by the electrophoresis measurements of a colloidal clay suspension.³⁶ Tris(2,2'-bipyridyl)-cobalt(III) ([Co(bpy)₃]³⁺ or tris(1,10-phenanthroline)cobalt(III). ([Co(phen)₃]³⁺) is added to colloidal dispersed sodium or cesium montmorillonite. The adsorption of these chelates is analyzed by Langmuir type plots. The amount of adsorbed chelate at saturation coverage, *a_s*, is calculated to be 2.8 and 1.6 meq per gram for both kinds of chelates when they are adsorbed by sodium and cesium montmorillonite, respectively. These values are about two and one times equivalents of CEC of a used clay, the CEC of these clays having been determined to be 1.2–1.5 meq per gram. Electrophoretic mobilities of clay colloids are measured as a function of the adsorbed amounts of the chelates (Fig. 13). In the absence of the chelates, the sign in the mobility of a clay is negative, indicating the dissociation of exchangeable cations for

TABLE IX
Surface areas of clay complexes as measured by nitrogen adsorption.³⁴

Clay	Complex salt	CEC-equivalents added ^a	N ₂ surface area, m ² /g			
			Heat treatment			
			160°C	450°C	550°C	
Hectorite	[Fe(phen) ₃]SO ₄	1	166	151	143	
		2	63	65	114	
		5	7	19	50	
		10	3	4	18	
	[Co(phen) ₃]SO ₄	5	10	13	46	
		[Ni(phen) ₃]SO ₄	5	2	4	29
Upton Montmorillonite	[Fe(phen) ₃]SO ₄	1	122	116	115	
		2	13	14	56	
		5	7	9	50	
		10	5	5	19	
Vermiculite	[Fe(phen) ₃]SO ₄	1	178	162	121	
		3	13	46	236	
		5	11	19	102	
	[Co(phen) ₃]SO ₄	3	9	18	217	
		[Ni(phen) ₃]SO ₄	3	7	31	220

^a The CEC-equivalents term refers to the quantity of complex salt in solution at the time of preparation of the clay complex.

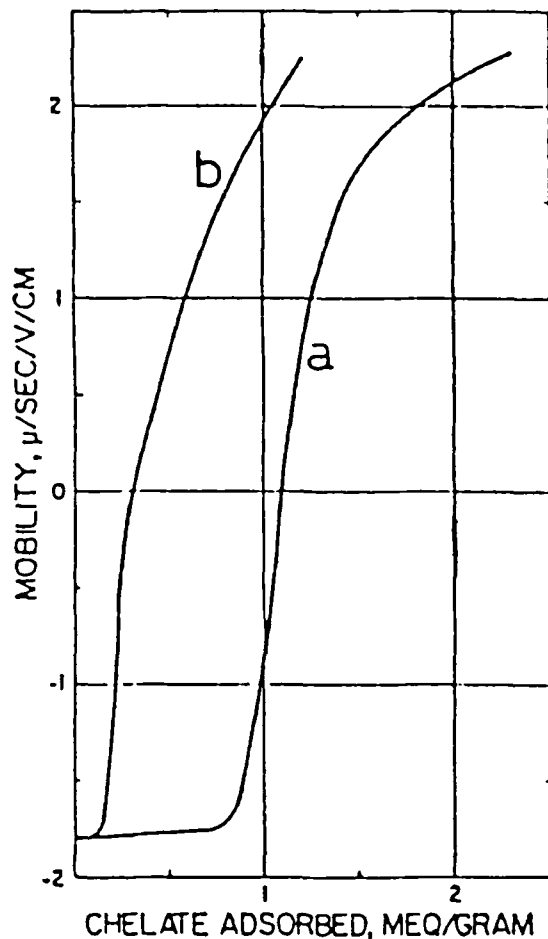


FIGURE 13 Electrophoretic mobilities of sodium (curve a) and cesium (curve b) montmorillonite, respectively, as a function of the adsorbed amounts of $[\text{Co}(\text{bpy})_3]^+$ and $[\text{Co}(\text{phen})_3]^{3+}$ ions.³⁶ Both chelate complexes give the same adsorption isotherm for the same clay.

negatively-charged clay layers. With increasing the adsorbed amount of a chelate, the mobility decreases to zero, then changes to a positive value, indicating that the particles become positively charged. The observed reversal of the sign in the mobility is a definite proof for the adsorption of the chelate beyond the CEC of a clay.

It should be mentioned here that such reversal of mobilities of a colloidal clay particle as observed above is never seen for the case of the adsorption of a simple metal ion like Co^{III} or Al^{III} or even a metal complex ion with small ligands such as $[\text{Co}(\text{NH}_3)_6]^{3+}$ or $[\text{Co}(\text{en})]^{+3}$.

The informations on the intermolecular interactions among the intercalated molecules within one layer are obtained by the dynamic investigation of the fluorescent emission from a bound complex. The transient change of the emission is followed after a suspension of $[\text{Ru}(\text{bpy})_3]^{2+}$ and sodium hectorite is illuminated by a 355 nm pulsed laser.³⁷ As shown in Figure 14, emission profiles are very much dependent on the intensity of an illuminated light pulse; that is, the life-time of an excited state of

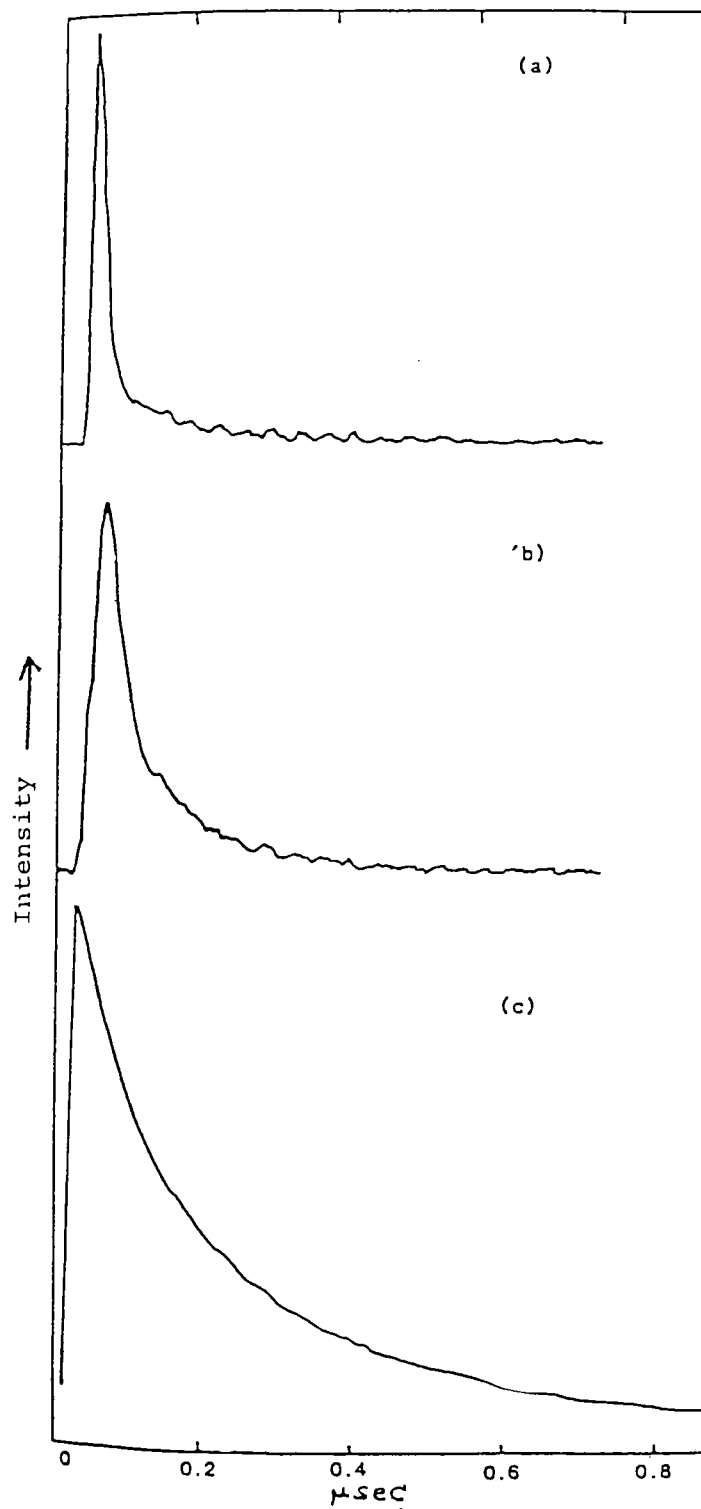


FIGURE 14 Emission decay profiles of $[\text{Ru}(\text{bpy})_3]^{2+}$ in a sodium montmorillonite suspension: (a) high-intensity excitation using nanosecond pulsed laser (355 nm), (b) same as (a) except that the pulse energy is attenuated by a factor of 5–7, and (c) low-intensity excitation using a triggered nitrogen gas lamp (337 nm).³⁷

TABLE X
Emission kinetics data^a of adsorbed $[\text{Ru}(\text{bpy})_3]^{2+}$ ^b as a function of $[\text{Zn}(\text{bpy})_3]^{2+}$ Concentration.³⁷

$10^5 \times$ $[\text{Zn}(\text{bpy})_3]^{2+}$, M	α^d	τ_1 , ^e ns	$1 - \alpha^f$	τ_2 , ^g ns	I^h
0	0.64	55	0.36	550	1
2	0.46	76	0.54	714	1.9
6	0.41	98	0.59	788	2.3
10	0.39	100	0.61	794	2.5

^a Parameters obtained from a double-exponential fitting routine. ^b 0.02 mM $[\text{Ru}(\text{bpy})_3]^{2+}$ in 2 g/L hectorite. ^c Added concentration of $\text{Zn}(\text{bpy})_3^{2+}$. ^d Fraction of total emission attributable to fast component at time zero. ^e Lifetime of fast component. ^f Fraction of total emission attributable to slow component at time zero. ^g Lifetime of slow component. ^h Relative integrated luminescence yield.

co-existing cations (Fig. 16a). The results for methylviologen are shown in Figure 16b, in which the Stern-Volmer plots are compared between the aqueous solution and the clay suspension. In water, methylviologen quenches the emission from excited $[\text{Ru}(\text{bpy})_3]^{2+}$ with the rate constant of $3 \times 10^8 \text{ M}^{-1} \text{ s}^{-1}$, while the same molecule does not quench the emission from excited $[\text{Ru}(\text{bpy})_3]^{2+}$ at all in a colloidal clay suspension. Since methylviologen cations are confirmed to be bound to a clay particle, it is postulated that the cations are unable to contact with excited $[\text{Ru}(\text{bpy})_3]^{2+}$ because these ions are spatially separated from each other as a result of segregation into the different clay layers (Fig. 15). In terms of the molecular interaction, the above results are explained by the principle that an intermolecular force is operative between the same kind of $[\text{Ru}(\text{bpy})_3]^{2+}$ molecules, leading to the adsorption beyond the CEC of a clay as well as the preferable aggregation within one layer. Such a force does not work between the molecules with no structural similarity such as between $[\text{Ru}(\text{bpy})_3]^{2+}$ and organic cations. The aggregate formation in one layer, therefore, occurs under distinct recognition of molecular structures.

In ending this section, one remark is added as for the segregation in the case of simple metal ions. It is reported that sodium ions and calcium ions are adsorbed by montmorillonite into different layers.³⁸ This demixing of metal ions is shown under such conditions that the layers containing calcium ions have two interlamellar water layers, while the layers containing sodium ions have only one water layer. Similar segregation has been observed for the simultaneous adsorption of a pair of ethylammonium and calcium ion by vermiculite.³⁹ Since the occurrence of the demixing depends on the kind of minerals, it is now suspected that the phenomena are related with the heterogeneity in the distribution of cation-exchange sites from one layer to another. In this respect, the causes for segregation for these molecules are different from what has been observed for the adsorption of $[\text{M}(\text{bpy})_3]^{2+}$ segregated from organic cations or simple metal ions.

5. RACEMIC ADSORPTION OF METAL CHELATES BY A COLLOIDAL CLAY

The preceding section presents the evidences that some metal complex ions like $[\text{M}(\text{bpy})_3]^{2+}$ interact intermolecularly when they are adsorbed in the interlayer space of a clay. Such interaction leads to the formation of an adsorbate aggregate within the surface of a single layer. It is not clarified yet, however, why the interaction is

only operative between the similar molecules such as $[\text{Ru}(\text{bpy})_3]^{2+}$ and $[\text{Ni}(\text{bpy})_3]^{2+}$ not between the dissimilar molecules such as $[\text{Ru}(\text{bpy})_3]^{2+}$ and methylviologen cation. Besides the reason is unclear why the attraction between bound $[\text{M}(\text{phen})_3]^{2+}$ ions are saturated at the adsorption of two-times excess of CEC. The most interesting question is whether any regularity exists in the arrangement of the adsorbed molecules in such an aggregate. Answers to the above questions have been given by a completely different approach toward the problems; that is, the stereochemical investigation on the stacking of metal complex ions in an interlamellar space.

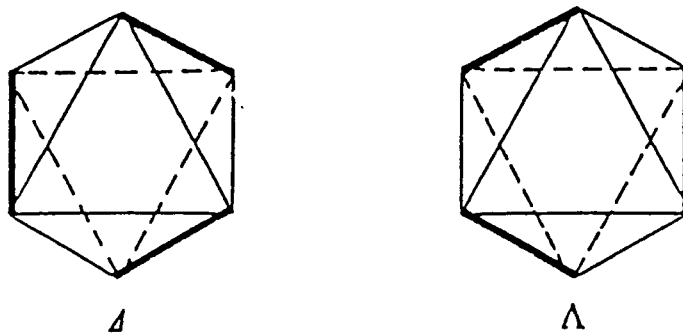
It has been examined if there is any selectivity on the adsorption of an optically active metal complex by a colloiddally dispersed clay particle.⁴⁰ The question has been motivated by the report that some amino acids and glucose are adsorbed stereoselectively by a colloidal suspension of naturally occurring sodium montmorillonite.⁴¹ L-amino acids and d-glucose are adsorbed almost 8 times more strongly by a clay than their optical antipodes. It is not clear whether a clay mineral is chiral or achiral in its crystal structure. Moreover, if a clay mineral is chiral, it is difficult to understand why one enantiomer of such a crystal exists in excess over its optical antipode.

For that purpose, the adsorption by a clay has been compared between the enantiomers of $[\text{Fe}(\text{phen})_3]^{2+}$ in a suspended condition. $[\text{Fe}(\text{phen})_3]^{2+}$ is chosen for the following reasons: i) the molecule is optically active, having the isomers normally denoted as Λ - and Δ -enantiomers under the IUPAC nomenclature method (Fig. 17A),⁴² ii) the isomers are resolved with ease by use of antimony tartrate salts,⁴³ and iii) the bound state of that molecule can be studied with various kinds of spectroscopies especially by the electronic absorption measurements due to its intense color in the visible region. As already remarked, a tris(2,2'-bipyridyl) chelate exhibits the characteristic change in its electronic spectrum when it is bound to a colloiddally dispersed clay (Fig. 10). A tris(1,10-phenanthroline) chelate also shows a similar change when it is bound to a clay. Such a change in the spectrum could be used as a measure of the binding of the chelate to a clay. In fact there is a strict linearity confirmed between the amount of the bound $[\text{Ru}(\text{bpy})_3]^{2+}$ and the increase of absorbance in its charge-transfer absorption from a metal to ligands.³²

The electronic absorption spectrum is measured for an aqueous suspension of $[\text{Fe}(\text{phen})_3]^{2+}$ and sodium montmorillonite.^{40,44} Figure 17B shows the increase of apparent extinction coefficient at 530 nm as a function of the ratio of [clay] to [chelate] for the three cases that the chelate is added as a Λ - or Δ -enantiomer or a racemic mixture. It is concluded that for both cases of Λ - and Δ -enantiomers the apparent extinction coefficient increases monotonously until it is saturated above [clay]/[chelate] = 2. Here the concentration of a clay is measured in terms of CEC. There is no stereoselectivity observed in the dependence of the spectral change on that ratio. It is concluded that both of the enantiomers of $[\text{Fe}(\text{phen})_3]^{2+}$ are adsorbed by a clay almost quantitatively, occupying two cation-exchange sites per molecule. When the same chelate is added as a racemic mixture, however, the apparent extinction coefficient increases more steeply until it levels off at the value of [clay]/[chelate] = 1. Thus it is derived that the racemic mixture is adsorbed in occupying one cation-exchange site per chelate. Since $[\text{Fe}(\text{phen})_3]^{2+}$ carries two positive charges per molecule, the racemic chelate is concluded to be adsorbed in two times excess of the CEC of a clay. It should be mentioned that the previously cited experiments on the adsorption of $[\text{M}(\text{phen})_3]^{2+}$ and $[\text{M}(\text{bpy})_3]^{2+}$ are all performed by using their racemic mixtures.³⁴⁻³⁶ It is thus clear that the excess adsorption beyond the CEC of a clay is restricted to the racemic mixtures of these chelates.

The electric dichroism measurements are performed on an aqueous suspension containing sodium montmorillonite and either enantiomeric or racemic $[\text{Fe}(\text{phen})_3]^{2+}$

(A)



(B)

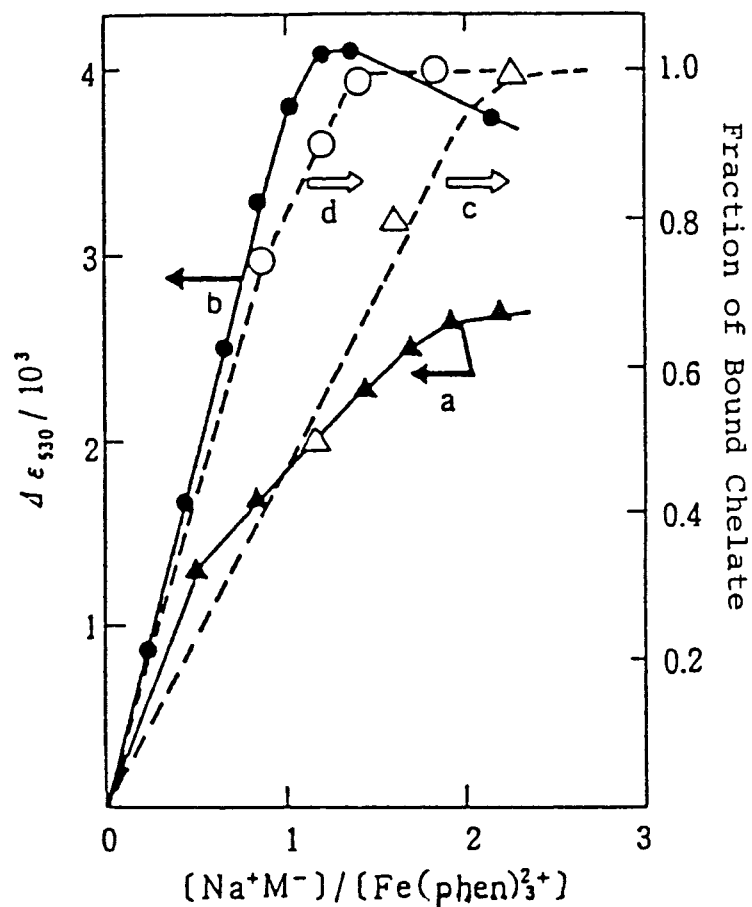


FIGURE 17 (A) Absolute configuration of a tris(chelated) complex.⁴² (B) Dependence of the apparent extinction coefficient at 530 nm on the ratio of [clay] to [chelate] when sodium montmorillonite is added to $[\text{Fe}(\text{phen})_3]^{2+}$ in an aqueous suspension.⁴⁴ The chelate is present as a pure enantiomer (a filled triangle) and as a racemic mixture (a filled circle). The vertical scale on the right-hand side is the dependence of the fraction of a bound chelate on the same ratio. The chelate is added as a pure enantiomer (an open triangle) and as a racemic mixture (an open circle).

ions.⁴⁴ In both cases, it is deduced that the molecules are adsorbed with their threefold symmetry axes perpendicular to the clay surface. There is no difference observed in their binding structures between the Λ - and Δ -[Fe(phen)₃]²⁺ enantiomers when they are added separately. This binding structure agrees with the previous presumption based on the X-ray diffraction measurements of $d(001)$ for a clay-chelate adduct.³⁴

The kinetics of the adsorption of [Fe(phen)₃]²⁺ by a colloiddally dispersed clay has been studied with a stopped-flow spectrophotometer.⁴⁴ After mixing a clay suspension with a solution of [Fe(phen)₃]²⁺, the transient increase of the absorbance at 530 nm is monitored. Figure 18 compares the absorption profiles among the following three systems: (i) a clay is mixed with enantiomeric [Fe(phen)₃]²⁺, (ii) a clay

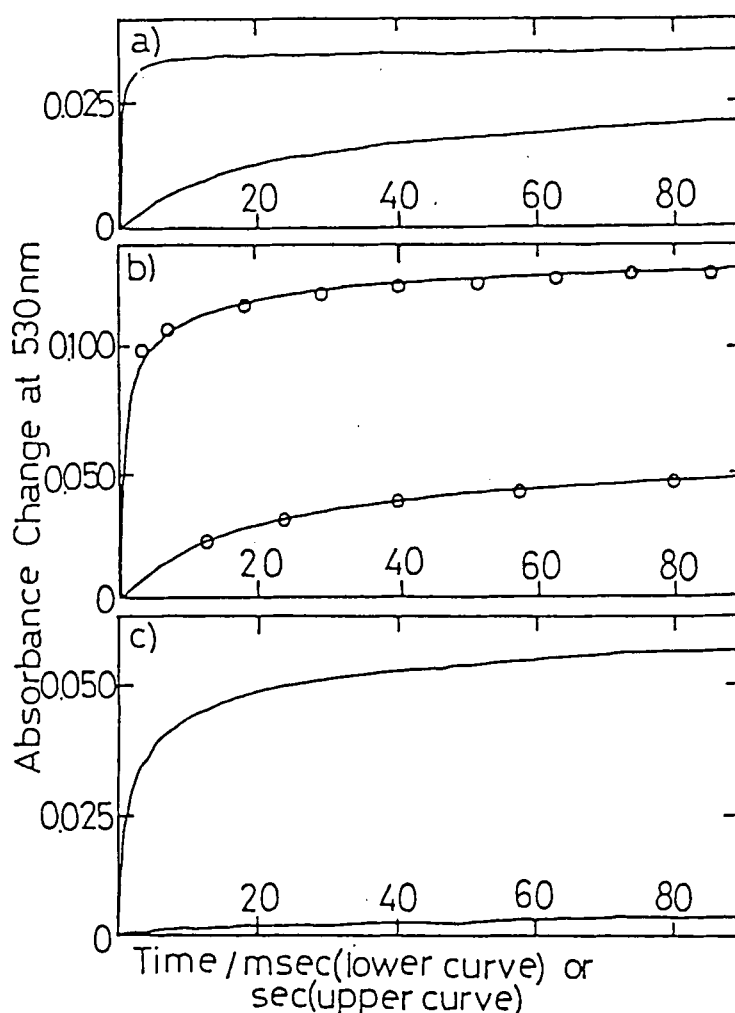


FIGURE 18 Transient increase of absorbance at 530 nm when the following two solutions are mixed in a stopped-flow apparatus: (a) enantiomeric [Fe(phen)₃]²⁺ and sodium montmorillonite, (b) racemic [Fe(phen)₃]²⁺ and sodium montmorillonite and (c) Λ -Fe(phen)₃]²⁺ and Δ -Fe(phen)₃]²⁺-montmorillonites.⁴⁴

is mixed with racemic $[\text{Fe}(\text{phen})_3]^{2+}$, (iii) a clay which has already exchanged enantiomeric $[\text{Fe}(\text{phen})_3]^{2+}$ is mixed with its antipodal $[\text{Fe}(\text{phen})_3]^{2+}$ isomer. For (i), the absorbance increase is completed within 100 ms after mixing. For (ii), the absorbance increase takes place by way of two stages, the first being completed within 100 ms and the second lasting beyond 80 s after mixing. For (iii), no rapid absorbance increase is observed in the time range of 100 ms and the absorbance increases slowly during 80 s after mixing. It is noted that the adsorption profile (ii) is equated to the sum of the profiles of (i) and (iii). It is deduced, therefore, that the adsorption of racemic mixture occurs by the succeeding two steps, the initial adsorption within CEC and the succeeding adsorption beyond CEC. These two steps correspond to processes (i) and (iii), respectively. The difference in adsorption rates between these two steps might reflect the difference in binding strength. The adsorption within CEC is strong because it is the process of electric neutralization, while the adsorption beyond CEC is weak because it is driven by the intermolecular attraction between the chelates of the same charge. The circumstances are coincident with the previously noted results that, when a clay containing two-CEC equivalents of $[\text{Fe}(\text{phen})_3]^{2+}$ is washed with water, only one CEC equivalent of $[\text{Fe}(\text{phen})_3]^{2+}$ remains on a clay.³⁴

It is tested whether the racemic adsorption as observed above takes place in other kinds of ion-exchange adsorbents such as a linear polyelectrolyte.⁴⁴ The adsorption by poly(styrene sulfonate) is studied for $[\text{Fe}(\text{phen})_3]^{2+}$ in an aqueous solution. Both enantiomeric and racemic $[\text{Fe}(\text{phen})_3]^{2+}$ ions are adsorbed up to the CEC of a polyelectrolyte. There is no excess adsorption observed for the racemic mixtures. It is concluded therefore that the racemic adsorption is a unique phenomenon to a layer clay mineral.

The above facts suggest that, when a racemic mixture of $[\text{Fe}(\text{phen})_3]^{2+}$ is adsorbed by a clay, a molecule is adsorbed as a unit of racemic pair rather than in a random distribution of optical isomers. Otherwise enantiomeric $[\text{Fe}(\text{phen})_3]^{2+}$ would also be adsorbed beyond CEC when the chelate is added in excess over a clay. In other words, racemic $[\text{Fe}(\text{phen})_3]^{2+}$ forms a racemic compound in the interlamellar region of a clay. The phenomena are denoted as "racemic adsorption" by a clay mineral. In order to seek the reasons for racemic adsorption, a molecular model is constructed for a possible structure of adsorbate aggregates. A tris(1,10-phenanthroline)metal(II) chelate is placed on a silicate sheet of montmorillonite with its threefold symmetry axis perpendicular to the surface. The three bottoms of the coordinated phenanthroline ligands make a regular triangle with the side lengths of about 6.5 Å. It is noted that these distances are close to the distances between the centers of neighboring SiO_4 hexagonal holes (5.5 Å) on a silicate sheet.⁴ Thus the bound chelate is possible to have its three hydrogen atoms in the ligands buried into the silicate surface. If this is the case, the chelate is rigidly fixed on the surface under the definite orientation (Fig. 19(a)). Based on the elemental compositions of a used montmorillonite (Table II), it is estimated that one cation-exchange site is allotted to every three hexagonal holes of a silicate sheet. For a clay in which enantiomeric $[\text{Fe}(\text{phen})_3]^{2+}$ is exchanged to one equivalent of CEC, the chelate occupies six hexagonal holes per molecule. The situations are depicted in Figure 19(b). For a clay in which racemic $[\text{Fe}(\text{phen})_3]^{2+}$ is exchanged to two equivalents of CEC, the chelate occupies three hexagonal holes per molecule as in Figure 19(c). It is at this point that a very strict stereochemical restriction appears in the arrangement of the bound isomers. In order to achieve such a high density of adsorption on a silicate surface as in (c), the bound isomers should be placed in an alternative way such as an isomer placed in between its optical antipodes. Otherwise, if a couple of $[\text{Fe}(\text{phen})_3]^{2+}$ enantiomers are placed at the neighboring sites, the phenanthroline ligands belonging to these facing chelates interfere sterically

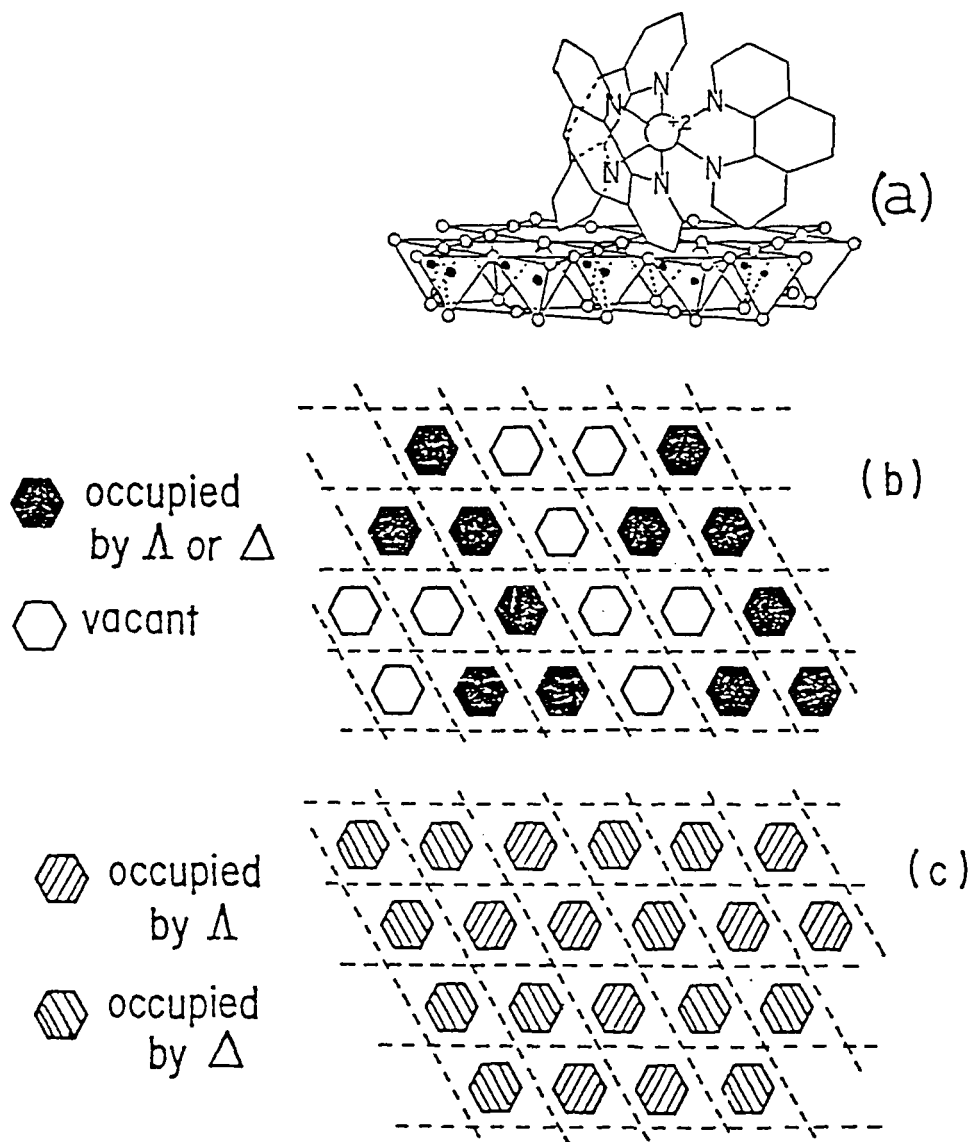


FIGURE 19 (a) Proposed structure of bound $[\text{Fe}(\text{phen})_3]^{2+}$ on a montmorillonite layer. (b) Proposed arrangement of enantiomeric $[\text{Fe}(\text{phen})_3]^{2+}$ on a layer. A hexagon denotes a hexagonal hole surrounded by six SiO_4^{4-} tetrahedrons on a silicate sheet. One chelate occupies six hexagons, so no interaction is expected among the chelates. (c) Proposed arrangement of racemic $[\text{Fe}(\text{phen})_3]^{2+}$ on a layer. One chelate occupies three hexagons. At such highly dense packing, the chelates should be arranged so as to form a bidimensional racemic compound.

with each other. Since the $d(001)$ for an adduct of a clay and racemic $[\text{Fe}(\text{phen})_3]^{2+}$ is measured to be 29 \AA ,⁴⁵ the interlayer space which accommodates racemic $[\text{Fe}(\text{phen})_3]^{2+}$ chelates has the height of about 20 \AA . Based on this, it is suspected that the racemic aggregate in (c) is not a monomolecular layer but a double layer in which the layer of one enantiomers, for example, Λ - $[\text{Fe}(\text{phen})_3]^{2+}$ is located a little

above the layer of the other enantiomer, or Δ -[Fe(phen)₃]²⁺. Even so, the same stereochemical restrictions are expected to be operative for achieving such close stacking.

The molecular model considerations as stated above lead to the following conclusions as to the conditions for the achievement of racemic adsorption by metal chelates on a solid surface:

(i) A bound chelate should be adsorbed up to such a density that it interacts with its neighbors stereochemically. In the case of cation-exchanging by a clay, a molecule carrying two positive charges is required to have a molecular radius longer than 5 Å. Otherwise it does not interact sterically with its neighbors. A molecule with less positive charge could be smaller to achieve the intermolecular interaction on a clay surface.

(ii) A surface should be bidimensional and capable of fixing a bound chelate under a definite orientation. Otherwise the strict stereochemical restriction does not arise in the stacking of a chelate as a molecular aggregate.

A direct evidence for the racemic adsorption has been obtained when a clay is added to a solution containing partially resolved metal complexes.^{44,46} If a metal complex is adsorbed racemically, the optical purity of a partially resolved solution would be improved by adding a clay to such a solution. This is expected because excessive racemic pairs are eliminated from the solution as a clay-chelate adduct. For that purpose, colloiddally dispersed sodium montmorillonite is added to an aqueous solution containing Λ -[Fe(phen)₃]²⁺ at an optical purity of 30%. After filtering the suspension, the filtrate is revealed to contain Λ -[Fe(phen)₃]²⁺ at an optical purity of 50%. The optical purity increases more by repeating the above procedures. This fact supports that the chelates are adsorbed by a colloidal clay as a racemic pair.

Another point of interest is concerned with the selectivity in the pairing of molecules in an interlamellar space. As already stated in the preceding section, there is some selectivity observed in the adsorption beyond the CEC of a clay.^{34,37} Such selectivity leads to the segregation of different kinds of ions among the layers (Fig. 15). The adsorption of two kinds of chelates by a colloidal clay suspension is studied by means of the electric dichroism and circular dichroism measurements.⁴⁷ In the electric dichroism studies, the amplitudes of the dichroism signal is used as a measure of the adsorbed amount of a chelate. This is based on the fact that a chelate exhibits the dichroism under the electric field pulse only when it is bound to a clay particle. As a free molecule, the chelate has too small dipole moment or polarizability to be orientated by the torque of electric field. In fact, the adsorbed amount of [Ru(phen)₃]²⁺, for example, is found to be proportional to the dichroism amplitude of the suspension. Figure 20 shows the dependence of the dichroism amplitude due to bound Λ -[Re(phen)₃]²⁺ on the ratio of an added enantiomer of a different kind (denoted by M*) to an initial Λ -[Ru(phen)₃]²⁺. For M* = Λ -[Ni(phen)₃]²⁺, the amplitude decreases monotonously to a saturated level which is about one-half of the initial value. The initial decrease of the dichroism amplitude indicates that bound Λ -[Ru(phen)₃]²⁺ is dissociated from a clay as it is replaced with Λ -[Ni(phen)₃]²⁺. In other words, Λ -[Ru(phen)₃]²⁺ and Λ -[Ni(phen)₃]²⁺ compete for the same binding sites on a clay. It should be noted here that the dichroism amplitude does not become zero but approaches some definite value at a large excess of Λ -[Ni(phen)₃]²⁺. The results are interpreted as an indication that a part of the initially bound Λ -[Ru(phen)₃]²⁺ is not replaced with Λ -[Ni(phen)₃]²⁺ but is attracted toward Λ -[Ni(phen)₃]²⁺ montmorillonite in excess of CEC. The same figure includes the plot of the dichroism amplitude in the case of Δ -[Ni(phen)₃]²⁺ as an added

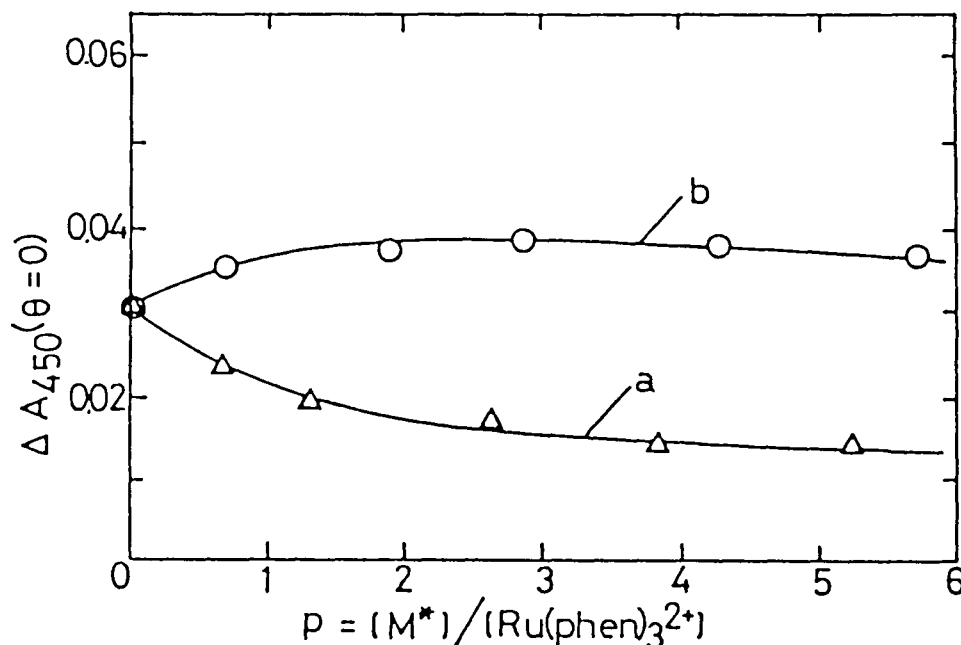


FIGURE 20 Plots of the dichroism amplitude at 450 nm for a parallel-polarized light when the enantiomers of $[\text{Ni}(\text{phen})_3]^{2+}$ is added to a colloidal suspension of Λ - $[\text{Ru}(\text{phen})_3]^{2+}$ montmorillonite.⁴⁷ Curves a and b correspond to the results for Λ - $[\text{Ni}(\text{phen})_3]^{2+}$ and Δ - $[\text{Ni}(\text{phen})_3]^{2+}$, respectively.

enantiomer. The amplitude stays at a constant value in the range of the ratio from 0 to 4. This means that Δ - $[\text{Ni}(\text{phen})_3]^{2+}$ does not replace bound Λ - $[\text{Ru}(\text{phen})_3]^{2+}$ at all. Most probably Δ - $[\text{Ni}(\text{phen})_3]^{2+}$ is adsorbed by Λ - $[\text{Ru}(\text{phen})_3]^{2+}$ montmorillonite by forming a diastereomeric pair with Λ - $[\text{Ru}(\text{phen})_3]^{2+}$. Such an antipodal pair between the different kinds of chelates would be called "pseudo-racemic". Similar plots are obtained when the enantiomers of $[\text{Fe}(\text{phen})_3]^{2+}$ are added to a solution of Λ - $[\text{Ru}(\text{phen})_3]^{2+}$ montmorillonite. In this case the monitoring light is adjusted to see solely the dichroism due to a bound Fe-chelate. The results are essentially identical with the ones obtained for the case of $M^* = [\text{Ni}(\text{phen})_3]^{2+}$, that is, the Λ -enantiomer of $[\text{Fe}(\text{phen})_3]^{2+}$ replace with bound Λ - $[\text{Ru}(\text{phen})_3]^{2+}$, while the Δ -enantiomer of $[\text{Fe}(\text{phen})_3]^{2+}$ is adsorbed by Λ - $[\text{Ru}(\text{phen})_3]^{2+}$ montmorillonite in excess over CEC. Thus pseudo-racemic adsorption is concluded to take place between different kinds of tris(1,10-phenanthroline) metal(II) chelates. In contrast with $[\text{M}(\text{phen})_3]^{2+}$, Λ - $[\text{Co}(\text{phen})_3]^{3+}$ is not found to make a pseudo-racemic pair with bound Λ - $[\text{Ru}(\text{phen})_3]^{2+}$.

This is attributed to the fact that $[\text{Co}(\text{phen})_3]^{3+}$ carries three positive charges that presents too high electric repulsion to be paired with $[\text{Ru}(\text{phen})_3]^{2+}$. On the same reason, $[\text{Co}(\text{en})_3]^{3+}$ does not make a racemic pair. Although $\text{cis-}[\text{CoCl}_2(\text{en})_2]^+$ carries one positive charge, the Δ -enantiomer of the chelate does not show pseudo-racemic adsorption toward Λ - $[\text{Ru}(\text{phen})_3]^{2+}$ montmorillonite. This is probably because the molecule has too small a radius to interact with $[\text{Ru}(\text{phen})_3]^{2+}$ on a clay surface.

The circular dichroism spectra are recorded on an aqueous suspension of Λ - $[\text{Ru}(\text{phen})_3]^{2+}$ montmorillonite.⁴⁷ Curve a in Figure 21 is the spectrum of Λ - $[\text{Ru}(\text{phen})_3]^{2+}$ in the absence of a clay. On adding a clay, the spectrum changes to

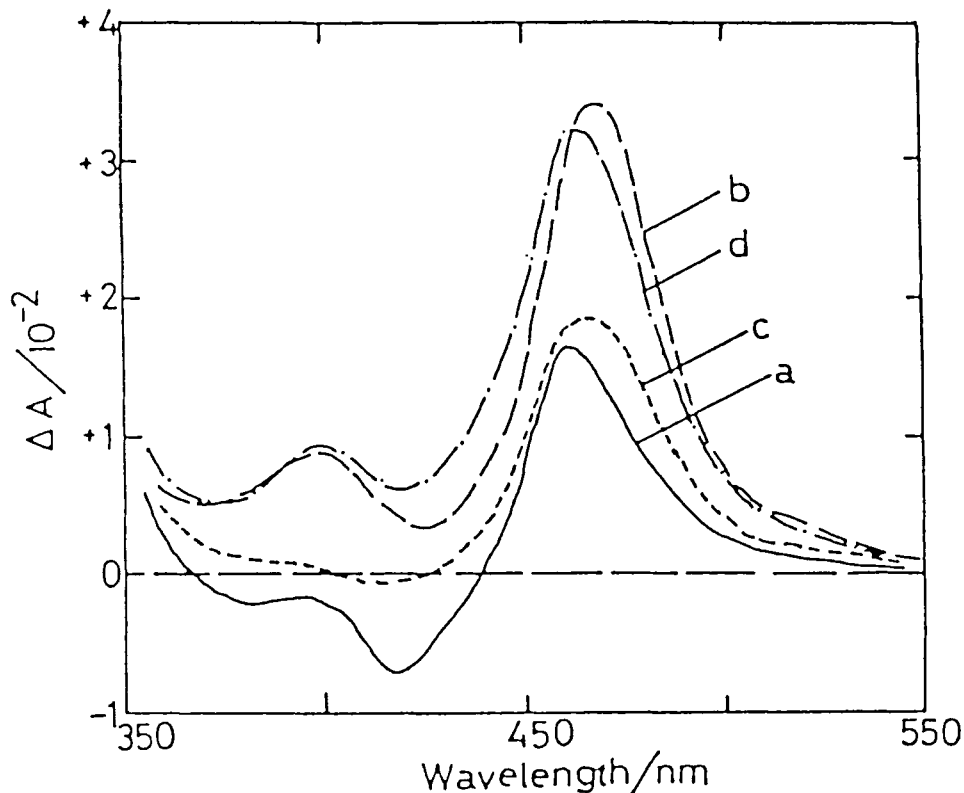


FIGURE 21 Effect of addition of sodium montmorillonite and the enantiomer of $[\text{Ni}(\text{phen})_3]^{2+}$ on the CD spectrum of $\Delta\text{-}[\text{Ru}(\text{phen})_3]^{2+}$: (a) no clay, (b) a clay added, (c) $\Delta\text{-}[\text{Ni}(\text{phen})_3]^{2+}$ added to (b), and (d) $\Lambda\text{-}[\text{Ni}(\text{phen})_3]^{2+}$ added to (b).⁴⁷

curve b, indicating the adsorption of the chelate to a clay. When $\Lambda\text{-}[\text{Ni}(\text{phen})_3]^{2+}$ is added, the spectrum changes to curve c, which is similar to that of a free Ru-chelate. This indicates that $\Lambda\text{-}[\text{Ru}(\text{phen})_3]^{2+}$ is dissociated from a clay by being replaced with added $\Lambda\text{-}[\text{Ni}(\text{phen})_3]^{2+}$. Oppositely when $\Delta\text{-}[\text{Ni}(\text{phen})_3]^{2+}$ is added, the spectrum changes little as shown by curve d, implying that bound $\Lambda\text{-}[\text{Ru}(\text{phen})_3]^{2+}$ is not dissociated in the presence of $\Delta\text{-}[\text{Ni}(\text{phen})_3]^{2+}$ enantiomer. These results are coincident with the previous conclusions obtained from the electric dichroism measurements. An interesting feature appears when racemic $[\text{Co}(\text{phen})_3]^{2+}$ is added to a $\Lambda\text{-}[\text{Ru}(\text{phen})_3]^{2+}$ clay suspension. Figure 22 illustrates the CD spectra in the region of 300 nm – 230 nm for that system. Curve c is the difference spectrum of $\Lambda\text{-}[\text{Ru}(\text{phen})_3]^{2+}$ montmorillonite suspension before and after the addition of racemic $[\text{Co}(\text{phen})_3]^{2+}$. The spectrum indicates that the Δ -isomer of some tris(1,10-phenanthroline) chelate is produced in excess in the suspension on addition of racemic $[\text{Co}(\text{phen})_3]^{2+}$. The results are interpreted by the assumption that racemic $[\text{Co}(\text{phen})_3]^{2+}$ which racemizes rapidly in a bulk solution, is converted to a little excess of $\Delta\text{-}[\text{Co}(\text{phen})_3]^{2+}$ in the presence of $\Lambda\text{-}[\text{Ru}(\text{phen})_3]^{2+}$ montmorillonite. This conversion is induced because the former isomer is more stabilized than its antipode by forming the pseudo-racemic pair with $\Lambda\text{-}[\text{Ru}(\text{phen})_3]^{2+}$ on a clay surface. In other words, $[\text{Co}(\text{phen})_3]^{2+}$ is anti-racemized to $\Delta\text{-}[\text{Co}(\text{phen})_3]^{2+}$ on a $\Lambda\text{-}[\text{Ru}(\text{phen})_3]^{2+}$

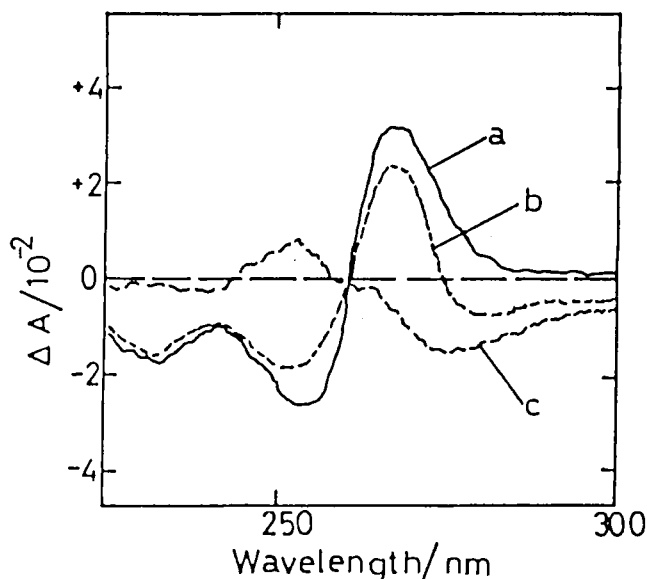


FIGURE 22 Effect of racemic $[\text{Co}(\text{phen})_3]^{2+}$ on the CD spectrum of an aqueous suspension of Δ - $[\text{Ru}(\text{phen})_3]^{2+}$ montmorillonite: (a) no $[\text{Co}(\text{phen})_3]^{2+}$ added, (b) racemic $[\text{Co}(\text{phen})_3]^{2+}$ added to (a), and (c) the difference between (a) and (b).⁴⁷

montmorillonite surface. The similar effect is observed when racemic $[\text{Fe}(\text{phen})_3]^{2+}$ is added to a suspension of Δ - $[\text{Ni}(\text{phen})_3]^{2+}$ montmorillonite. As shown in Figure 23, the new CD absorption is induced in two steps at 400–600 nm where Δ - $[\text{Ni}(\text{phen})_3]^{2+}$ alone has no detectable absorption under those conditions; the initial instantaneous appearance of CD as shown by curve a is followed by the further gradual change as shown by curves b – e. The results are interpreted by the mechanism that Λ - $[\text{Fe}(\text{phen})_3]^{2+}$ is first adsorbed by Δ - $[\text{Ni}(\text{phen})_3]^{2+}$ clay stereoselectively, and then Δ - $[\text{Fe}(\text{phen})_3]^{2+}$ is also adsorbed by a clay after it is converted to the Λ -isomer in a bulk medium. As a result, initial racemic $[\text{Fe}(\text{phen})_3]^{2+}$ is accumulated as the Λ -isomer to almost 60% of optical purity. Moreover the Λ -isomer produced in excess in the above system does not racemize at all in at least three days. The fact implies that the pseudo-racemic layer composed of Δ - $[\text{Ni}(\text{phen})_3]^{2+}$ and Λ - $[\text{Fe}(\text{phen})_3]^{2+}$ on a clay surface is so rigidly packed that neither of the component complexes is capable of racemization. In a homogeneous solution, such anti-racemization is known as a Pfeifer's effect which is caused by addition of appropriate chiral reagent to a racemic mixture.⁴⁸ For example, Λ - $[\text{Ni}(\text{phen})_3]^{2+}$ is enriched with the equilibrium constant of 1.14 at 25°C when 2% of cinchonium sulfate is added to racemic $[\text{Ni}(\text{phen})_3]^{2+}$.⁴⁹ The large displacement of the racemization equilibrium observed in a clay suspension as above is apparently attributed to the solid-like nature of the interlamellar complex. That is, the racemic or pseudo-racemic layer in such a space is so highly packed that it is regarded as a solid phase. Thus it is protected from the attack of water molecules in a bulk medium. This would reduce very much the racemization rates of intercalated complexes.

In the foregoing section, the intermolecular force is reported to be negligible between $[\text{Ru}(\text{bpy})_3]^{2+}$ and organic cations such as methylviologen (Fig. 15). The CD spectral study indicates that such interaction does take place under appropriate conditions.

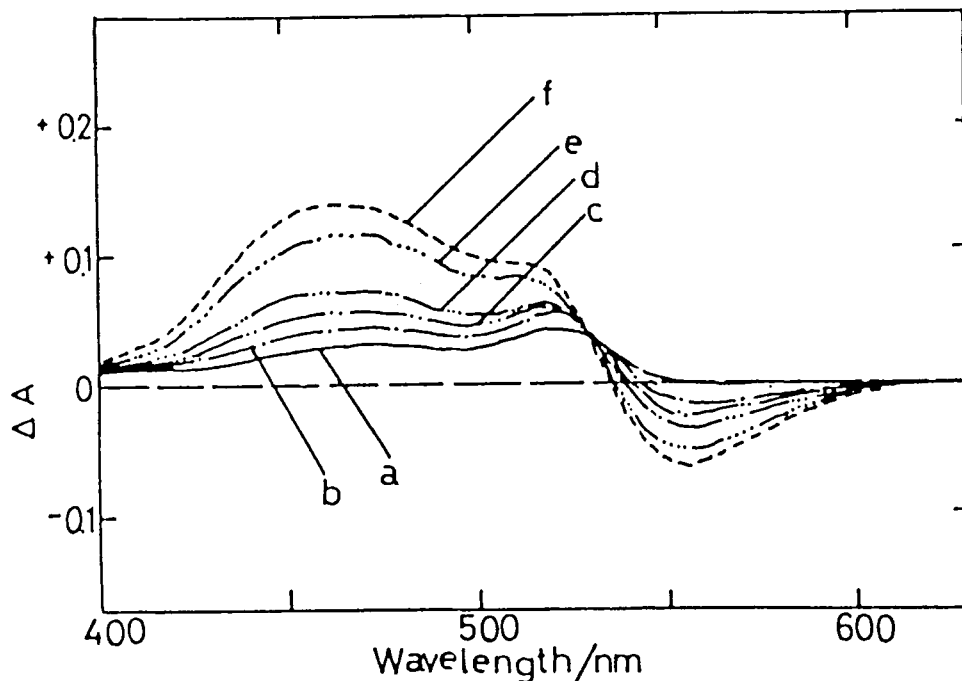


FIGURE 23 Induction of CD absorption when racemic $[\text{Fe}(\text{phen})_3]^{2+}$ is added to an aqueous suspension of Δ - $[\text{Ni}(\text{phen})_3]^{2+}$ montmorillonite.⁴⁷ The spectrum is recorded at (a) 2 min, (b) 5 min, (c) 15 min, (d) 30 min, and (e) 3 hr after $[\text{Fe}(\text{phen})_3]^{2+}$ is added to the suspension, (f) is the spectrum when Λ - $[\text{Fe}(\text{phen})_3]^{2+}$ is added to a Δ - $[\text{Ni}(\text{phen})_3]^{2+}$ montmorillonite suspension.

Figure 24 shows the induced CD spectra when the derivatives of Acridine Orange cations are added to a suspension of Δ - $[\text{Ni}(\text{phen})_3]^{2+}$ montmorillonite. The dye molecules which are achiral as a free species become optically active in their electronic spectrum when they are bound to the clay-chelate adduct. It is deduced that Acridine Orange dye cations are arranged in a chiral way on such an adduct. The van der Waals interactions would be responsible for the attraction of the dye cations towards the bound chelates.

Stereoselectivity is also confirmed from the kinetic point of view.⁵⁰ Adsorption rates are compared between the Λ - and Δ -enantiomers of $[\text{Fe}(\text{phen})_3]^{2+}$ by colloiddally dispersed Δ - $[\text{Ni}(\text{phen})_3]^{2+}$ montmorillonite. The initial rate of absorbance increase is about 50 times higher for Λ - $[\text{Fe}(\text{phen})_3]^{2+}$ than for Δ - $[\text{Fe}(\text{phen})_3]^{2+}$. The results mean that the stereoselectivity in adsorption by a clay-adduct is not only of thermodynamic nature but also of kinetic one.

A clay adduct with racemic $[\text{Fe}(\text{phen})_3]^{2+}$ should contain external anions in the solid state because the cationic chelate is adsorbed in excess over CEC. The presence of such anions is examined with the Auger electron spectroscopies (A.e.s.) for a solid sample of $[\text{Fe}(\text{phen})_3]^{2+}$ montmorillonite.⁵¹ From the A.e.s. transition peaks, antimony tartrate anion is found to be included in the sample which has adsorbed racemic $[\text{Fe}(\text{phen})_3]^{2+}$ antimony tartrate. To this contrary, the sample which has adsorbed Λ - $[\text{Fe}(\text{phen})_3]^{2+}$ antimony tartrate does not contain antimony tartrate anions. These results provide an additional evidence for the fact that adsorption beyond CEC occurs only for racemic $[\text{Fe}(\text{phen})_3]^{2+}$.

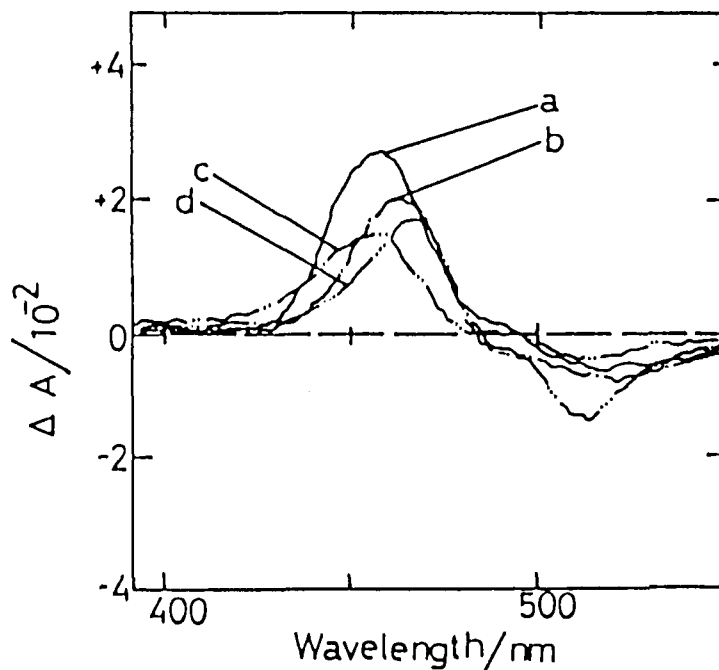


FIGURE 24 Induction of CD absorption when an N-alkylated Acridine Orange derivatives is added to an aqueous suspension of Δ -[Ni(phen)₃]²⁺ montmorillonite.⁴⁷ An added cation is (a) Acridine Orange cation, (b) *N*-methyl Acridine Orange cation, (c) *N*-ethyl Acridine Orange cation and (d) *N*-*n*-propyl Acridine Orange cation.

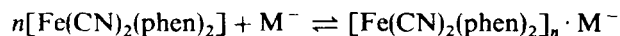
Racemic adsorption by a clay is also ascertained for dicyanobis(1,10-phenanthroline)iron(II) ([Fe(CN)₂(phen)₂] and dicyanobis(2,2'-bipyridyl)iron(II) ([Fe(CN)₂(bpy)₂]).⁵² Although these complexes carry no charge, they are still adsorbed by montmorillonite strongly. Probably the highly polarizable chelates are attracted towards a clay through an ion-dipole interaction with the permanent negative charge of a clay layer. Table XI includes the adsorption data in which n and K_b denote the

TABLE XI
Binding equilibria of iron complexes with colloiddally dispersed sodium montmorillonite at 20°C.⁵²

complex	n^a	K_b/M^{-b}
[Fe(CN) ₂ (phen) ₂] racemic	1.75	4.1×10^5
enantiomeric	1.33 – 0.74	$(0.31 – 1.3) \times 10^5$
[Fe(CN) ₂ (phen) ₂] ⁺ racemic	0.90 ^c	$> 10^6$ ^c
enantiomeric	0.55 ^c	$> 10^6$ ^c
[Fe(CN) ₂ (bpy) ₂] racemic	2.2	1.8×10^6
enantiomeric	1	$\sim 10^5$

^a Number of adsorbed metal chelates per cation-exchange site. ^b Binding constant.
^c n and K_b were obtained from the decrease of free metal complex by centrifuging

number of adsorbed chelate per cation-exchange site and the binding constant according to the equation below, respectively.



It is noted that n for a racemic mixture is always about twice for an enantiomeric chelate and K_b for a racemic mixture is larger than for an enantiomer. Since these dicyanobischelate complexes have bulky planar ligands like $[\text{M}(\text{phen})_3]^{2+}$, they are expected to interact with their neighbors stereoselectively. Higher values of n for these chelates than $[\text{M}(\text{phen})_3]^{2+}$ ($n = 1$ and 0.5 for a racemic mixture and an enantiomer, respectively (Fig. 17)) reflects the situations that the smaller area is occupied per one molecule for the former than for the latter. Besides it should be added that racemic $[\text{Fe}(\text{CN})_2(\text{phen})_2]$ exhibits remarkably low solubility in comparison to enantiomeric $[\text{Fe}(\text{CN})_2(\text{phen})_2]$: 7.0×10^{-5} M and 7.9×10^{-4} M at 15°C for a racemic mixture and an enantiomer, respectively. As a result, $[\text{Fe}(\text{CN})_2(\text{phen})_2]$ forms racemic crystal from an aqueous solution. Thus tendency for racemic pairing of this chelate has an origin already in its own properties.

Racemic adsorption is observed for a bis(chelated) complex. Bis(1-(2-pyridylazo)-2-naphthol)cobalt(III) ($[\text{Co}(\text{PAN})_2]^+$ (Fig. 25)) is adsorbed by colloidal dispersed sodium montmorillonite.⁵³ The upper and lower parts of Figure 26A show the changes of electronic spectra when optically active $(-)-[\text{Co}(\text{PAN})_2]^+$ and racemic $[\text{Co}(\text{PAN})_2]^+$ are adsorbed by a clay. The absorbance at 644 nm increases more for a racemic mixture than for an enantiomer. Besides the number of chelate per cation-exchange site is 0.5 and 1.0 for the racemic and enantiomeric chelates, respectively. The system is studied with the electric dichroism measurements. $[\text{Co}(\text{PAN})_2]^+$ has two major bands in the wavelength region of 400–700 nm. These bands arise from the $\pi - \pi^*$ transitions in the coordinated PAN ligands.⁵⁴ The transition moments for the bands at 450 nm and around 600 nm lie in the long and short axes of the bound PAN ligands, respectively. Analyzing the wavelength dependence of the observed electric dichroism amplitudes, the chelates are concluded to be bound on a clay surface as schematically shown in Figure 26B. The figure indicates that enantiomeric $[\text{Co}(\text{PAN})_2]^+$ occupies two thirds of the surface, while racemic $(\text{Co}(\text{PAN})_2)^+$ covers the whole surface by forming a double layer: one layer consists of $(-)$ -enantiomer and the other of $(+)$ -enantiomer. Under such a closely packed state, the ligands of the neighboring racemic pair are stacked nicely with each other.

Table XII summarizes the results of the absorption studies in this section. From the table, the conditions for a chelate realizing racemic adsorption on a clay are given

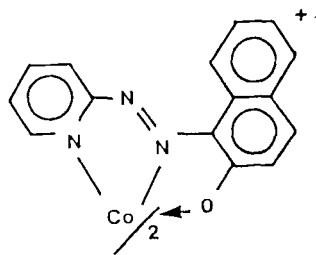


FIGURE 25 Structure of $[\text{Co}(\text{PAN})_2]^+$.

TABLE XII
The Chelates which show the racemic adsorption and do not show the
racemic adsorption in binding to a colloidal clay

Chelates showing racemic adsorption	Chelates not showing racemic adsorption
$[\text{Fe}(\text{CN}_2(\text{phen})_2)]^a$	$[\text{Co}(\text{en})_3]^{3+ a}$
$[\text{Fe}(\text{CN}_2(\text{byp})_2)]^a$	$[\text{Co}(\text{glycinato})_2(\text{phen})^+]^d$
$[\text{Fe}(\text{CN}_2(\text{phen})_2)]^{+ a}$	$[\text{Co}(\text{phen})_3]^{3+ d}$
$[\text{Fe}(\text{CN}_2(\text{byp})_2)]^{+ a}$	
$[\text{Fe}(\text{phen})_3]^{2+ b}$	
$[\text{Ni}(\text{phen})_3]^{2+ b}$	
$[\text{Co}(\text{PAN})_2]^{+ c}$	

^a byp = 2,2'-bipyridyl⁵² ^b Ref. 40. ^c Ref. 53. ^d Unpublished results.

as follows:

- (i) The charge of a chelate is 0, +1, and +2 (not +3).
- (ii) The chelate possesses two or three planar ligands whose sizes are larger than 10 Å.

In ending this section, two additional works are remarked in connection with the chiral aggregation phenomena. One is concerned with the aggregation of tris(1,10-phenanthroline) metal(II) chelate in a homogeneous solution. From the proton NMR chemical shifts of a deuterated water solution of $[\text{Ru}(\text{phen})_3]^{2+}$, it is confirmed that the chelates form the aggregates above the concentration of 0.01 M at room temperature (28°C).⁵⁵

The NMR shifts are different between the racemic and enantiomeric solutions of the chelate, indicating that the interaction in such an aggregate is stereospecific. Figure 27 shows the probable configuration of a dimeric aggregate of a racemic pair. The phenanthroline ligand of one chelate is placed over the phenanthroline ligand of the other. In contrast to the racemic dimer, the dimer of an enantiomeric pair is more labile and is not possible to be stacked as closely as shown in the figure. The results support the present view in the aspect that a $[\text{M}(\text{phen})_3]^{2+}$ ion is possible to be stacked stereoselectively.

The other work is concerned with the monolayer formation of surfactant molecules. Both chiral and racemic 12-hydroxyoctadecanoic acids (12HOA) form a monolayer at the interface of water and air.⁵⁶ The monolayers of both acids undergo a two-dimensional phase transition from the expanded monolayer composed of bent chain molecules to the condensed monolayer composed of straight chain molecules. It is confirmed that racemic 12HOA forms a racemic molecular compound in the condensed monolayer phase as shown in Figure 28. The results provide another example that a racemic mixture is packed on a bidimensional surface as a racemic compound. Evidence for "two-dimensional resolution" is reported in a monolayer of racemic N- α -methylbenzylstearamide.⁵⁷ The racemic film of this compound gives a higher surface free energy than the film of an enantiomer. Based on this, the racemic film is compressed in seeding with the crystal of an R-enantiomer. As a result, the film becomes predominant in an S-enantiomer by depositing an R-enantiomer on the crystal.

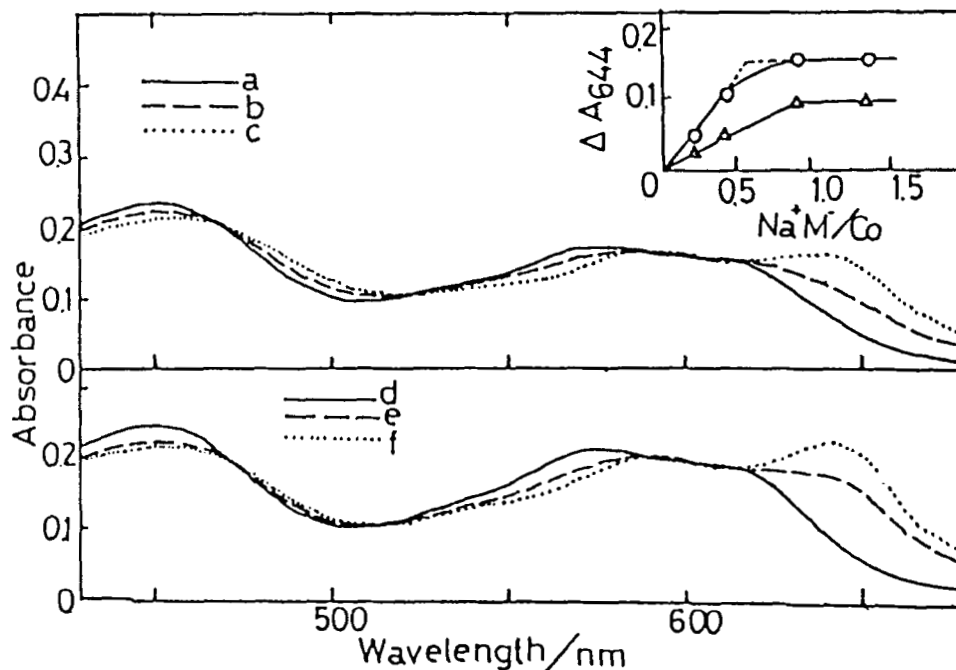


FIGURE 26A The effects of sodium montmorillonite on the electronic spectrum of $[\text{Co}(\text{PAN})_2]^+$.⁵³ (Upper) (a) (—) isomer in the absence of a clay, (b) and (c) a clay added. (Lower) (d) racemic chelate in the absence of a clay, (e) and (f) a clay added. The insert is the dependence of the increase of absorbance at 644 nm on the ratio of [clay] to [chelate].

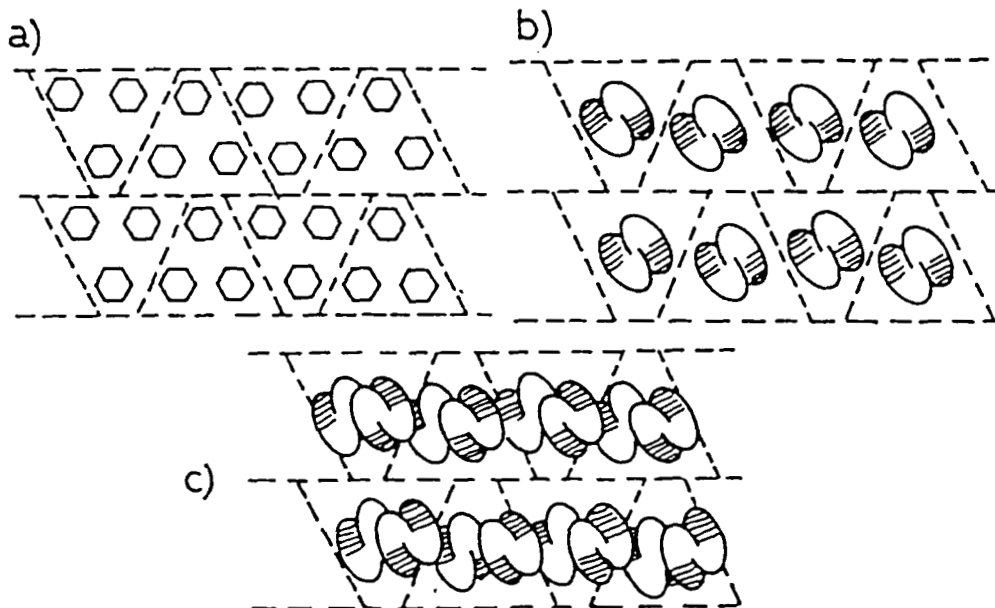


FIGURE 26B (a) Overview drawing of a silicate sheet of montmorillonite layer. A hexagon indicates a hexagonal hole surrounded by six SiO_4 tetrahedrons. The area surrounded by dotted lines corresponds to one cation-exchange site. (b) A proposed bound state of enantiomeric $[\text{Co}(\text{PAN})_2]^+$ ions. (c) A proposed bound state of racemic $[\text{Co}(\text{PAN})_2]^+$. The adsorbate layer is a double-molecular layer in which (—) and (+) isomers constitute homochiral layers.

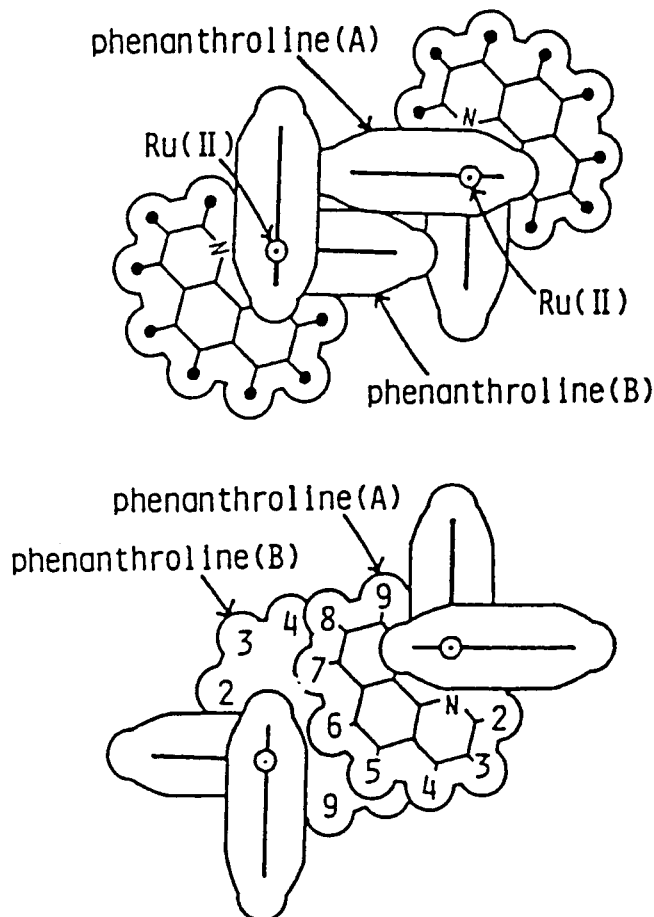


FIGURE 27 Probable configuration of a pair of Λ - and Δ -[Ru(phen)₃]²⁺ ions in the M₂X and M₂X₂ aggregates (X = anion): the elevation (top) and the plane (bottom).⁵⁵

6. CHROMATOGRAPHIC RESOLUTION BY USE OF CLAY-CHELATE ADDUCTS

In the previous section, the adsorption of some racemic metal chelates beyond the CEC of a clay is described and rationalized in terms of stereoregular stacking between the adjacent molecules within a bidimensional silicate sheet of a clay layer. A similar kind of pairing is observed even between the diastereomeric pair of different chelates in which one enantiomer is delta and the other lamda (previously named "pseudo racemic" pair). Such a formation of a racemic or pseudo-racemic pair is restricted to the chelates satisfying certain stereochemical conditions. When these phenomena are examined from the practical point of view, there are three possible ways of application conceived as below:

(i) The optical purity of a partially resolved solution is improved through the adsorption by a clay. This is attained by the elimination of an excess racemic pair in the form of a clay-chelate adduct as schematically shown in Figure 29a.

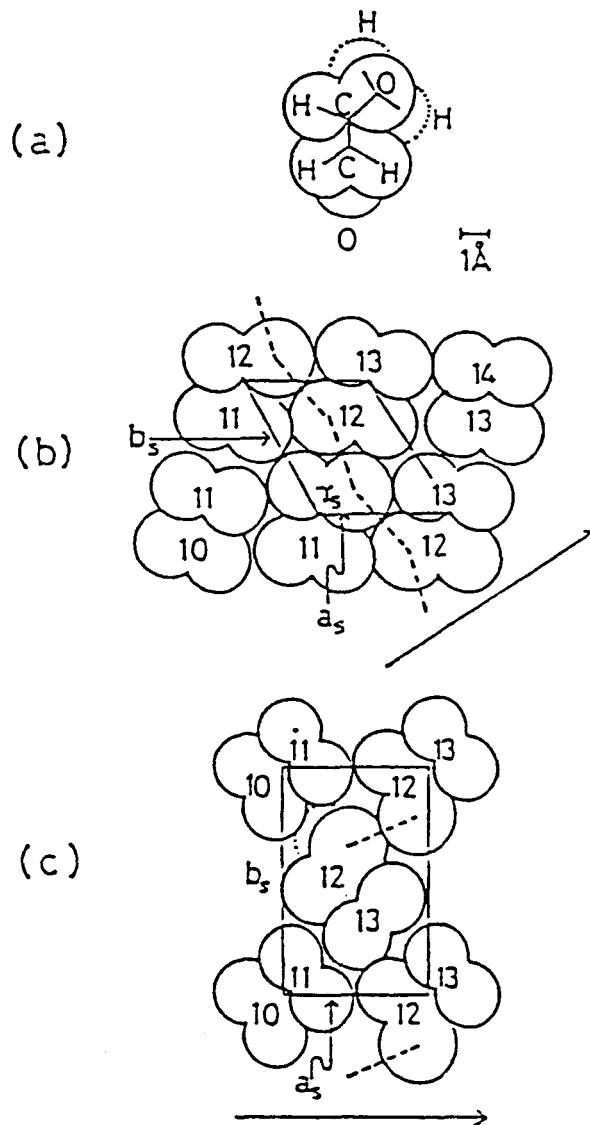
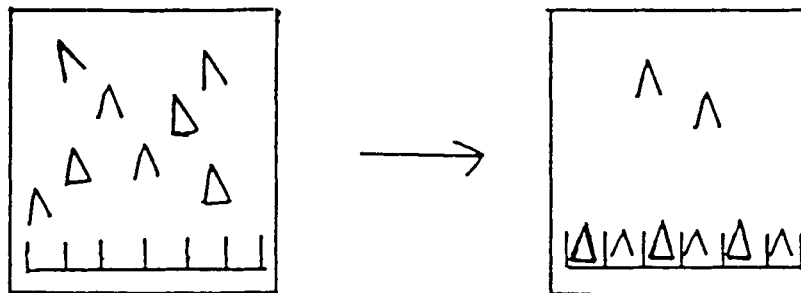


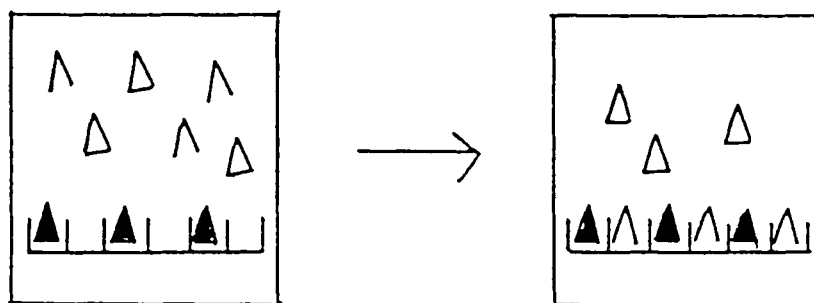
FIGURE 28 Molecular models for monolayers of chiral and racemic 12-hydrooctadecanoic acid (12HOA).⁵⁶ (a) A projection of a straight chain molecule of (R)-12HOA on a plane perpendicular to the chain axis; (b) proposed packing model for (R)-12HOA in the condensed monolayer state; (c) proposed packing model for the racemic 12HOA in the condensed monolayer state. The $a_s b_s$ planes are in the sheet of the paper, to which the molecular axis is perpendicular for racemic 12HOA, but not for (R)-12HOA. The direction of the water surface is denoted by an arrow.

(ii) The optical resolution of a racemic mixture is performed by forming a diastereomeric pair on a clay surface. In this method, an ion-exchange adduct of a clay and an optically active chelate is used as a resolving agent. If the formation of a diastereomeric pair takes place stereoselectively, either one of an enantiomer of the racemic mixture would be removed from a solution by being adsorbed on such a clay-chelate adduct (Fig 29b).

(a) Improvement of Optical Purity



(b) Optical Resolution



(c) Asymmetric Synthesis

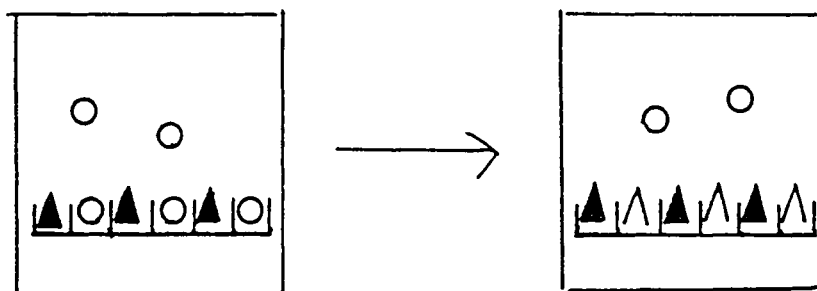


FIGURE 29 Three possible ways for application of racemic adsorption of metal chelates by a clay: (i) Improvement of optical purity of a partially resolved solution. Δ and Λ denote racemic isomers. (ii) Optical resolution of racemic mixtures by use of a clay-chelate adduct as a resolving agent. \blacktriangle denotes a preadsorbed optically active chelate, and Δ and Λ are added racemic chelates. (iii) Asymmetric synthesis by use of a clay-chelate adduct as a chiral adsorbent. \circ denotes a prochiral reactant and Λ a chiral product.

(iii) The asymmetric synthesis is accomplished by utilizing an ion-exchange adduct of a clay and an optically active chelate as a chiral adsorbent. In this method, after a prochiral molecule is adsorbed by such an adduct, it is chemically converted to an optically active molecule. Here the steric interactions of a prochiral reactant with a preadsorbed optically active chelate are expected to lead to the preferential formation of either one enantiomer of the product molecule (Fig. 29c).

An application of (i) has already been described in the preceding section on a solution of partially resolved $[\text{Fe}(\text{phen})_3]^{2+}$.^{44,46} This method is regarded as an extension of the method improving the optical purity of a solution by racemic crystallization. By condensing a partially resolved solution, an excessive racemic mixture is eliminated in the form of racemic crystal. Since a greater part of optically active compounds have a tendency to form a racemic crystal rather than a conglomerate, the method is widely used to improve the purity of an optically active molecule.⁵⁸ An advantage in the usage of a clay as an adsorbent might lie in the fact that it is applicable for a very dilute solution of a resolved species. As having been shown in Figure 30, for example, $[\text{Fe}(\text{phen})_3]^{2+}$ is purified from an aqueous solution at the concentration as low as 10^{-5} M.

The present section is concerned with the method (ii). There have been a number of chiral adsorbents devised for the purpose of resolving racemic mixtures.⁵⁹ However, no report has been found to use an ion-exchange adduct of a clay and a chelate for such a purpose. The method is therefore of practical interest as providing a new type of resolving agent.

The racemic mixtures of $[\text{Fe}(\text{phen})_3]^{2+}$, $[\text{Fe}(\text{bpy})_3]^{2+}$, $[\text{Ru}(\text{phen})_3]^{2+}$, $[\text{Ru}(\text{bpy})_3]^{2+}$ and $[\text{Co}(\text{phenylalaninato})(\text{en})_2]^{2+}$ are added to an aqueous suspension of Λ -

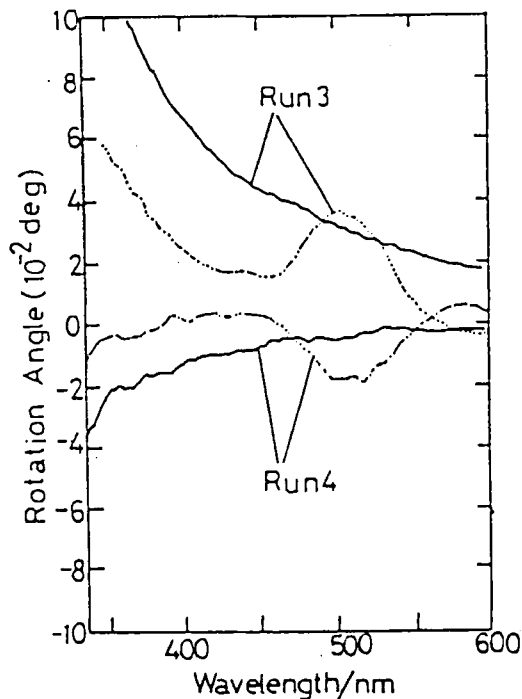


FIGURE 30 ORD spectra of runs 3 and 4 in Table XIII.³⁷ The solid and dotted curves are for the solutions before and after filtering through a membrane filter, respectively.

$[\text{Ni}(\text{phen})_3]^{2+}$ montmorillonite.⁴⁰ The mixture is passed through a membrane filter and the filtrate is analyzed by the UV and optical rotatory dispersion (ORD) spectroscopies. The results are given in Figure 30 and Table XIII. According to the results, when racemic $[\text{Fe}(\text{phen})_3]^{2+}$ is added to Λ - $[\text{Ni}(\text{phen})_3]^{2+}$ montmorillonite, the filtrate contains Λ - $[\text{Fe}(\text{phen})_3]^{2+}$ as an excess enantiomer. Thus racemic $[\text{Fe}(\text{phen})_3]^{2+}$ is successfully resolved because Δ - $[\text{Fe}(\text{phen})_3]^{2+}$ is eliminated from a solution, forming a diastereomeric pair with Λ - $[\text{Ni}(\text{phen})_3]^{2+}$ on a clay. $[\text{Fe}(\text{bpy})_3]^{2+}$ is resolved in the same mechanism. $[\text{Ru}(\text{phen})_3]^{2+}$ and $[\text{Ru}(\text{bpy})_3]^{2+}$ are not resolved in the same procedure. The previous results on the electric dichroism measurements (Fig. 20) have shown that $[\text{Ru}(\text{phen})_3]^{2+}$ montmorillonite discriminates the chirality of an $[\text{Ni}(\text{phen})_3]^{2+}$ molecule effectively. The failure of resolution in the case of $[\text{Ru}(\text{phen})_3]^{2+}$ seems to contradict with those results. The answer to this peculiarity is uncertain yet. One possibility is that a very condensed condition is realized when a solution is passed through a membrane filter. Under this condition, both enantiomers of $[\text{Ru}(\text{phen})_3]^{2+}$ might be adsorbed with no stereoselectivity. $[\text{Co}(\text{L-phenylalanine})_2]^{2+}$ is not resolved at all probably because this molecule is too small to interact with preadsorbed Λ - $[\text{Ni}(\text{phen})_3]^{2+}$ on a clay surface.

$[\text{Fe}(\text{CN})_2(\text{phen})_2]$ is also resolved by use of colloiddally dispersed Λ - $[\text{Ni}(\text{phen})_3]^{2+}$ montmorillonite (Table XIV).⁵³ In this case, a methanol-water mixture is used to achieve the appropriate solubility of racemic $[\text{Fe}(\text{CN})_2(\text{phen})_2]$. Although $[\text{Fe}(\text{CN})_2(\text{phen})_2]$ possesses only two bulky ligands in contrast with Λ - $[\text{Ni}(\text{phen})_3]^{2+}$, the molecule interacts with Λ - $[\text{Ni}(\text{phen})_3]^{2+}$ stereoselectively.

It is a natural consequence to extend the above results to the column chromatographic resolution of racemic mixtures on an ion-exchange adduct of a clay and a chelate. Such an adduct is prepared simply by mixing an optically active chelate to a colloidal suspension of a clay. For example, one CEC-equivalent amount of Δ - $[\text{Ni}(\text{phen})_3]\text{Cl}_2$ is added to a suspension of sodium montmorillonite.^{60,61} Δ - $[\text{Ni}(\text{phen})_3]^{2+}$ is exchanged into a clay instantly and the resultant adduct of Δ - $[\text{Ni}(\text{phen})_3]^{2+}$ montmorillonite is precipitated as a pink gel. After filtering the gel, the precipitate is dried and ground into a powder of about 100–200 mesh. The material is poured into a glass filter to a thickness of about 1 cm. It should be mentioned that an adduct as prepared in this way is no longer colloidal in water and stable enough to be eluted with water solvent at an appropriate flow rate of 0.1–1 mL per minute. In this respect, sodium montmorillonite becomes a more appropriate substance for a packing material in chromatography by exchanging sodium ions with $[\text{Ni}(\text{phen})_3]^{2+}$ complexes. Probably the intercalated $[\text{Ni}(\text{phen})_3]^{2+}$ plays a bridging agent in connecting the upper and lower layers of a clay. This results in the reduction of swelling capability in water and in the increase of a particle size. Similar effects are observed by exchanging other $[\text{M}(\text{phen})_3]^{2+}$ ions and $[\text{M}(\text{bpy})_3]^{2+}$ ions in sodium montmorillonite.

$[\text{Co}(\text{acac})_3]$ is tried to be resolved on the above column.⁶⁰ Since $[\text{Co}(\text{acac})_3]$ is neutral and possesses no functional groups on its periphery, it has been resisting against the resolution by a simple resolving agent such as tartrate anion and cinchonium cation.⁶² It is expected that $[\text{Co}(\text{acac})_3]$ stacks stereoselectively with preadsorbed $[\text{Ni}(\text{phen})_3]^{2+}$ on a clay surface just in the similar way as $[\text{M}(\text{phen})_3]^{2+}$ and other bulky chelates do. Figure 21 shows the chromatogram when racemic $[\text{Co}(\text{acac})_3]$ is placed on the column and eluted with water and succeedingly with methanol. On eluting $[\text{Co}(\text{acac})_3]$ with water, about half of mounted $[\text{Co}(\text{acac})_3]$ is separated from the column. No $[\text{Ni}(\text{phen})_3]^{2+}$ is removed from the column, indicating that $[\text{Ni}(\text{phen})_3]^{2+}$ is bound to a clay by much stronger force than $[\text{Co}(\text{acac})_3]$. In this sense, preadsorbed $[\text{Ni}(\text{phen})_3]^{2+}$ is regarded as a part of a stationary phase not as a simple ion-exchange species. The rest of $[\text{Co}(\text{acac})_3]$ is recovered by flowing

TABLE XIII
Effects of adsorption on clay of a solution containing two kinds of metal chelates.^a

run	solution I ^a	solution II ^b
1	$\frac{1}{2}(+) [Ni(phen)_3]^{2+} \cdot 2ClO_4^- (2.7 \times 10^{-4} M)$	$(+) [Ni(phen)_3]^{2+} (1.4 \times 10^{-4} M)$
2	$\frac{1}{2}(+) [Fe(phen)_3]^{2+} + \frac{1}{2}(-) [Fe(phen)_3]^{2+} \cdot 2ClO_4^- (2.2 \times 10^{-4} M)$	$(+) [Fe(phen)_3]^{2+} (0.6 \times 10^{-4} M)$
3	$\frac{1}{2}(+) [Ni(phen)_3]^{2+} \cdot 2ClO_4^- + \frac{1}{2}(-) [Fe(phen)_3]^{2+} \cdot 2ClO_4^- (2.2 \times 10^{-4} M)$	$(-) [Ni(phen)_3]^{2+} (0.2 \times 10^{-4} M)$
4	$\frac{1}{2}(+) [Ni(phen)_3]^{2+} \cdot 2ClO_4^- + \frac{1}{2}(-) [Fe(bpy)_3]^{2+} \cdot 2ClO_4^- (2.1 \times 10^{-4} M)$	$(-) [Fe(phen)_3]^{2+} (0.5 \times 10^{-4} M)$
5	$\frac{1}{2}(+) [Fe(phen)_3]^{2+} + \frac{1}{2}(-) [Fe(bpy)_3]^{2+} \cdot 2ClO_4^- (1.8 \times 10^{-4} M)$	$(+) [Ni(phen)_3]^{2+} (0.5 \times 10^{-4} M)$
6	$\frac{1}{2}(+) [Ni(phen)_3]^{2+} \cdot 2ClO_4^- + \frac{1}{2}(-) [Ru(phen)_3]^{2+} \cdot 2ClO_4^- (1.9 \times 10^{-4} M)$	$(+) [Fe(bpy)_3]^{2+} (0.8 \times 10^{-4} M)$
	$\frac{1}{2}(+) [Ni(phen)_3]^{2+} \cdot 2ClO_4^- (1.8 \times 10^{-4} M)$	$(-) [Fe(bpy)_3]^{2+} (0.5 \times 10^{-4} M)$
	$\frac{1}{2}(+) [Co(en)_2(L-palan)]^{2+} + \frac{1}{2}(-) [Co(en)_2(L-palan)]^{2+} \cdot 2I^- (2.0 \times 10^{-4} M)^c$	$(+) [Fe(bpy)_3]^{2+} (0.1 \times 10^{-4} M)$
		$(+) [Ni(phen)_3]^{2+} (0.4 \times 10^{-4} M)$
		$(+) [Ru(phen)_3]^{2+} (0.4 \times 10^{-4} M)$
		$(-) [Ni(phen)_3]^{2+} (0.2 \times 10^{-4} M)$
		$(+) [Co(en)_2(L-palan)]^{2+} (0.8 \times 10^{-4} M)$
		$(-) [Co(en)_2(L-palan)]^{2+} (0.8 \times 10^{-4} M)$

^a An initial solution containing two kinds of metal chelates. ^b The same solution filtered through a membrane filter after $(2-3) \times 10^{-6} M Na^+ M^-$ was added. ^c L-palan = L-phenylalanine; en = ethylenediamine.

TABLE XIV
Optical resolution of racemic $[\text{Fe}(\text{CN})_2(\text{phen})_2]$ at the expense of $\Lambda\text{-}[\text{Ni}(\text{phen})_3](\text{ClO}_4)_2$ ^{a,53}

run	initial soln		final soln ^b		
	$[\text{Fe}(\text{CN})_2(\text{phen})_2]/10^{-4} \text{ M}$	$\Lambda\text{-}[\text{Ni}(\text{phen})_3]^{2+}/10^{-4} \text{ M}$	$\Lambda\text{-}[\text{Fe}(\text{CN})_2(\text{phen})_3]/10^{-4} \text{ M}$	$\Delta\text{-}[\text{Fe}(\text{CN})_2(\text{phen})_2]/10^{-4} \text{ M}$	$\Lambda\text{-}[\text{Ni}(\text{phen})_3]^{2+}/10^{-4} \text{ M}$
1	1.8	1.3	0.85	0.35	0.80
2	1.8	1.0	0.90	0.40	0.50
3	1.8	0.70	0.90	0.40	0.25
4	1.8	0.40	0.80	0.50	0.0
5 ^c	7.0	10.0	0.50	0.50	0.0

^aThe solvent contained 10–30% methanol for all runs. ^bThe concentrations in a supernatant when the initial solution was centrifuged after addition of $1.0 \times 10^{-4} \text{ M Na}^+ \text{M}^-$ to it. ^cA solid of $\Delta\text{-}[\text{Ni}(\text{phen})_3]^{2+}$ -montmorillonite was added to a $[\text{Fe}(\text{CN})_2(\text{phen})_2]$ solution.

methanol. Methanol is used as it is a better solvent for $[\text{Co}(\text{acac})_3]$. By measuring the ORD spectra of collected fractions, it is seen that the water eluate contains Λ - $[\text{Co}(\text{acac})_3]$ and the methanol eluate Δ - $[\text{Co}(\text{acac})_3]$ as excess enantiomers. The optical purity is attained to be 36% and 32% for water and methanol eluates, respectively. The optical purity is improved up to 72% by passing the water eluate one more time through the same column. Table XV compares the chromatographic results among various kinds of adsorbents. It is concluded that the present clay-chelate adduct is outstanding in its high resolving efficiency in spite of its short length of a used column. Although the column does not attain the complete resolution of $[\text{Co}(\text{acac})_3]$, the peaks of resolved enantiomers are separated very much from each other (Fig. 31). It is therefore suspected that the mechanism of chirality recognition

TABLE XV
Comparison of resolution efficiency among various adsorbents

packing material	column length	optical purity ^a	Ref.
D-lactose	230 cm	9 %	62
sephadex exchanging Δ - $[\text{Ni}(\text{phen})_3]^{2+}$	80 cm	19 %	63
Δ - $[\text{Ni}(\text{phen})_3]^{2+}$ montmorillonite	2.5 cm	36 %	60

^aOptical purity of a fraction containing a less retaining enantiomer.

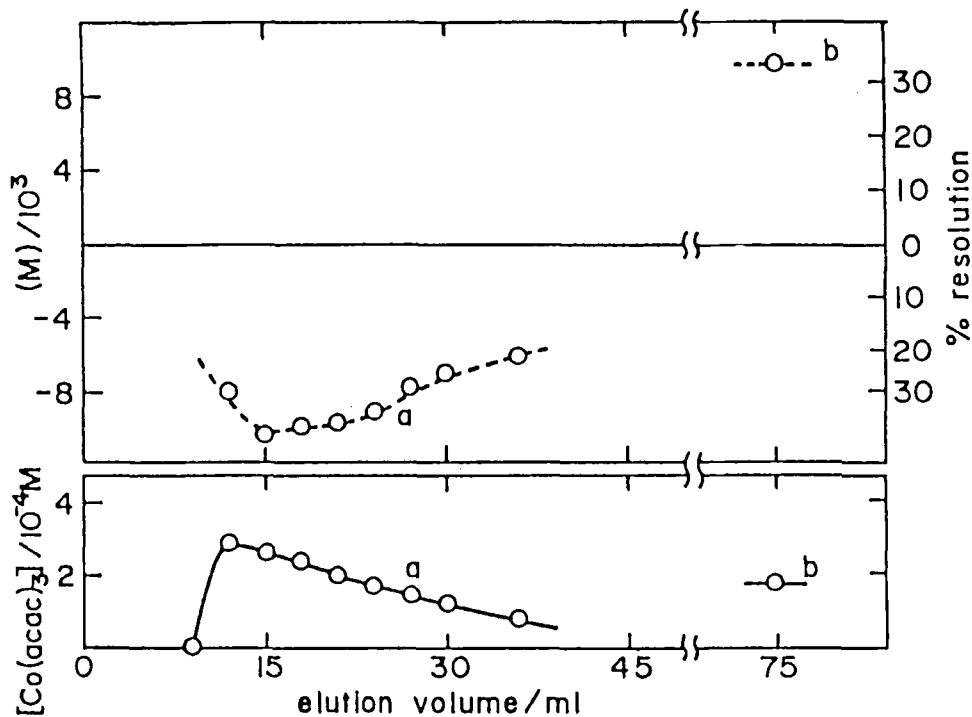


FIGURE 31 Elution curve of $[\text{Co}(\text{acac})_3]$ placed on a 2.5-cm-long column of Δ - $[\text{Ni}(\text{phen})_3]^{2+}$ montmorillonite.⁶⁰ Curve a and plot b are eluted with water and methanol, respectively. Solid (lower) and dotted (upper) curves are the concentration and the molecular rotation of $[\text{Co}(\text{acac})_3]$ at 530 nm, respectively.

is strictly stereoselective on the clay column and that some other factors might lower the total optical purity of a collected fraction. From the chromatogram, the long tailing of the resolved peak is concluded to be a main cause for the apparently low optical purity. It is also noted that the clay adduct is too adsorbing Δ -[Co(acac)₃], a more retained enantiomer in the present case. Most of Δ -[Co(acac)₃] is removed only with methanol. It is presumed that these effects are caused by the layer structures of the clay-chelate adduct. The enantiomers might penetrate the interlamellar space of an adduct so that they are not easily removed by a poor solvent.

Another point of interest concerning the results in Figure 31 is the mechanism of resolution of [Co(acac)₃] on the present column. Δ -[Co(acac)₃] is eluted after Λ -[Co(acac)₃], implying that the former is more strongly adsorbed by the column than the latter. This order of the affinity is opposite to the previously observed results on the resolution of [Fe(phen)₃]²⁺ or [Fe(bpy)₃]²⁺ by Δ -[Ni(phen)₃]²⁺ montmorillonite (Table XIII), since the Λ -enantiomers of these chelates show higher affinity towards the adduct. By use of the molecular stacking model, it is sought what type of stacking is possible when the enantiomer of [Co(acac)₃] approaches the surface of Δ -[Ni(phen)₃]²⁺ montmorillonite. Δ -[Co(acac)₃] is stacked closely with Δ -[Ni(phen)₃]²⁺ on a clay when the former is placed over the head of the latter with their threefold axes in the same vertical line (Fig. 32a). Under such a conformation, the three methyl groups in acetylacetonato ligands in [Co(acac)₃] are located above the phenanthroline ligands in [Ni(phen)₃]²⁺. This type of stacking (denoted as "enantiomeric" stacking) is different from the previous pseudo-racemic stacking between two opposite enantiomers of tris(phenanthroline) complexes. Δ -[Co(acac)₃] preferring the position as in Figure 32a would not penetrate the interlamellar space

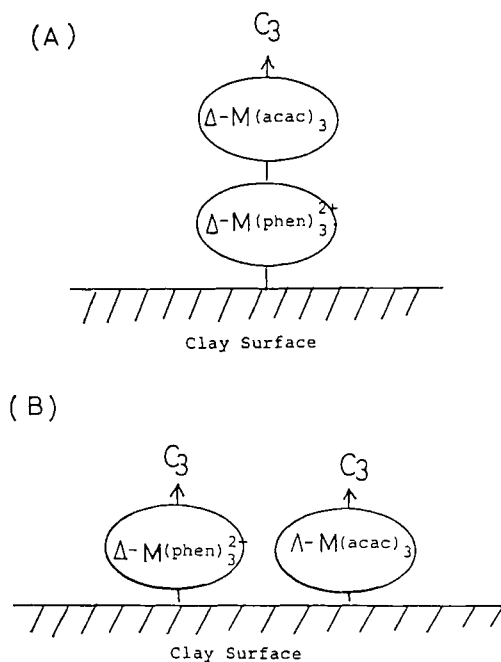


FIGURE 32 Possible modes of stacking between the enantiomers of [M(phen)₃]²⁺ and [M(acac)₃]: (a) over-the-head stacking (or enantiomeric stacking) between Δ -[M(phen)₃]²⁺ and Δ -[M(acac)₃] and (b) side-by-side stacking (or racemic stacking) between Δ -[M(phen)₃]²⁺ and Λ -[M(acac)₃].⁶⁶

unless the layers of the clay adduct expand in water solvent. Such expansion of the basal spacing of the column material, however, is not detected on the adsorption of $[\text{Co}(\text{acac})_3]$.⁶¹ Therefore the binding as in Figure 32a would be possible only on an external surface where no spatial restriction is imposed by the upper layer. As for Λ - $[\text{Co}(\text{acac})_3]$, the enantiomer is expected to prefer the position by the side of Δ - $[\text{Ni}(\text{phen})_3]^{2+}$ as shown in Figure 32b. This conformation is the same as the racemic or pseudo-racemic stacking of $[\text{M}(\text{phen})_3]^{2+}$ enantiomers. The reason that Δ - $[\text{Co}(\text{acac})_3]$ in Figure 32a is more retained than Λ - $[\text{Co}(\text{acac})_3]$ in Figure 32b is considered as below: when adsorption of $[\text{Co}(\text{acac})_3]$ is studied by colloiddally dispersed sodium montmorillonite, the chelate shows no affinity toward a clay.⁶⁰ The fact seems reasonable since $[\text{Co}(\text{acac})_3]$ is unlikely to be attracted to montmorillonite by electrostatic or ion-dipole forces. This inertness towards a clay might donate $[\text{Co}(\text{acac})_3]$ the tendency that the chelate is located far apart from a clay surface in contrast to $[\text{M}(\text{phen})_3]^{2+}$. $[\text{M}(\text{phen})_3]^{2+}$ is adsorbed by a clay as close to its surface as possible (Figure 19a). Based on this, the enantiomeric stacking as in Figure 32a is expected to be more stabilized than the racemic or pseudo-racemic (more shortly racemic) stacking as in Figure 32b.

From the statistical viewpoint, it will depend on the coverage of a preadsorbed chelate which of stacking mode is preferred between Figures 32a and b. At the low coverage, preadsorbed Δ - $[\text{Ni}(\text{phen})_3]^{2+}$ is mostly present as an isolated species on a layer. Under such circumstances, the area surrounding Δ - $[\text{Ni}(\text{phen})_3]^{2+}$ is all available to the racemic binding of Λ - $[\text{Co}(\text{acac})_3]$ as in Figure 32b. At high coverage, preadsorbed Δ - $[\text{Ni}(\text{phen})_3]^{2+}$ forms an aggregate on a clay surface so that there is little room left for the adsorption of Λ - $[\text{Co}(\text{acac})_3]$. Under these circumstances, however, Δ - $[\text{Co}(\text{acac})_3]$ would be adsorbed over the head of Δ - $[\text{Ni}(\text{phen})_3]^{2+}$ on an external surface with no difficulty (enantiomeric binding). Prompted by the above expectation, the adsorption of racemic $[\text{Co}(\text{acac})_3]$ by Δ - $[\text{Ni}(\text{phen})_3]^{2+}$ -exchanged montmorillonite is studied at various ratios of $[\text{Ni-chelate}]$ to $[\text{clay}]$ (Table XVI).⁶⁰ At low exchanging level, Λ - $[\text{Co}(\text{acac})_3]$ is more strongly adsorbed by a clay, while, at high exchanging level or as the whole sites are occupied by Δ - $[\text{Ni}(\text{phen})_3]^{2+}$, Δ - $[\text{Co}(\text{acac})_3]$ is more strongly adsorbed by a clay. The results agree with the above statistical consideration.

In order to elucidate the effects of the structure of a resolved chelate on the selectivity between the racemic (Fig. 32a) and enantiomeric (Fig. 32b) stackings, bis(acetylacetonato) (amino acidato) cobalt(III) chelate is resolved on a column of Δ - $[\text{Ni}(\text{phen})_3]^{2+}$ montmorillonite.⁶⁴ The structure of a resolved chelate is varied by

TABLE XVI
Adsorption of $[\text{Co}(\text{acac})_3]$ on sodium montmorillonite ($\text{Na}^+ \text{M}^-$) in the presence of Δ - $[\text{Ni}(\text{phen})_3](\text{ClO}_4)_2$ 60

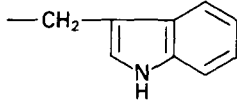
Run	Δ - $[\text{Ni}(\text{phen})_3]^{2+} / 10^{-4} \text{ M}^a$	adsorbed $[\text{Co}(\text{acac})_3] / 10^{-4} \text{ M}^b$	excessive isomer in the solvent/ 10^{-5} M^c
1	0.0	less than 0.2	none
2	1.4	0.5	0.4 (Δ)
3	2.9	0.9	0.8 (Δ)
4	4.0	2.1	1.5 (Δ)
5	5.8	2.5	8.0 (Λ)

^aThe initial amount of Δ - $[\text{Ni}(\text{phen})_3](\text{ClO}_4)_2$, which was present in a solution of $1.42 \times 10^{-3} \text{ M}$ $[\text{Co}(\text{acac})_3]$ and $1.1 \times 10^{-3} \text{ M}$ $\text{Na}^+ \text{M}^-$.

^bThe adsorbed amount of $[\text{Co}(\text{acac})_3]$ on a clay, which was obtained by centrifuging the solution.

^cThe excessive optical isomer of $[\text{Co}(\text{acac})_3]$, which was present in a supernatant solution.

TABLE XVII
Resolution of $[\text{Co}(\text{acac})_2(\text{L})]$ on a $\Delta\text{-}[\text{Ni}(\text{phen})_3]^{2+}$ montmorillonite column⁶⁴



(A)

L	Side-chain structure	Preferred enantiomer ^a	$[M]_{500}$
GlyO	-H	Λ	-11 000
AlaO	-CH ₃	Λ	-5 300
ValO ^b	-CH(CH ₃) ₂	Δ	+1 100
LeuO ^c	-CH ₂ CH(CH ₃) ₂	Δ	+600
SerO ^d	-CH ₂ OH	Λ	-3 100
ThreO ^e	-CH(OH)CH ₃	Δ	+5 300
ProO	-CH ₂ CH ₂ CH ₂ -	Λ	-940
MetO	-CH ₂ CH ₂ SCH ₃	Δ	+7 300
PheO	-CH ₂ Ph	Δ	+4 900
TrpO	(A)	Λ	-5 900
acac		Δ	+24 000

^a The configuration of an enantiomer bound to the column more firmly than its optical antipode. ^b Valinate. ^c Leucinate. ^d Serinate. ^e Threoninate.

coordinating various kinds of amino acids. Table XVII lists the chromatographic results when the chelate is eluted with water or methanol-water mixture. All of the investigated ten chelates are resolved at least partially on the column. The absolute configuration of a resolved chelate is determined from their ORD spectra.⁶⁵ It is noteworthy how delicately the configuration of a preferred enantiomer is dependent on the side chain structure of a coordinated amino acid. Some rules are derived from the results in the table.

(i) When an amino acid has a small side chain, the Λ -isomer shows stronger affinity toward the column, that is, the adsorption is racemic with respect to preadsorbed $[\text{Ni}(\text{phen})_3]^{2+}$.

(ii) When an amino acid has a long alkyl chain, the Δ -isomer shows stronger affinity toward the column, or the adsorption is enantiomeric with respect to preadsorbed $[\text{Ni}(\text{phen})_3]^{2+}$.

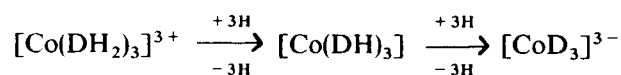
(iii) The exceptions for the above rules are the chelates coordinating proline and tryptophan. These chelates are adsorbed racemically although they have a bulky side chain.

Rule (i) is understandable if one admits that the present type of a chelate has an intrinsic affinity towards a silicate sheet of a clay due to the interaction of a coordinated amino acid with a clay. Thus it will prefer the racemic stacking because the stacking allows the chelate to be close to a clay surface. Rule (ii) is rationalized in terms of the situations that a chelate with a bulky side chain is not racemically adsorbed because it is not accommodated in the narrow side space of preadsorbed $[\text{Ni}(\text{phen})_3]^{2+}$. It will prefer the wider space over the head of $[\text{Ni}(\text{phen})_3]^{2+}$ on an external surface for the enantiomeric adsorption. Since tryptophan is itself adsorbed most strongly

among the amino acids in Table XVII, the chelate containing tryptophan ligand would prefer the racemic stacking in spite of its bulky side chain. The coordinated tryptophan would be deformed in such a narrow space. The reason for exceptional behaviour of the prolinato chelate is not clear yet.

[Co(acac)₃], [Cr(acac)₃], [Cr(3-nitroacetylacetonato)₃] and [Rh(acac)₃] are resolved on a column of Λ-[Ru(phen)₃]²⁺ montmorillonite (Table XVIII).^{66,67} [Ru(phen)₃]²⁺ montmorillonite is more suitable for a column material than [Ni(phen)₃]²⁺ montmorillonite since [Ru(phen)₃]²⁺ does not racemize at all. [Ni(phen)₃]²⁺ racemizes gradually when it is adsorbed by a clay. According to Table XVIII, [Co(acac)₃], which has shown enantiomeric adsorption towards [Ni(phen)₃]²⁺ montmorillonite, is adsorbed racemically on [Ru(phen)₃]²⁺ montmorillonite when it is eluted with water. Probably the vacant space for racemic adsorption is larger for [Ru(phen)₃]²⁺-exchanged clay than [Ni(phen)₃]²⁺-exchanged clay because the former chelate has an ionic radius about 0.1 Å larger than the latter.⁶⁸ Notably, in case that the same chelate is eluted with 1:2 (v/v) water-methanol, the chirality preference is reversed or it shows the enantiomeric adsorption. [Cr(acac)₃] and [Rh(acac)₃] show the enantiomeric adsorption when they are eluted with water-methanol mixtures. Observed solvent effects on the chirality selectivity are not clarified yet. However, the effects might be related to the swelling capability of the clay material under the above eluting solvents. That is, in water, the clay adduct is able to swell enough to allow the penetration of a resolved chelate in the interlamellar region. In that region, racemic stacking is more probable than enantiomeric one so that the chelate would show racemic adsorption in water. In methanol or other organic solvents, the clay adduct does not swell very much so that only an external surface is available for adsorption. In such a region, both racemic and enantiomeric adsorptions are possible and the latter mode is preferred due to the low affinity of acetylacetonato chelates towards a clay surface.

Tris(dimethylglyoximato)cobalt(III) ([Co(DH)₃]) carries no charge and possesses no functional groups that are possible to interact with any resolving agent. Thus the chelate just like [Co(acac)₃] is difficult to be resolved with ordinary ionic resolving reagents. There has been no report on the resolution of that compound. [Co(DH)₃] is placed on a column of Λ-[Ru(phen)₃]²⁺ montmorillonite and eluted with water.⁶⁷ The chelate is successfully resolved and the UV and CD spectra of the more retained enantiomer are shown in Figure 33. By applying the exciton-splitting theory to the positive and negative peaks below 300 nm,⁶⁹ the enantiomer is concluded to have Λ-configuration. Thus [Co(DH)₃] shows the enantiomeric adsorption. The UV and CD spectra of resolved [Co(DH)₃] are both affected by the pH of a solution. This is ascribed to the following protonation equilibria:



in which DH₂ and D denote the neutral and dianion forms of dimethylglyoxime, respectively. [Co(DH)₃] is not found to racemize for 200 hours at room temperature. Thus due to the above protonation equilibria, [Co(DH)₃] could function as an acid-base catalyst with stereoselectivity.

Anionic complexes are also resolved on the present column of a clay-chelate adduct. Tris(1-nitroso-2-naphthol-3,6-disulphonato)cobalt(III) ([Co(nitroso-R)₃]⁶⁻) is a tris(chelated) complex with six negative charges.⁷⁰ The chelate is placed on the Λ-[Ru(phen)₃]²⁺ montmorillonite column and eluted with water.⁶⁷ The CD spectrum of a collected fraction exhibits very complex changes as shown in Figure 34. A

TABLE XVIII
Chromatographic results for $[\text{M}(\text{acac})_3]$ on a Λ -[Ru(phen) $_3$] $^{2+}$ -montmorillonite column⁶⁷

Chelate amount (mole)	Eluent	Volume of fraction (ml)	Concentration (10^{-3} M)	Molecular rotation and wavelength (nm)	Resolution (%) and enantiomer in excess	Column size (cm \times cm O.D.)
$[\text{Co}(\text{acac})_3]$ ($8 \cdot 10^{-6}$)	Water	2	0.8	-19,000 (480)	61 (A)	0.5 \times 1
		2	0.8	-13,000	43 (A)	
		2	0.5	+2000	7 (A)	
		2	0.2	+18,000	60 (A)	
		2	0.1	+20,000	67 (A)	
$[\text{Co}(\text{acac})_3]$ ($6 \cdot 10^{-5}$)	Methanol	2	0.7	+21,000	70 (A)	1 \times 1
		2	1.3	+200 (480)	7 (A)	
		2	7.8	+300	1 (A)	
$[\text{Cr}(\text{acac})_3]$ ($1.2 \cdot 10^{-5}$)	Water-methanol (2:1)	2	1.0	0	0	0.5 \times 1
		2	0.7	-3000	10 (A)	
		2	1.7	-2800 (570)	20 (A)*	
		2	2.3	+800	6 (A)	
		2	0.5	+7000	50 (A)	
$[\text{Cr}(\text{acac})_3]$ ($2.2 \cdot 10^{-5}$)	95% Methanol	2	8.0	-300 (570)	2 (A)*	0.5 \times 1
		2	2.3	+800	6 (A)	
$[\text{Cr}(3\text{-NO}_2\text{-acac})_3]$ ** ($5.6 \cdot 10^{-5}$)	Chloroform	2	4.3	+320 (570)	(A)	1 \times 1
		2	4.3	+50	(A)	
		2	8.6	0	(A)	
		2	10.00	-50	(A)	
		2	1.4	-710	(A)	
$[\text{Rh}(\text{acac})_3]$ ($8.0 \cdot 10^{-6}$)	Water-methanol (2:1)	1	0.8	+5900 (433)	50 (A)***	2 \times 1.2
		1	11.5	+4000	33 (A)	
		2	7.3	+2600	22 (A)	
		2	4.1	-2900	24 (A)	
		6	2.7	-6300	52 (A)	
		4	1.6	-10,000	83 (A)	

* Based on $[\text{M}]_{570} = -14,000$ [Δ -Cr(acac) $_3$] and $+14,000$ [Λ -Cr(acac) $_3$]. These values were obtained by comparing the ORD and CD spectra of the same solution.

** 3-NO $_2$ -acac denotes 3-nitroacetylacetonate.

*** Based on $[\text{M}]_{433} = +11,800$ [Δ -Rh(acac) $_3$] and $-11,800$ [Λ -Rh(acac) $_3$]. The values were estimated as in footnote.

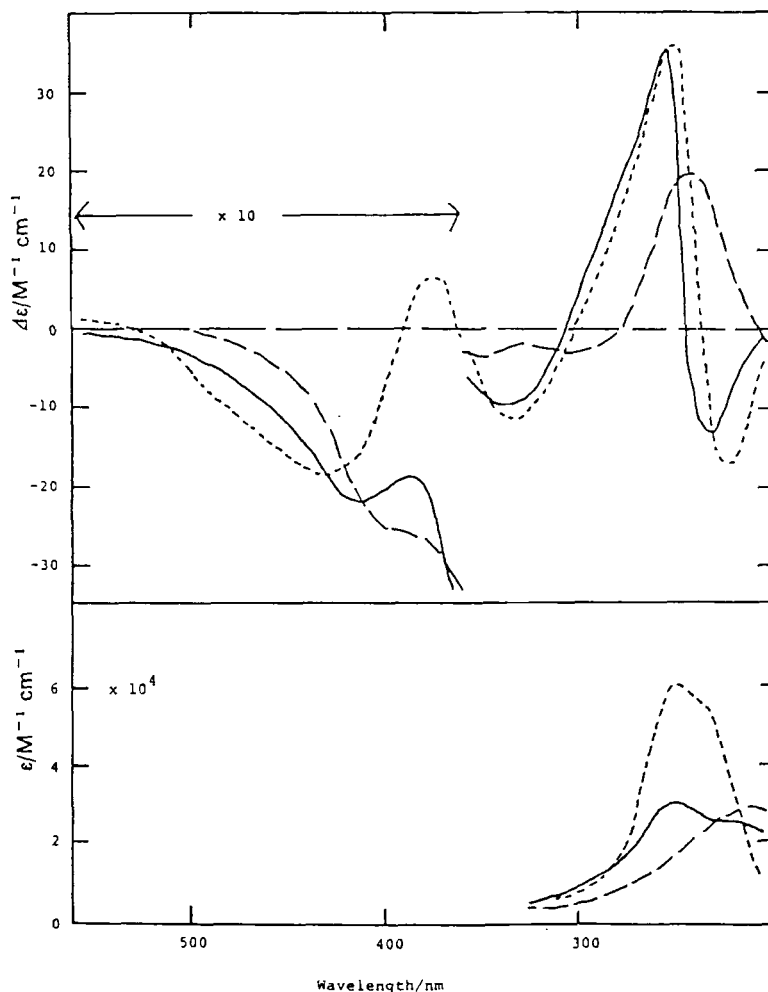


FIGURE 33 CD (upper) and electronic absorption (lower) spectra of partially resolved tris(dimethylglyoximate)cobalt(III): (-----) neutral pH, (.....) 0.1 M NaOH, and (- · - · -) 0.1 M HClO₄.⁶⁷

nitroso-R ligand is coordinated to a cobalt(III) ion through one oxygen and one nitrogen atoms. There exist two geometrical isomers named *fac*- and *mer*-isomers since the chelate belongs to a $M(a-b)_3$ type complex. The change of the CD spectra is therefore interpreted by the assumption that the chelate is resolved to two types of optical isomers. As a result, the eluant in Figure 34 contains four kinds of isomers. Although the pure CD spectra of these isomers are not determined, it is concluded from the spectral changes that the more retained isomers are always of Δ -configuration. In deducing this conclusion, the exciton-splitting theory is applied to the two peaks in the wavelength range of 300–500 nm.⁶⁹ The resolved isomers racemize at a unimolecular rate constant of $1.9 \times 10^{-5} \text{ s}^{-1}$ at 20°C and pH = 5. As another anionic chelate, tris(catecholate)arsenate(V) ($[\text{As}(\text{cat})_3]^-$) is also resolved on the same column.⁶⁷ The more retaining enantiomer is found to be Λ - $[\text{As}(\text{cat})_3]^-$ in contrast to the case of $[\text{Co}(\text{nitroso-R})_3]^{6-}$. As is mentioned in Section 2, an anion-exchange site of a clay is thought to exist at the edge of its microcrystalline.^{11,12} If the aionic complexes

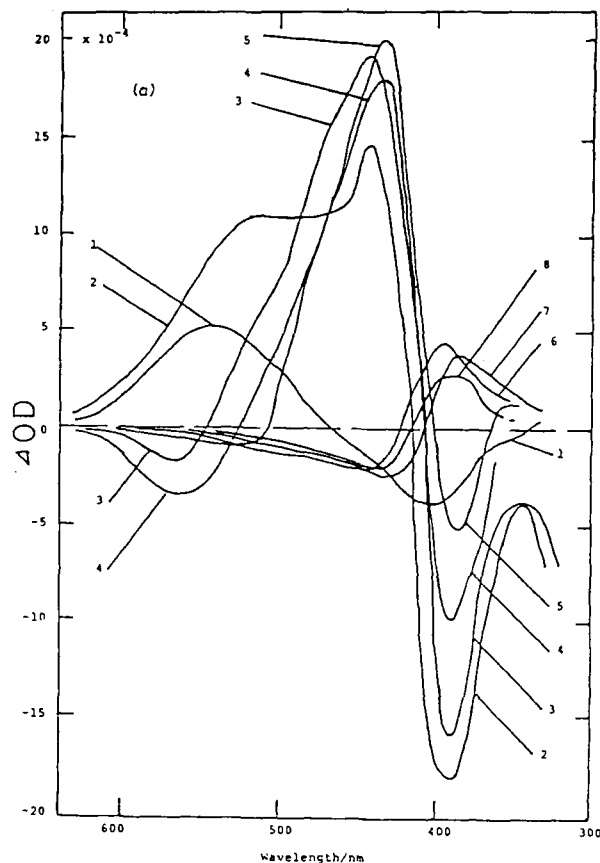


FIGURE 34 CD spectra of the fractions in eluting tris(1-nitroso-2-naphthol-3,6-disulphonato)cobalt(III) anion with water on a Λ -[Ru(phen)₃]²⁺ montmorillonite column.⁶⁷

investigated above are adsorbed at such a region, they are unlikely to interact with preadsorbed Λ -[Ru(phen)₃]²⁺ chelates in an interlayer space. The achievement of resolution of the above two complexes are, therefore, thought to be an indication that the anionic chelates are also adsorbed either on a flat region of an external surface or in the interlayer space of a clay.

Bis(chelated) complexes are resolved on the same column. An investigated chelate is a Co^{II} or Co^{III} complex with terdentate pyridylazo ligands (Fig. 25).⁶⁷ These complexes have been shown to be adsorbed racemically by a colloiddally dispersed clay.⁵³ Thus the planar aromatic groups in the Co-complexes are expected to stack with [Ru(phen)₃]²⁺ stereoselectively. As a result, [Co(α PAN)₂]⁺, [Co(β PAN)₂]⁺, [Co(β PAN)₂] [Co(5-Cl-PADAP)₂]⁺ and [Co(PAR)₂]⁺ are all found to be resolved on the column. Some of the CD spectra of resolved complexes are shown in Figures 35a and b. The absolute configurations of the enantiomers are suspected on the basis of the exciton-splitting interpretation⁶⁹ for the two oppositely signed peaks in the wavelength region of about 400–700 nm. Based on this, the Λ -enantiomers are concluded to show higher affinity towards a column. Only one exception is [Co(5-Cl-PADAP)₂]⁺, for which the Δ -isomer is a more retained enantiomer. The structural origin for these selectivities is not clarified yet. [Co(β PAN)₂]⁺ does not

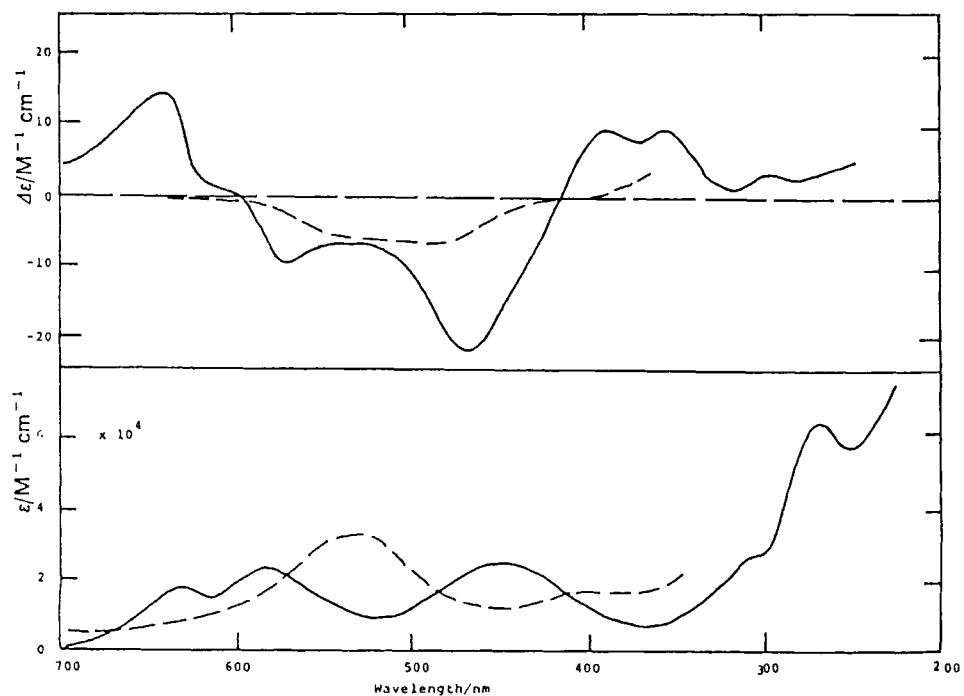


FIGURE 35A CD (upper) and electronic absorption (lower) spectra for the ethanol effluents of $[\text{Co}(\beta\text{PAN})_2]^+$ (----) and $[\text{Co}(\beta\text{PAN})_2]$ (—).^{6,7}

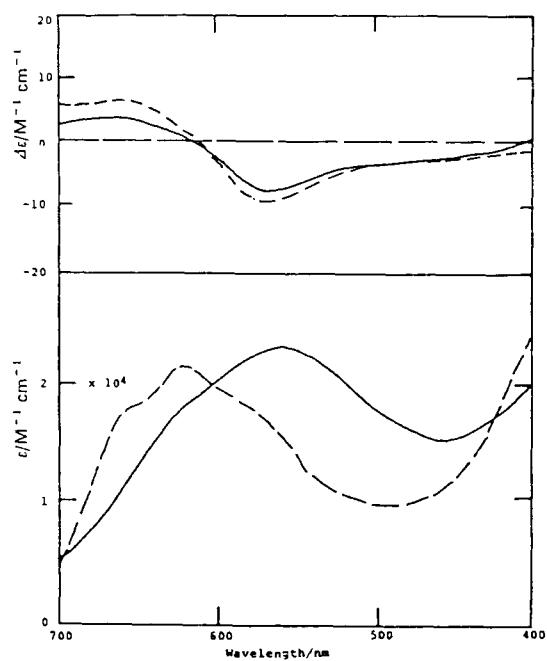


FIGURE 35B CD (upper) and electronic absorption (lower) spectra for the ethanol effluents of $[\text{Co}(\alpha\text{PAN})_2]^+$ (----) and $[\text{Co}(\alpha\text{PAN})_2]$ (—).^{6,7}

racemize at all at room temperature. Notably $[\text{Co}(\beta\text{PAN})_2]$ does not racemize at least within the investigated period (two days). This is an unusual result since most of Co(II) complexes racemize rapidly due to its ligand replacement lability.⁷² The present one provides a rare case for the inertness of a Co^{II} complex.

Adsorption toward Δ - $[\text{Ni}(\text{phen})_3]^{2+}$ montmorillonite column is compared among $[\text{Co}(\text{acac})_2(\text{gly})]$, $[\text{Co}(\text{acac})(\text{gly})_2]$ and *mer*- $[\text{Co}(\text{gly})_3]$.⁷³ The results are shown in Figure 36. With water as an eluting solvent, $[\text{Co}(\text{acac})_2(\text{gly})]$ and $[\text{Co}(\text{acac})(\text{gly})_2]$ are resolved partially, while *mer*- $[\text{Co}(\text{gly})_3]$ is not resolved at all. *mer*- $[\text{Co}(\text{gly})_3]$ is adsorbed too weakly by the column. In both of the resolved chelates, the Λ -isomers are more retained enantiomers.

Tris(bathophenanthrolinedisulfonato)iron^{II} ($[\text{Fe}(\text{BPS})_3]^{4-}$) and tris(bathophenanthroline)iron^{II} ($[\text{Fe}(\text{BS})_3]^{2+}$) (Fig. 37a) are resolved by use of either Δ - $[\text{Ni}(\text{phen})_3]^{2+}$ or Λ - $[\text{Ru}(\text{phen})_3]^{2+}$ montmorillonite.⁷⁴ Figure 37b show the CD spectra of the resolved enantiomers. The spectra are similar to that of $[\text{Fe}(\text{phen})_3]^{2+}$ enantiomers so that the configurations of the chelates are determined with little ambiguity. Both of the complexes are adsorbed in the pseudo-racemic mode; that is, the antipodal enantiomer with respect to preadsorbed $[\text{M}(\text{phen})_3]^{2+}$ show higher affinity toward the column. Since these chelates are too bulky to penetrate the interlamellar space of a clay- $[\text{M}(\text{phen})_3]^{2+}$ adduct, they are suspected to be adsorbed on an external surface. By studying the racemization kinetics of these chelates, it is derived that $[\text{Fe}(\text{BPS})_3]^{4-}$ racemizes only through the dissociation of a coordinated ligand (intermolecular path). The results are in marked contrast with the racemization of $[\text{Fe}(\text{phen})_3]^{2+}$ since $[\text{Fe}(\text{phen})_3]^{2+}$ racemizes mainly by the path of intramolecular re-organization of the ligands.⁷⁵ In such an intramolecular path, $[\text{Fe}(\text{phen})_3]^{2+}$ expands its metal-ligand bonds in the activated state. Therefore the absence in the intramolecular path for $[\text{Fe}(\text{BPS})_3]^{4-}$ is rationalized by assuming that an expanded state is difficult for $[\text{Fe}(\text{BPS})_3]^{4-}$ to realize because high energy is required to separate negatively-charged BPS ligands from divalent iron^{II} ion. In the intermolecular path, such high energy is compensated by solvation of a dissociated BPS^{2-} molecule in water.

Optically active α -amino acids are attempted to be resolved on a column of Λ - $[\text{Ru}(\text{phen})_3]^{2+}$ montmorillonite.⁷⁶ No amino acid is resolved to a detectable level except for proline. It is suspected that the resolution of proline might have something to do with the ring structure of that molecule. To ensure this hypothesis, a number of aliphatic molecules with a ring structure have been attempted on the same column. As a result, five other compounds are resolved as listed in Table XIX, although the attained optical purity is low. When these molecules are packed with preadsorbed $[\text{M}(\text{phen})_3]^{2+}$ on a molecular model, it is seen that they are too small to show any stereoselectivity. Thus the reason for resolution of the above cyclic compounds is not certain. One possibility is that these molecules are resolved as the form of a dimer or trimer. The dimer formation of proline is already reported in a homogeneous solution.⁷⁷

In the above chromatographic attempts, an adsorbent material is a neat adduct of montmorillonite exchanging optically active $[\text{M}(\text{phen})_3]^{2+}$. From the practical point of view, such an adduct has a few disadvantages as a packing material. Firstly, the material has a layer structure so that a part of a placed molecule penetrates deeply the interlamellar region. Under such circumstances, adsorption takes much time to attain equilibrium. This slowness in equilibration rate seems to be responsible for the observed large tailing in the separated species (Fig. 31). Secondly, as is suspected in the above paragraph, the interlamellar region and the external surface of the adduct are likely to behave in a different way in selecting a preferred enantiomer. For example, the racemic stacking mode in Figure 32a is possible only in an interlamellar region,

A. YAMAGISHI

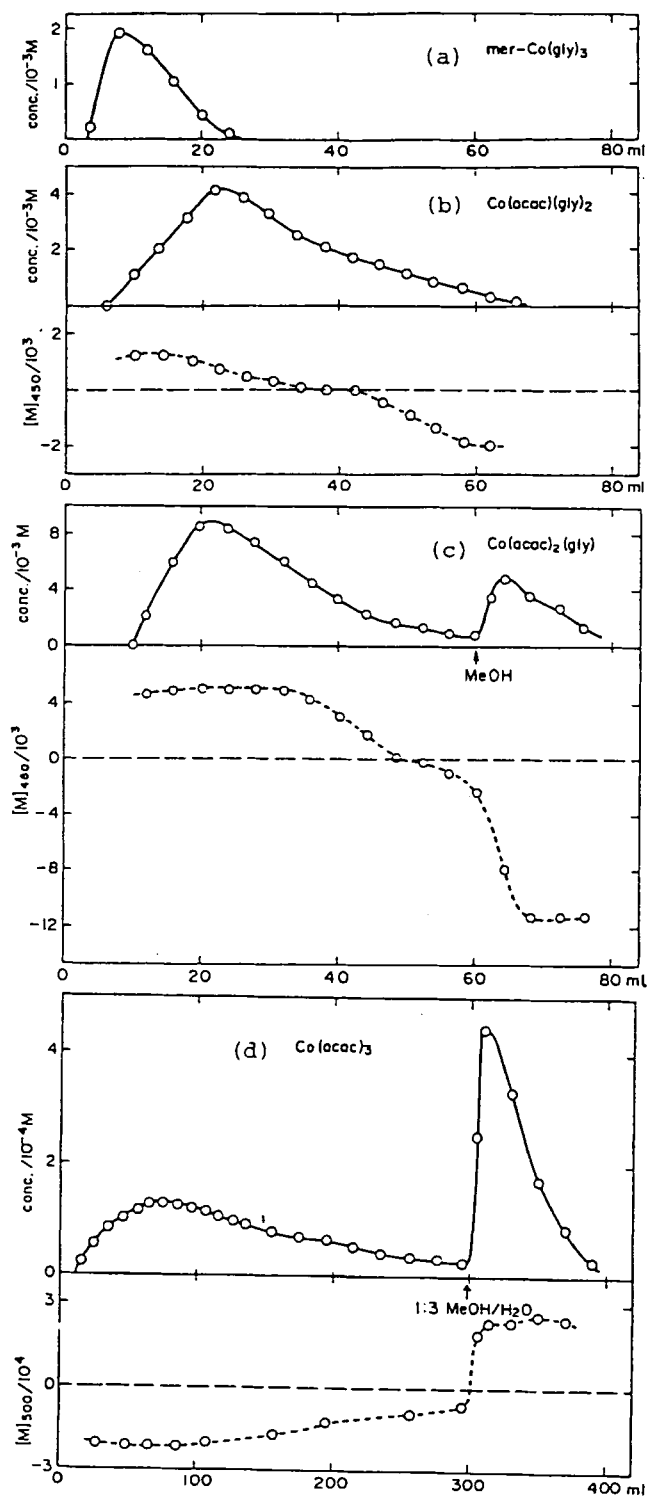


FIGURE 36 Elution curves of (a) $mer-[Co(gly)_3]$, (b) $[Co(acac)(gly)_2]$, (c) $[Co(acac)_2(gly)]$, and $[Co(acac)_3]$ on a column of Δ -[Ni(phen)₃]²⁺ montmorillonite.⁷³

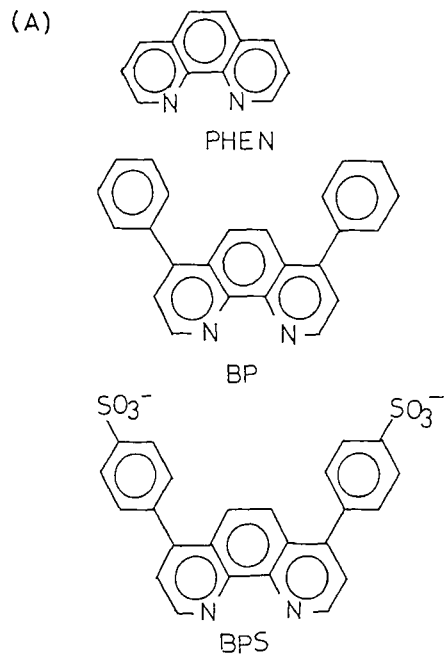


FIGURE 37A (A) Structures of 1,10-phenanthroline (PHEN), bathophenanthroline (BP) and bathophenanthroline disulfonate (BPS).

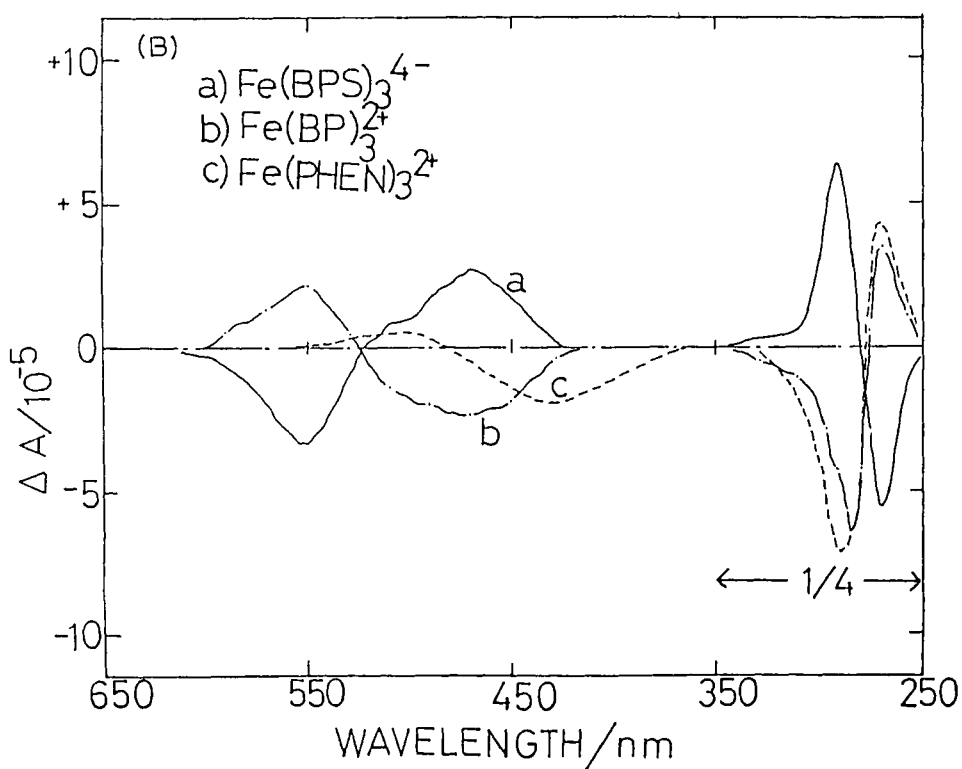


FIGURE 37B (B) CD spectra of (a) partially resolved tris(bathophenanthroline disulfonate)iron(III), (b) partially resolved tris(bathophenanthroline)iron(III), and (c) $\Delta\text{-}[\text{Fe}(\text{phen})_3]^{2+ \cdot 74}$

TABLE XIX
Chromatographic data of resolution on a Λ -[Ru(phen)₃]²⁺ montmorillonite column^{a,76}

DL-compound	maximum molecular rotation ^b	maximum resolution (%) ^b	configuration
proline	-33(+34) at 250 nm	3.8(3.9)	L(D)
5-oxo-proline	+390(-1000) at 230 nm	12(30)	L(D)
5-methyl-2-pyrrolidinone	+250(-1220) at 230 nm	-(-)	L(D)
dihydro-5-methyl-2(3H)-furanone	+20(-39) at 250 nm	-(-)	D(L)
2-piperidine carboxylic acid	-11(+54) at 300 nm	6.8(33)	L(D)
4-thiazolinecarboxylic acid	+42(-115) at 300 nm	5.0(14)	D(L)

^a Water is used as a eluting solvent.

^b Values of the first and the last effluents are shown out and in the bracket.

while the enantiomeric stacking mode in Figure 32b is possible in both of the interlamellar and external regions. These opposite trends in chirality selection will lower the overall efficiency of resolution. Thirdly, it is very difficult to obtain a uniform size of particles when the material is prepared by reaction between a colloiddally dispersed clay and a metal chelate. Even after selecting particles of a constant size, the material would be collapsed into finer particles during the chromatographic procedures. In order to overcome these defects pertaining to the layer structure of a clay, there are two ways conceivable to modify the materials.

(i) To prepare a rigid uniform particle of clay in such a way that the plates of a clay crystalline are aggregated in edge-to-face manners.

(ii) To coat a rigid particle of a uniform size such as a silica gel particle with a thin film of a clay-chelate adduct.

The first method has been applied for sodium bentonite powder.⁷⁸ An aqueous suspension of a clay is sprayed with a high-speed rotating nozzle under the conditions that the inlet and outlet temperatures are maintained at 250 and 90°C, respectively. The material thus prepared has a size of about several hundreds angstrom and certainly a "card-house" structure with many cavities. The powder exhibits a high efficiency in separating ring-substituted dimethylanilines with high-performance-liquid chromatography (HPLC). The example of separation is shown in Figure 38.

The second method is applied to the present type of a clay-chelate adduct.⁷⁹ A silica gel of a uniform particle size is added to a suspension of sodium montmorillonite and boiled to dryness. The solid is then immersed in an aqueous solution containing an optically active metal complex. The complex is adsorbed in a clay film coating in silica gel particle. The material is poured into a column tube in a slurry and used for HPLC. The resolution of tris(acetylacetonato) complex is attempted on this column to check the resolution efficiency. Figure 39a shows the chromatogram when [Co(acac)₃] is eluted with water on the column of a silica gel coated with a film of Λ -[Ru(phen)₃]²⁺ montmorillonite.

(i) The whole part of a placed chelate is eluted with water eluent, giving the clearly separated two peaks. The tailing is much more reduced than when neat [M(phen)₃]²⁺ montmorillonite is used as a column material (Fig. 31).

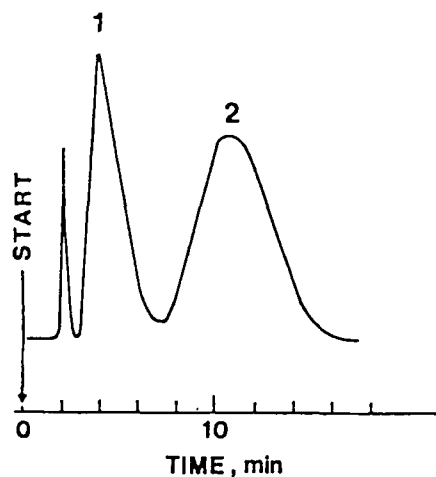


FIGURE 38 Separation of (1) 2,6- and (2) 2,5-dimethylaniline by a preheated quasi-spherical particles of bentonite column (12×0.46 cm).⁷⁸ Elution conditions: by 5% isopropanol in hexane at 0.5 ml/min flow rate and detected at 237 nm.

(ii) The order of the enantiomers removing from the column is that the first is a Δ -isomer and the second a Λ -isomer irrespective of the difference in metal ions in $[M(\text{acac})_3]$.

The above results are considered to be an indication that there exists one kind of binding sites preferring the enantiomeric adsorption uniformly on the column. Besides the flow of an eluant becomes uniform due to the uniform size of a packed material. These effects might be realized because a clay-chelate adduct takes a thin film form so that adsorption occurs dominantly on an external surface of a clay. The penetration into an interlamellar space is reduced.

Figure 40(a) shows the effects of the flow rate on the separation factor or the optical purity of a fraction collected at the minimum of a chromatogram.⁸⁰ Figure 40(b) shows the effect of the column temperature on the same quantities. The separation factor is little affected with the variations of the flow rate and the column temperature. To this contrary, the optical purity of a collected fraction increases with the decrease of the flow rate and shows the maximum around 20°C. It is deduced that the main factor in determining the optical purity of a collected fraction or practically the resolution efficiency is the extent of the overlap between the separated enantiomers and that the peak width is determined mostly by the unequilibrium in the adsorption process between a mobile phase and a solid adsorbent. Comparing the width of the peak in Figure 39 with that of a peak on a column packed with a bare silica gel, it is concluded that the penetration of a molecule in an interlayer space still takes place in Figure 39 even when it is reduced in comparison with a neat clay-chelate adduct.

The resolution of an organic molecule is attempted on a column of a silica gel coated with Λ - $[\text{Ru}(\text{phen})_3]^{2+}$ montmorillonite. If a molecule has a planar group such as phenyl or naphthyl groups or an aliphatic ring group, it is likely to stack with preadsorbed $[\text{Ru}(\text{phen})_3]^{2+}$ just like a tris(acetylacetonato) chelate in Figure 32. Based on this, such molecules as listed in Figure 41 are tried to be resolved.⁷⁹⁻⁸¹ These all possess bulky planar groups which will be likely to interact with $[\text{Ru}(\text{phen})_3]^{2+}$ intermolecularly. As a result, most of the studied molecules are resolved at least partially except for the ones underlined in the figure. The following points are

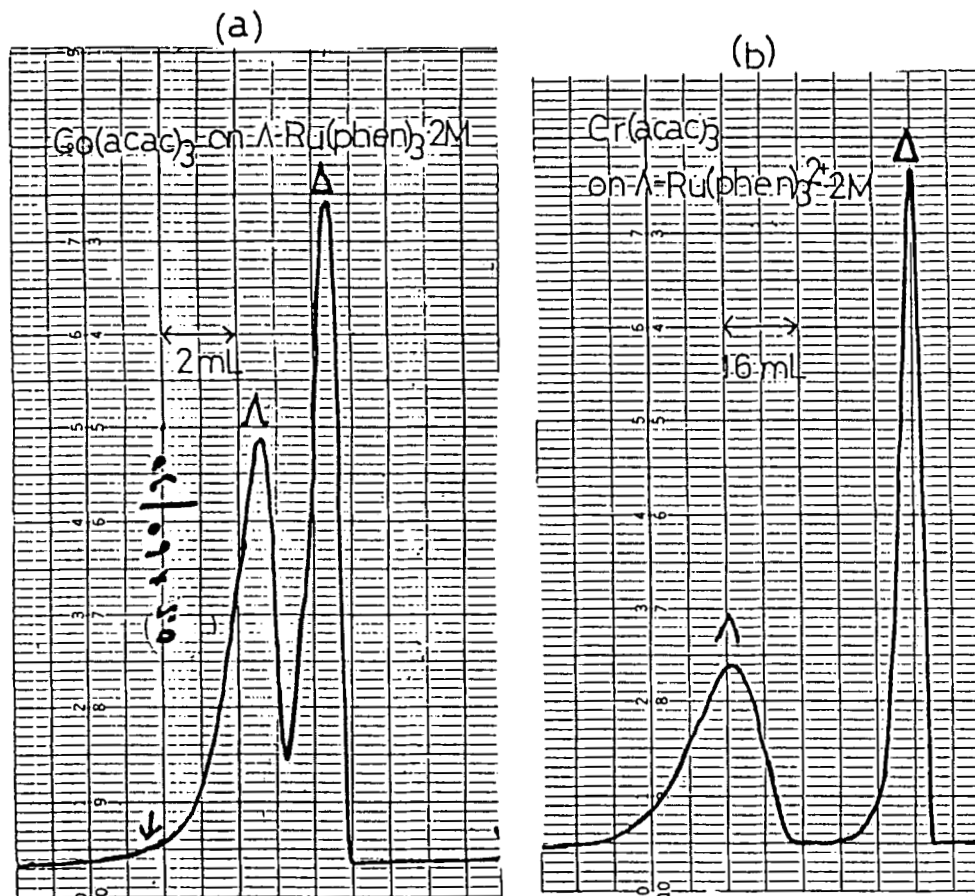
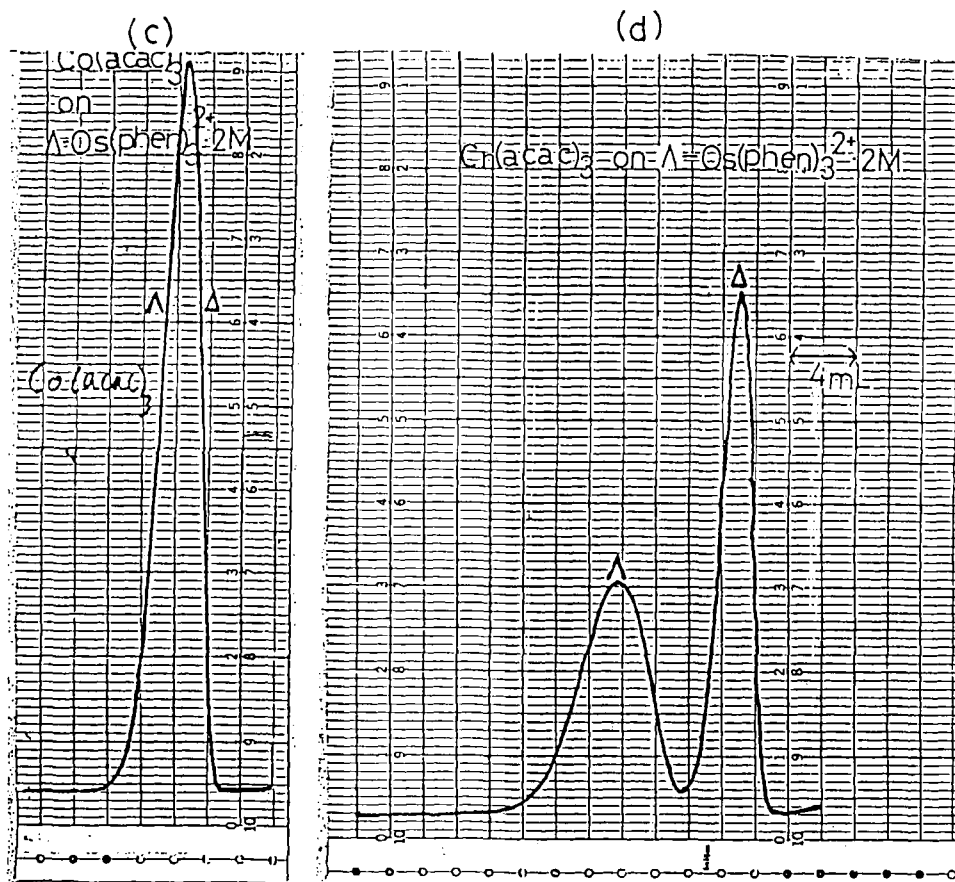


FIGURE 39 Chromatograms of tris(acetylacetonato)metal(III) ($[M(acac)_3]$) eluted with water on a column of a silica gel coated with Λ - $[M(phen)_3]^{2+}$ montmorillonite:⁶⁰ column size 20×0.4 cm (i.d.), flow rate 0.5 mL/min and temperature 25°C . (a) $[Co(acac)_3]$ on a silica gel coated with Λ - $[Ru(phen)_3]^{2+}$

noteworthy as to the mechanisms in chirality recognition and also from the viewpoints of practical utility:

(i) 1,1'-Binaphthol (II) and its analogues (III) and (IV) are resolved almost completely. 2,2'-Bromobinaphthol (V) is not resolved at all. From these results, it is deduced that the substituents at the 2 and 2' positions of binaphthyl should be electron-donating in order to achieve resolution. It seems to be an indication that the stacking interaction between Λ - $[Ru(phen)_3]^{2+}$ and a resolved molecule is achieved partly by the charge-transfer forces in which the former acts as an electron acceptor. From the practical point of view, optically active binaphthol derivatives have been useful as a chiral ligand in hydrogenation of ketone with metal hydrides.⁸² So far several chiral adsorbents are reported to achieve the chromatographic resolution of this compound.⁸³ Comparing the present results with those reported ones, the present clay chelate adducts are easier to prepare and free from chemical deterioration such as oxidation or hydrolysis.



montmorillonite and (b) $[\text{Cr}(\text{acac})_3]$ on the same column as (a), (c) $[\text{Co}(\text{acac})_3]$ on a silica gel coated with $\Lambda\text{-}[\text{Os}(\text{phen})_3]^{2+}$ montmorillonite, and (d) $[\text{Cr}(\text{acac})_3]$ on the same column as (c).

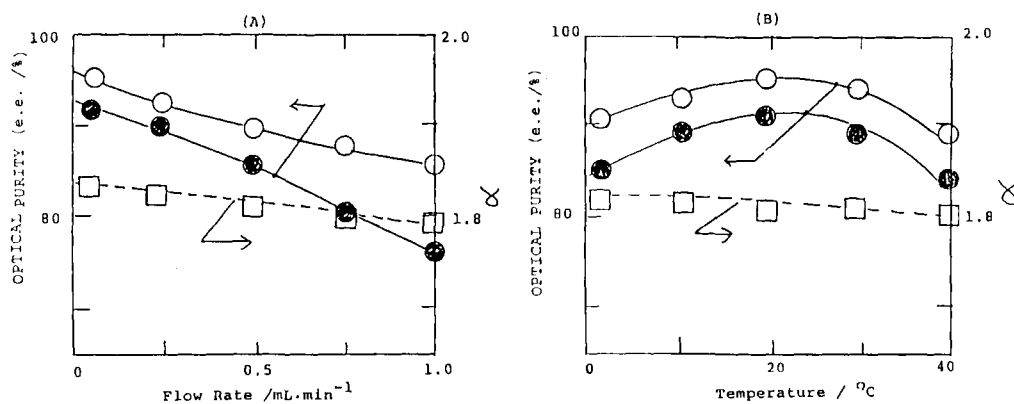


FIGURE 40 (A) Effects of the flow rate on the optical purity of a first fraction collected at the minimum in Figure 55 (a) (left) and on the separation factor of the two resolved peaks (right).⁸¹ (B) Effects of column temperature on the optical purity (left) and the separation factor (right).

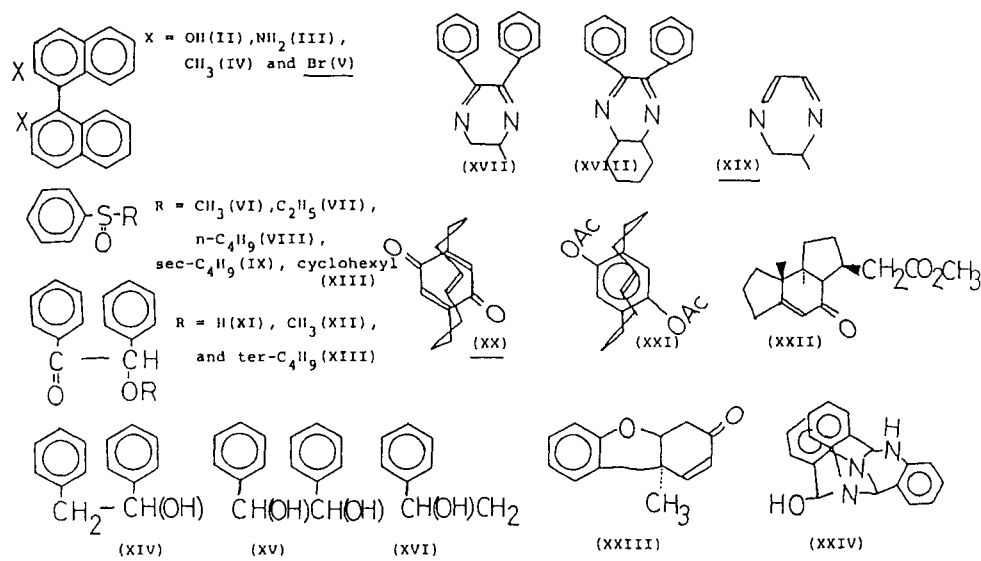


FIGURE 41 Organic molecules tried to be resolved on a column of a silicic acid coated with Λ -[Ru(phen)₃]²⁺ montmorillonite.^{80,81} The compounds are all resolved at least partially except for the underlined ones.

(ii) Phenyl alkyl sulfoxides are resolved ((VI) – (X)). An optically active sulfoxide is now used as an intermediate for the enantioselective synthesis of cycloalkanones.⁸⁴ Efficient resolution is achieved when an attached alkyl group is bulky such as cyclohexyl (X) or *sec*-butyl (IX). The fact assists the occurrence of the stacking of an alkyl group in a sulfoxide with the phenanthroline ligands in a [Ru(phen)₃]²⁺ chelate.

(iii) 1,2-Diphenylethane derivatives are resolved ((XI) – (XV)), while a monophenylethane (XVI) is not resolved at all. In addition, the carbonyl group seems to enhance the resolution efficiency when the results on three benzoin derivatives are compared ((XI) – (XIII)). Probably the ion-dipole interaction plays some role in binding these molecules to a clay.

(iv) 2,3-Dihydropyrazine derivatives are resolved when they are attached with phenyl groups ((XVII) and (XVIII)). It again assists the stacking model between a resolved molecule and [Ru(phen)₃]²⁺.

(v) A bridged *p*-benzoquinone is not resolved while its precursor, a bridged *p*-hydroquinone diester (XXI), is resolved completely. In this case, too, the electron-donating property seems to be important for resolution. Interestingly, a photoinduced intramolecular adduct of (XX), (XXII), is resolved almost completely. It is noted that the compound has three fused aliphatic rings just like alkaloids. The present column is, therefore, expected to resolve the class of natural alkaloid compounds.

7. ASYMMETRIC SYNTHESSES BY USE OF ADSORPTION ON A CLAY MINERAL

This section describes the attempts to achieve an asymmetric synthesis of an optically active molecule by utilizing an adduct of a clay and a metal chelate. The principle of

the method has been already explained in the foregoing section (Fig. 29(c)). Before going into the detailed results on the method, the previous works concerning with this topic are briefly reviewed.

Clay minerals have been utilized in asymmetric syntheses in the following three ways:

- (i) A clay has been claimed to catalyze reactions stereoselectively.
- (ii) A clay is used as an adsorbent of a reactant in asymmetric syntheses.
- (iii) A clay is used as an adsorbent immobilizing a catalyst for asymmetric reactions.

We first review the first possibility (i). There have been a number of investigations on the utility of a clay for catalytic reactions. The catalytic activities of a clay which arise partly from a proton from an intercalated water molecule and partly from a coordinatively unsaturated metal ion in a clay layer have been found to catalyze several synthetic reactions. They are, for instance, ether formation,⁸⁵ addition of acids to alkenes,⁸⁶ the breakdown or dimerization of esters,⁸⁷ decomposition of organic amines,⁸⁸ elimination of hydrogen sulphide from thiols,⁸⁹ and dehydration of alcohols.⁹⁰ For these reactions, cations in a clay have been replaced with transition metal ions such as Cu^{II} , Fe^{III} , Cr^{II} , Co^{II} and Ni^{II} . Although none of these reactions are concerned with asymmetric syntheses, some of the reactions either produce or convert the racemic mixtures of optically active molecules. Thus in the presence of a certain chiral additive, the reactions would be modified to apply for asymmetric syntheses.

In contrast to the above synthetic approach, there have been reported a few experimental results on the possibility of stereoselective adsorption and asymmetric syntheses by a naturally occurring clay mineral. It is reported, for example, that an amino acid is polymerized to a polypeptide stereoselectively in an aqueous suspension of kaolinite.⁹¹ In the presence of 0.5 g of kaolinite dispersed in 5 mL of water, 0.01 M of aspartic acid is polymerized at 90°C for 32 days. Figure 42 compares the amount of a chemically converted amino acid monomer for the three cases of S- and racemic and R-amino acid. It is concluded that a clay catalyzes preferably the polymerization of S-amino acid. The structural origin for such stereoselectivity is speculated. It is postulated that there exists an asymmetric structure along the edge line of a kaolinite microcrystalline due to the arrangement of vacant sites in the coordination around an aluminium atom. If the polymerization of an amino acid is catalyzed by such a site, it is expected to proceed stereoselectively.⁹³⁻⁹⁵

Concerning with the second approach (ii), a clay has been utilized as an adsorbent of reactants for organic reactions. For example, oxidation of sulfide is performed by sodium metaperiodate which is mounted on montmorillonite.⁹⁶ In this way, an inorganic reagent insoluble in organic media is conveniently used for the synthesis in a nonpolar solvent. In this example, a clay is used merely as a substituent for a supporting material such as alumina or silica. As a more interesting example, a reagent which is supported by a clay exhibits an enhanced reactivity than in a free state. Iron^{III} nitrate impregnated on bentonite belongs to these attempts.⁹⁷ The reagent is easily prepared by dissolution of iron^{III} nitrate nonahydrate in acetone, to which bentonite clay is added. The reagent oxidizes a variety of alcohol in organic solvents quantitatively as given in Table XX. The enhancement in oxidizing activity by Fe^{III} is confirmed by comparing the results of control experiments in the table. As for the mechanisms of the oxidation reactions, a nitrous ester is found to be formed as an intermediate.⁹⁸ The role of Fe^{III} in a clay is not clarified yet. The results are interesting if they are compared with the enhanced oxidizing power of Fe^{III} intercalated in a clay layer.³⁴ The same reagent combined with 4-*t*-butylphenol forms a catalytic system

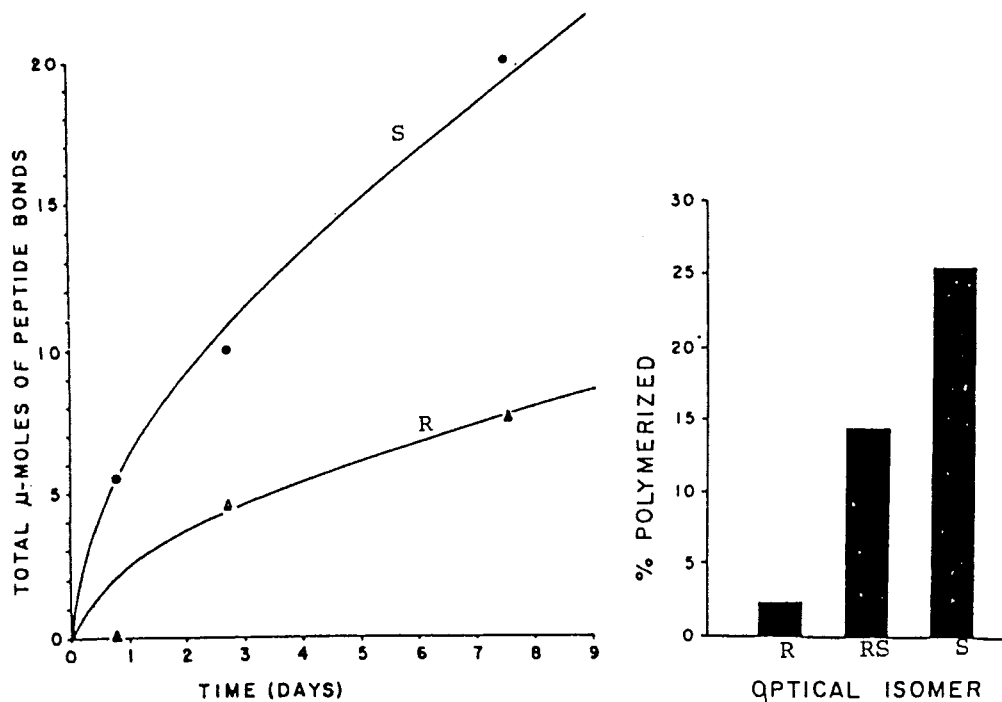


FIGURE 42 (A) Plots showing rates of peptide bond formation in solutions of S- (or L-) and R- (or D-) aspartic acid heated in the presence of kaolinite: (an open circle) S-aspartic acid and (an open triangle) R-aspartic acid.⁹¹ (B) Relative amounts of aspartic acid isomer polymerized on kaolinite after 32 days.

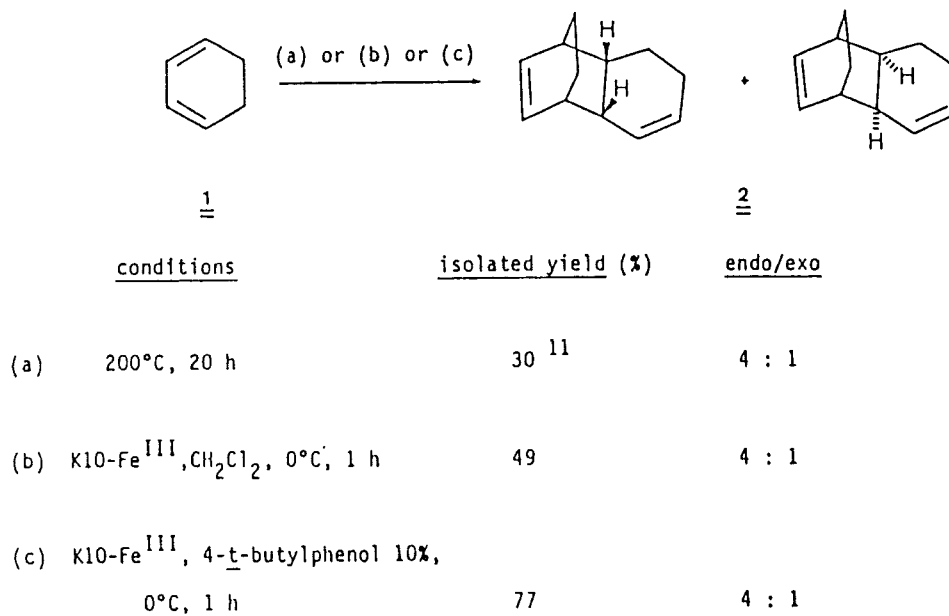
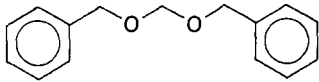
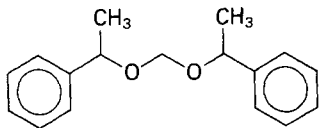
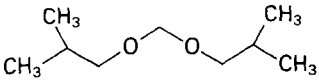
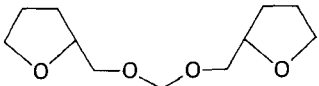
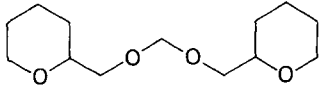


FIGURE 43 Diels-Alder reaction of unactivated dienophile in the presence of a clay.⁹⁹

TABLE XX
Formaldehyde dialkyl acetals (3) from dihalomethanes(I) alcohols (2), and aqueous base using a clay catalyst⁹⁷

3	Yield ^a [%] (Method)	b.p./torr [°C]	b.p./torr[°C] reported or molecular formula
a 	95(A)	192°/17	179–182°/11
b 	83 ^b (A)	207–208°/25	C ₁₇ H ₂₀ O ₂ (256.3458)
c $n\text{-C}_4\text{H}_9\text{-O-CH}_2\text{-O-CH}_2\text{-C}_4\text{H}_9\text{-n}$	80(A)	182°/760	179.4°/760° 181.8°/760°
d 	77(A)	115–117°/40	207.3°/760°
e 	58 ^b (B)	211–213°/100	
f 	79 ^b (B)	131–134°/0.7	

^aYield of isolated pure product. The purity was found to be by G.L.C. analysis. The structures of all products were fully established by microanalyses (high-resolution M.S. for volatile compounds). I.R. and ¹H-N.M.R. data.

^bThe product is a 1:1 mixture of d, l and meso diastereoisomer according to the ¹H-N.M.R. spectrum.

for unactivated dienophiles to undergo Diels-Alder condensations.⁹⁹ Some of the attempted reactions are shown in Figure 43. It is noted that the reaction proceeds in a stereospecific way. Therefore the method would be modified to achieve asymmetric syntheses on adding some chiral reagents to the system.

As for the third possibility (iii), a layer structure of a clay has been noted to achieve a novel function when a catalyst is intercalated between the layers. Cationic hydrogenation catalyst precursors of the type RhL_n (L = triphenylphosphine; $n = 2, 3$) have been intercalated in hectorite by the *in-situ* reaction of triphenylphosphine with rhodium^{II} acetate dimer.¹⁰⁰ The catalyst prepared in this way exhibits the remarkable specificity in the hydrogenation of an alkyne with respect to the molecular size of a substrate. The observed specificity is accounted for in terms of the spatial restriction of an interlayer space on the stability of a coordinate alkyne. Relatively small alkynes

TABLE XXI
Asymmetric hydrogenation of α -acetamidoacrylic acid catalysed by CLAY-[RhCODPNNP (+ and -)]¹⁰¹

Catalyst [α]	1st cycle			2nd cycle			3rd cycle		
	O.Y.	Reaction e.e. %	[α] time (h)	O.Y.	Reaction e.e. %	[α] time (h)	O.Y.	Reaction e.e. %	[α] time (h)
Hectorite - [Rh(CODPNNP)(+)]	-0.475(S)	72.0	1	-0.475	72.0	1,5	-0.495	75.0	2
Bentonite - [Rh(CODPNNP)(-)]	+0.450(R)	68.0	2	+0.450	68.0	4	+0.440	66.0	6
Nontronite - [Rh(CODPNNP)(-)]	+0.450(R)	61.0	3	+0.450	68.0	4	+0.465	70.0	5
Halloysite - [Rh(CODPNNP)(-)]	+0.360(R)	55.0	2	+0.420	64.0	4	+0.445	67.0	6,5

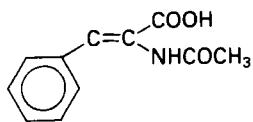
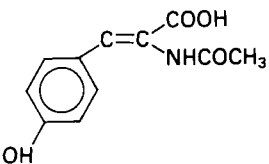
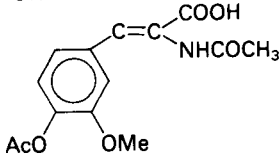
such as 1-hexyne and 2-hexyne shows the initial reduction rates which are comparable for the reduction with the homogeneous catalysts, while larger alkynes such as diphenylacetylene that exceed the critical size of the height of an interlamellar space (7.7 Å) are hydrogenated with the rates 100 times lower than homogeneous rates.

It is rather straight forward to extend the above results to asymmetric catalytic systems, in which an asymmetric catalyst is intercalated in a clay. An insoluble chiral complex of rhodium¹ aminophosphine is supported on four kinds of clays.¹⁰¹ In all systems studied, an amino acid precursor such as α -acetamidoacrylic acid has been hydrogenated with good chemical yield. The attained optical yields depend on the nature of supporting materials very much as given in Table XXI. In contrast to the homogeneous systems, the catalytic chelate acquires greater stability against the decomposition by hydrogen molecules. The effect is attributed to the coordination of water molecules to a rhodium atom in the chelate.

A similar attempt has been reported by immobilizing rhodium complexes of the type $[\text{Rh}(\text{diene})(\text{diphos}^*)]^+$, where diphos* is a chiral bidentate diphosphine ligand, in an interlamellar space of hectorite.¹⁰² Table XXII gives the results on the asymmetric hydrogenation of prochiral olefins with such a catalyst. The same level of optical yield has been attained between the immobilized and homogeneous systems.

We now describe the method of symmetric syntheses by using an adduct of a clay and an optically active chelate. In this method, the adduct is used as a chiral adsorbent either of a reactant or of a catalyst. It is expected that the steric control due to the intermolecular interaction of a reactant or a catalyst with a preadsorbed metal chelate induces asymmetry in a reaction product. Thus this method is classified to (ii) or (iii), depending on which of a reactant or a catalyst is adsorbed by the adduct before starting a reaction.

TABLE XXII
Asymmetric hydrogenation of prochiral olefins with $\text{Rh}(\text{NBD})(4\text{Me-(R)-Prophos})^+ \text{ a,102}$

Substrate	Optical yield (%)	
	Inter. catalyst	Homo. catalyst
	89.6	92.6
	78.5	72.0
	95.1	95.3

^a Reactions were carried out at 25°C, 1 atm pressure, in 95% ethanol. The chemical yields were >98% in each case.

Firstly are mentioned the attempts of using a clay-chelate adduct as an adsorbent of a prochiral reactant. When a neutral molecule, 1-(2-pyridylazo)-2-naphthol (Hpan), is added to an aqueous suspension of Δ -[Ni(phen)₃]²⁺ montmorillonite, a new CD peak appears around 500 nm.¹⁰³ Since Hpan is itself achiral and has an absorption peak at 475 nm, the observed CD peak is ascribed to Hpan molecules bound to the clay-chelate adduct. The results imply that the bound molecules experience an

TABLE XXIII
Asymmetric syntheses of metal chelates and organic molecules by use of Δ -Ni(phen)₃²⁺ · montmorillonite.^{103,104}

	Reactant	Product	Optical Yield (confg.)
(a)	PANH	$\xrightarrow[\text{Co}^{2+}]{\text{O}_2}$ [Co(PAN) ₂] ⁺	30 % ((-) _D)
(b)		$\xrightarrow{\text{NaBH}_4}$ CH(OH)CH(OH)	5 % (S, S-)
(c)		$\xrightarrow{\text{NaBH}_4}$ CH ₂ -CH(OH)	50 % (S)
(d)		$\xrightarrow{\text{Fe}^{3+}}$	3 % (R)
(e)		$\xrightarrow{\text{NaIO}_4}$	45 % (S)
(f)		$\xrightarrow{\text{NaIO}_4}$	0 %
(g)		$\xrightarrow{\text{H}_2/\text{Co (dmg)}_2}$	0 %

asymmetric field due to optically active Δ -[Ni(phen)₃]²⁺. When Co^{II} ion is added to the suspension, the mixture changes from orange to green, indicating that a complex, [Co(pan)₂]⁺, is formed. The complex is removed by washing with methanol from the clay-chelate adduct and analyzed with ORD spectra. As a result, (-)-[Co(pan)₂]⁺ is formed with the optical purity of 30%. It is known from the chromatography that this isomer exhibits a stronger affinity toward a column of Δ -[Ni(phen)₃]²⁺ montmorillonite.⁶⁷ Thus the observed induction of optical activity might arise from the steric control of Δ -[Ni(phen)₃]²⁺ when Hpan ligands attack a Co^{II} ion on a clay surface.

Similar experiments are performed for the reduction of benzil with NaBH₄ to 1,2-diphenylethane-1,2-diol.¹⁰³ In this case, the (S,S)-isomer is produced with the optical purity of less than 5%. The extremely low value of the optical purity is ascribed to the formation of large amount of a meso-isomer. Table XXIII lists the experimental results of the asymmetric syntheses based on this method.

The most promising system among the investigated reactions is the oxidation of alkyl phenyl sulfide with sodium metaperiodate.¹⁰⁴ According to this oxidation method, an alkyl phenyl sulfide is adsorbed by a clay-chelate adduct and is converted to a corresponding sulfoxide with an appropriate oxidizing agent. A typical procedure is as follows. Alkyl phenyl sulfide (about 10⁻⁶ mol) is adsorbed by colloidal dispersed Δ -[Ni(phen)₃]²⁺ montmorillonite (about 10⁻⁵ mol in terms of CEC of a clay). The adsorbed sulfide is oxidized with excess amount of NaIO₄ in water. The mixture is washed with methanol to extract the sulfoxide. The optical purity of sulfoxide thus obtained is analyzed with CD spectral. The results are compiled in Table XXIV. The highest optical yield of 78% is attained for the oxidation of cyclohexyl phenyl sulfide

TABLE XXIV
Asymmetric oxidation of alkyl phenyl sulfide adsorbed by delta-tris(1,10-phenanthroline)nickel(II) montmorillonite in water.¹⁰⁴

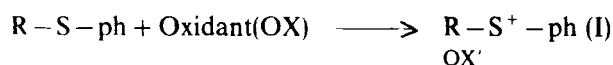
sulfoxide	oxidant	T/°C	Sulfone/%	sulfoxide/%	(e.e./%)
cyclohexyl-S-ph	NaIO ₄	0	0	90	(28)
same	same	10	0	95	(46)
same	same	20	3	92	(73)
same	same	25	5	90	(78)
same	same	30	5	90	(62)
same	H ₂ O ₂	25	0	95	(8)
same	K ₂ O ₂ S ₈	25	0	75	(42)
same	<i>m</i> -chloro- perbenzoic acid	25	10	90	(62)
methyl-S-ph	NaIO ₄	25	15	95	(0)
ethyl-S-ph	same	25	10	90	(9)
<i>n</i> -butyl-S-ph	same	25	5	90	(75)
<i>sec</i> -butyl-S-ph	same	25	5	90	(65)
benzyl-S-ph	same	25	0	95	(70)

^a An ion-exchange adduct of a clay and Δ -[Ni(phen)₃]²⁺ was prepared by adding the stoichiometric amount of the metal chelate to a colloidal solution of sodium montmorillonite. The reaction conditions are described in the text. An oxidant was added in about 100 times excess over a sulfide except for *m*-chloroperbenzoic acid which was added in an equimolar amount to the sulfide.

^b The optical purity of a produced sulfoxide is given in terms of per cent of enantiomeric excess of S-isomer (e.e.). A pure enantiomer of S-sulfoxide was obtained as a less retained species when the racemic mixture was chromatographed on a column of Δ -[Ru(phen)₃]²⁺ montmorillonite. The e.e. was calculated from the ratio of apparent $\Delta\epsilon$ at 245 nm of a sample to $\Delta\epsilon$ of a pre S-enantiomer in the CD spectra.

at 25°C. This optical yield is much higher than the values obtained by asymmetrically-modified peroxides (1–10%).¹⁰⁵ The yield is comparable to the best known results by the use of Ti(O-*i*-Pr)/(*R,R*)-diethyl tartrate/water/*t*-BuOOH (the modified Sharpless reagent).¹⁰⁶ With this reagent, various kind of aryl methyl sulfides are homogeneously oxidized to sulfoxides at the optical yield of 5–91% at –17 – –20°C. The optical yield is lowered appreciably when the reaction is conducted at room temperature. On the contrary, the present method gives the highest optical yield around 25°C. In this respect, the present method seems more versatile in synthetic use than the reported ones.

The bulkiness of an alkyl group in a sulfide has a decisive effect on the efficiency of asymmetric induction.¹⁰⁴ Methyl phenyl sulfide, for example, gives no optically active sulfoxide with the same oxidant. Most probably, an oxidized intermediate (I), which exists in two isomeric forms as a free state, forms on the clay adduct:



The alkyl group in such an intermediate interacts with the phenanthroline ligands in the Ni^{II}-chelate to stabilize either one of the isomeric forms. Thus a small group like methyl group is inefficient in inducing the optical activity of a product molecule.

As an additional remark, a sulfone is produced as a by-product as seen in Table XXIV. This is unusual because the homogeneous oxidation of an alkyl phenyl sulfide with NaIO₄ never produces higher oxidation molecules like sulfone.¹⁰² The results indicate that a clay plays a catalytic role in causing the further oxidation of a sulfoxide. One possibility is that a transition metal ion included in a crystal lattice of a clay such as Fe^{II} might act as a catalyst in the present systems.

As the second attempt for asymmetric syntheses by use of a clay-chelate adduct, the electrochemical studies on a clay-coated electrode are described. In this method, an electrode is coated with a thin film of a clay-chelate adduct. Since a clay itself does not undergo any oxidation-reduction processes under the electric potential, an electrode coated with a pure clay is inactive on scanning the external voltage. However, if a metal complex ion which is possible to be either oxidized or reduced is incorporated in such a clay film, the modified electrode becomes now electroactive. If an incorporated metal complex is regarded as a catalyst, the method is classified to approach (iii).

These kinds of clay-modified electrodes are first reported in the case of an SnO₂ glass electrode coated with a film of sodium montmorillonite.¹⁰⁸ The electrode is prepared simply by immersing an SnO₂ glass in an aqueous suspension of sodium montmorillonite. In the suspension, poly(vinyl alcohol) is added as a sticker for a clay film on an SnO₂ glass surface. With no additives incorporated in a clay film, the electrode is found to be electro-inactive (curve (a) in Fig. 44a). [Ru(bpy)₃]²⁺ is incorporated into the film by soaking an electrode in an aqueous solution of the chelate. The electrode thus prepared is now electroactive, showing the reversible oxidation-reduction peaks as seen in curve b in Figure 44a. From the dependence of the cathodic peak current on the square of the scan rate (Fig. 44b), the apparent diffusion coefficient of [Ru(bpy)₃]²⁺ in a clay film is estimated to be about 10⁻¹¹ cm²/s. It is unclear what kind of mechanism of electron-transfer is responsible for this observed mobility of bound chelates.

When a clay is compared with other kinds of materials ever used as an electrode-modifier, it has the following advantages:

(i) A clay itself is electrolytically inactive so that a wide range of voltage sweep is possible without causing any electrochemical degradation.

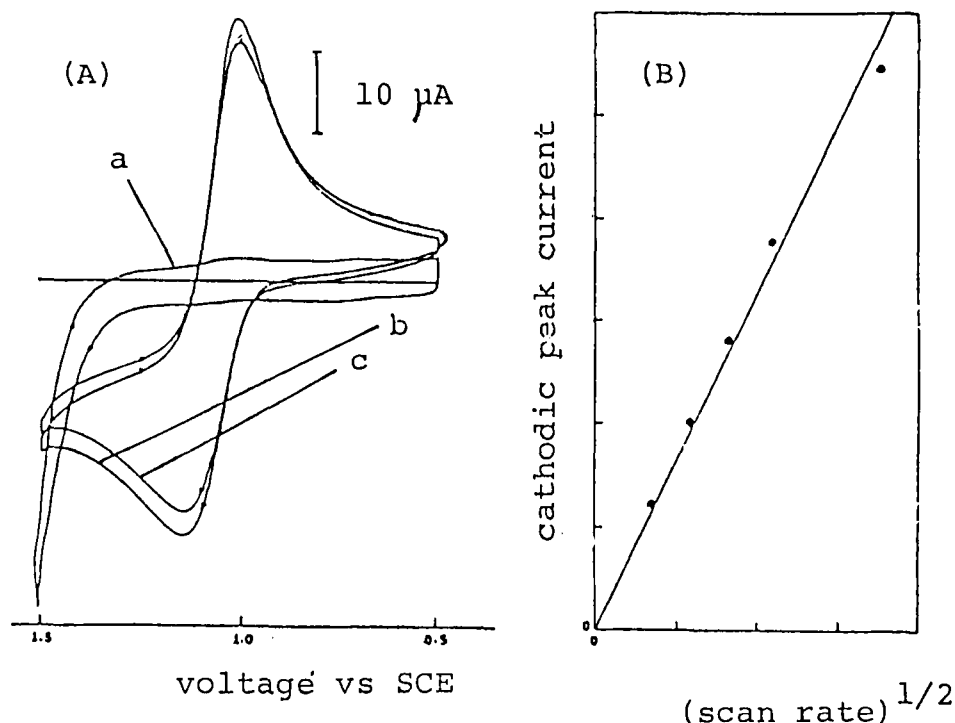


FIGURE 44 (A) Cyclic voltammograms for $[\text{Ru}(\text{bpy})_3]^{2+}$ incorporated into clay films on SnO_2 electrodes, in the absence (a) and in the presence (b, c) of colloidal Pt/poly(vinyl alcohol); (b) initial scan, (c) 50th scan. Voltammograms are recorded in 0.1 M Na_2SO_4 .¹⁰⁸ (B) Plot of the cathodic peak current versus the square root of the scan rate for the electroactive film.

(ii) A clay has a layer structure so that it is easy to construct a well-oriented thin film free from mechanical defects such as cracks and holes. The film is strengthened by mixing some additives like poly(vinyl alcohol) or colloidal platinum particle.

(iii) A clay is capable of including a certain type of metal chelates very firmly such as tris(1,10-phenanthroline) and tris(2,2'-bipyridyl) chelates. These included chelates make a clay film electro-active due to their own reversible redox changes. A film of a clay-chelate adduct thus prepared is possible to exhibit any selectivity in electrochemical processes due to the stereochemical interactions of the chelate with a reactant.

(iv) From a practical aspect, a clay is inexpensively available in a purified form.⁶ Thus the system would be easily extended to a larger scale if some selective electrochemical reactions are realized on such a clay-modified electrode.

Motivated by the above works, the asymmetric electrochemical reactions are attempted by use of a clay-modified electrode. For this purpose, an optically active metal chelate is incorporated in a clay film instead of using a racemic mixture. Figure 45(a) shows the cyclic voltammogram when an SnO_2 glass electrode is coated with a film of Δ - $[\text{Ru}(\text{phen})_3]^{2+}$ montmorillonite.¹⁰⁹ An electrode solution contains merely 0.05 M Na_2SO_4 . No $[\text{Ru}(\text{phen})_3]^{2+}$ is removed from an electrode, showing that a clay film is so strongly sorptive for this chelate. When an electrode solution contains Δ - $[\text{Ru}(\text{phen})_3]^{2+}$, no significant change is observed in the cyclic voltammogram (curve a in Fig. 45(b)). In contrast, the voltammogram changes considerably when an electrode

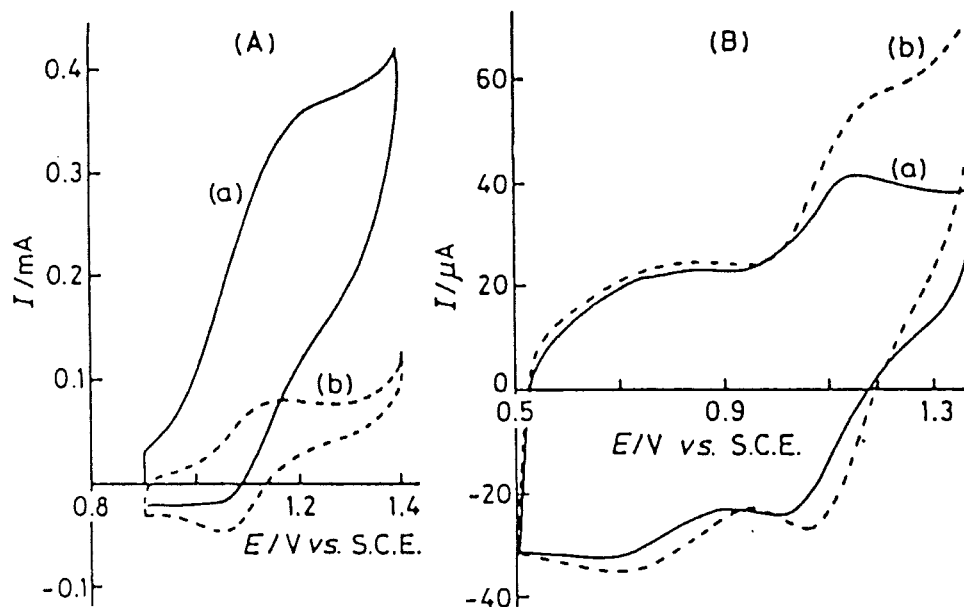


FIGURE 45 (A) Cyclic voltammogram at 50 mV/s in 0.05 M Na_2SO_4 for $\Delta\text{-}[\text{Ru}(\text{phen})_3]^{2+}$ incorporated into a clay film on SnO_2 electrodes. (a) initial scan, and (b) about 20th scan.¹⁰⁹ (B) Cyclic voltammograms at about 15th scan of 0.2 V/s: (a) an aqueous $\Delta\text{-}[\text{Ru}(\text{phen})_3]^{2+}$ solution, and (b) an aqueous $\Lambda\text{-}[\text{Ru}(\text{phen})_3]^{2+}$ solution.

solution contains $\Lambda\text{-}[\text{Ru}(\text{phen})_3]^{2+}$ (curve b in Fig. 45(b)). The current increases by almost 1.5 times at the anodic peak. Notably the observed effect of $\Lambda\text{-}[\text{Ru}(\text{phen})_3]^{2+}$ is reversible or curve (b) reverts to curve (a) when the solution is replaced with a solution of $\Delta\text{-}[\text{Ru}(\text{phen})_3]^{2+}$ again. The results suggest that $\Delta\text{-}[\text{Ru}(\text{phen})_3]^{2+}$ is repelled from the $\Delta\text{-}[\text{Ru}(\text{phen})_3]^{2+}$ montmorillonite film, while $\Lambda\text{-}[\text{Ru}(\text{phen})_3]^{2+}$ in the electrolytic solution penetrates the clay film until the $\Lambda\text{-}[\text{Ru}(\text{phen})_3]^{2+}$ is oxidized to $\Delta\text{-}[\text{Ru}(\text{phen})_3]^{3+}$ at the SnO_2 electrode. Thus the results confirm that a film of a clay-metal chelate adduct makes an SnO_2 electrode stereoselective towards a redox reaction of the same kind of metal chelate. The above results are extended to the electrochemical oxidation of racemic $[\text{Co}(\text{phen})_3]^{2+}$ on the same electrode.¹¹⁰ After electrolyzing the solution of racemic $[\text{Co}(\text{phen})_3]^{3+}$, it is found that $\Lambda\text{-}[\text{Co}(\text{phen})_3]^{3+}$ is formed with the optical purity of 7%. Although the observed stereoselectivity is low, the clay-chelate adduct is shown to be a modifier for asymmetric electrolytic oxidation.

The same modified electrode is applied to achieve the electrolytic production of an optically active organic molecule. Phenyl alkyl sulfide is oxidized on an SnO_2 glass electrode coated with $\Lambda\text{-}[\text{Ru}(\text{phen})_3]^{2+}$ montmorillonite.¹¹⁰ Figure 46 exhibits the effect of cyclohexyl phenyl sulfide on the cyclic voltammogram of such an electrode. On adding the sulfide, the peaks due to the oxidation-reduction of $[\text{Ru}(\text{phen})_3]^{2+}$ in a clay disappears to result in the almost monotonous increase of the current with the potential (curve a to curve b in the figure). Curve b might correspond to the irreversible oxidation of sulfide to sulfoxide. It is unclear, however, why the redox process due to bound $[\text{Ru}(\text{phen})_3]^{2+}$ ceases on the addition of sulfide. One possibility is that sulfide penetrates the clay film until it covers the SnO_2 electrode surface completely. Interestingly the potential at which the oxidation of sulfide starts is read to be 1.05 V

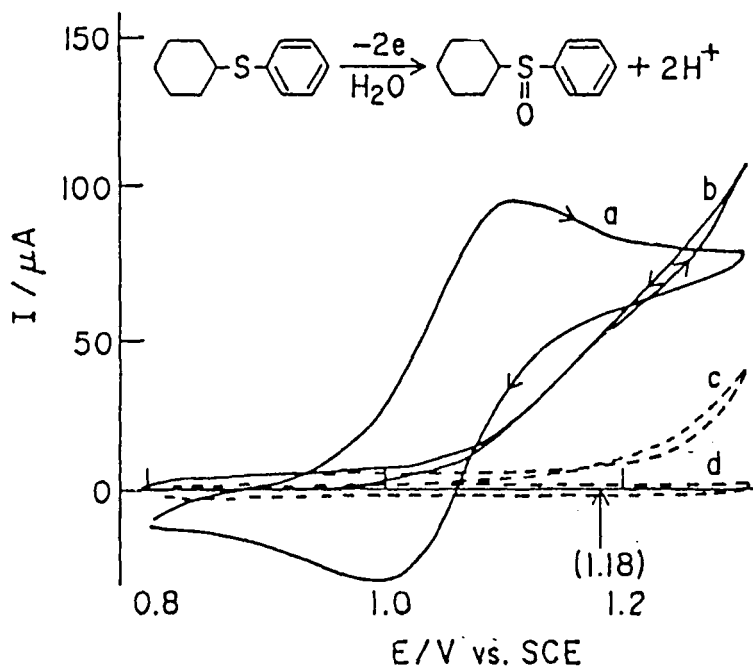


FIGURE 46 Cyclic voltammograms for Δ -[Ru(phen)₃]²⁺ incorporated into montmorillonite films on SnO₂ glass electrodes: (a) no sulfide, (b) in the presence of sulfide. (c) Cyclic voltammogram of sulfide on SnO₂ electrode. (d) Cyclic voltammogram of sulfide on a Δ -[Ni(phen)₃]²⁺ montmorillonite-coated SnO₂ electrode. All solvents are 40% (v/v) acetonitrile-water (modified from ref. 110.)

vs. SCE from curve b, which is appreciably lower than the potential at which sulfide is oxidized on a bare SnO₂ glass electrode (about 1.2 V vs. SCE from curve c in the same figure). In other words, the clay film acts as a catalyst in oxidizing the sulfide electrochemically. For such a catalytic activity, a clay should include a metal chelate which is oxidizable at that potential. This is concluded because no oxidation of sulfide takes place on an electrode coated with Δ -[Ni(phen)₃]²⁺ montmorillonite. Thus some interaction of a sulfide with Δ -[Ru(phen)₃]²⁺ in a clay film causes the oxidation of sulfide at lower potential.

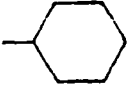

Table XXV lists the results of the electrochemical oxidation of four kinds of sulfides. The attained optical yields in the table are comparable to the previous electrooxidation of sulfides on a polymer-coated electrode.¹¹¹ In case of cyclohexyl phenyl sulfoxide, for example, the asymmetric yield obtained at room temperature is one third of that of the best known results by use of a platinum electrode coated with poly(L-valine). As is noted in the oxidation by NaIO₄,¹⁰⁴ the alkyl group is important in determining the magnitude of asymmetric yield. Methyl phenyl sulfide does not produce optically active sulfoxide at all. The similar mechanism in asymmetric induction as postulated above in the colloiddally dispersed system¹⁰⁴ would hold in the electrolytic oxidation.¹¹²

8. POSSIBLE ROLE OF A CLAY IN THE ORIGIN OF CHIRALITY

It is generally accepted that there existed primordial chemical processes in which simple inorganic and organic molecules were converted chemically into biological

TABLE XXV

Electrochemical oxidation of phenyl alkyl sulfide to phenyl alkyl sulfoxide on an SnO_2 -glass electrode coated with $\Lambda\text{-Ru}(\text{phen})_3^2+$ montmorillonite; $\text{Ph-S-R} \rightarrow \text{Ph-S-R}^{\text{a,110}}$

-R	Excess enantiomer	Optical yield/% ^b	Chemical yield/%
-CH ₃	R-(+) _D	0	100
-C ₂ H ₅	R-(+) _D	5	100
-CH(CH ₃)C ₂ H ₅	R-(+) _D	20	70
	R-(+) _D	15	60
-CH ₂ - 	R-(+) _D	5	100

^aAbout 10^{-4} M of sulfide in 0.08 M Na_2SO_4 30% (v/v) $\text{CH}_3\text{CN} + \text{H}_2\text{O}$ was electrolyzed at 1.3 V vs. SCE at room temperature.

^bEstimated from the circular dichroism spectra on the basis of $\Delta\epsilon_{240} = 10$.

constituents before initial organisms appeared on the earth. The process, ordinarily called chemical evolution, was thought to have existed about $2 - 4 \times 10^9$ years ago.¹¹³

Clay minerals were present abundantly on the earth at that period as a consequence of diagenetic actions of volcanic rocks or ashes. Since the postulate by Bernal in early 1950's,¹¹⁴ a number of investigators have tried to establish the role of clay minerals in the chemical evolution. It has been reported that clays catalyze the polymerizations of amino acids and nucleotides and also concentrate biological constituents selectively.¹¹⁵⁻¹¹⁸ Clay crystals are thought to have functioned as a first organism preceding the organism made of organic molecules.^{119,120}

As to the origin of optical activity, a clay has been claimed to adsorb stereoselectively some of amino acids or glucose and to catalyze stereoselectively the polymerization of amino acids.^{41,91} There are, however, great arguments on the validity of these results.¹²¹ No structural evidences have been presented yet as to the optical activity of clay minerals.

In the following, we propose a postulate as to the origin and amplification of optical activity on the basis of the present results. The postulate involves the participation of an optically active metal chelate as a key compound.

(i) Optical activity was first generated in the form of a configurationally optically-active metal chelate such as a bis(chelated) or tris(chelated) complex rather than as an asymmetric carbon compound as observed in today's bioorganisms.

(ii) The initial chirality was then transferred to other kinds of chelates through various mechanisms such as those by the formation of diastereomeric pairs between the initial chelate and another kind of chelate. Such transfer of chirality continued until an optically-active chelate satisfying the conditions for racemic adsorption by a clay (Table XII) was produced.

(iii) Once such an optically-active chelate was formed, the optical purity of the chelate was improved by the racemic adsorption by a clay (Fig. 29a). This took place

at the bottom of the primitive sea which dissolved the chelate at a very dilute concentration. As a result, the ocean contained a pure enantiomer.

(iv) The purified chelate was adsorbed by a clay and formed a layer of a clay-chelate adduct. This layer worked as a chiral adsorbent for optical resolution or asymmetric syntheses. At this stage, optically-active organic molecules appeared.

As for the postulate (i), in comparison to an organic molecule such as amino acid or glucose, a metal complex is possible to interact more readily with an external asymmetric physical field such as magnetic, electric or electromagnetic field. This is, of course, due to the facts that a metal complex absorbs a light in wider wavelength region, and that it often possesses electric, magnetic or quadrupole moments. For example, racemic tris(oxalato)chromium(III) anti-racemizes under the circularly polarized light.¹²² Simultaneous resolution is more possible for a metal complex than for a simple organic molecule. For example, a certain cobalt(III) complex with an amino acid ligand is proved to be simultaneously resolved, although the amino acid itself does not resolve simultaneously.¹²³

As for the postulates (iii) and (iv), the previous results in Section 6 reveal that a chelate is adsorbed racemically by a clay if it has a ligand larger than about 10 Å and has an electric charge from zero to two. For example, metal complexes of purines or pyrimidines are large enough to satisfy these conditions. However, these complexes are mostly labile and cannot stay as a pure enantiomer. A countermeasure for this would be a metal complex with *N*(1)-oxide nucleotides. In contrast to natural nucleotides, this modified nucleotides form much more stable complexes with various bi-valent metal ions.¹²⁴ Therefore it would be interesting to study the adsorption behaviour of these chelates in the presence of a clay from a viewpoint of a molecule responsible for the propagation of chirality.

REFERENCES AND NOTES

1. A. Weiss, *Clays and Clay Minerals*, **10**, 191 (1963).
2. S.L. Swartzen-Allen and E. Matijevic, *Chem. Rev.*, **74**, 385 (1974).
3. A. Hadding, *Z. Krist.*, **58**, 108 (1923).
4. L. Pauling, *Proc. Natl. Acad. Sci., U.S.A.*, **16**, 123 (1930).
5. G.W. Brindly and G. Brown, *Crystal Structures of Clay Minerals and Their X-Ray Identification* (Mineralogical Society, London, 1980), p. 5.
6. Cited from the catalogue of Kunimine Ind. Co. Ltd (Japan).
7. B.K.G. Theng, *The Chemistry of Clay-Organic Reactions* (Adam Hilger, Bristol, 1974) Chap. 1.
8. *American Petroleum Institute Research Project 49, Reference Clay Minerals* (Columbia University, New York, 1951) (through ref. 2).
9. Ref. 5, Chap. 3.
10. Ref. 7, Chaps. 2-7.
11. H. Van Olphen, *An Introduction to Clay Colloid Chemistry* (Interscience Publishers, New York, 1963), p. 90.
12. N. Kohyama, *Abstracts of the 8th International Clay Conference*, 125 (1985).
13. I. Shainberg and W.D. Kenper, *Soil Sci. Soc. Amer. Proc.*, **30**, 707 (1966).
14. S. Yamanaka, *J. Phys. Chem.*, **78**, 42 (1974).
15. T.J. Pinnavaia, *Science*, **220**, 365 (1983).
16. J.W. Jordan, *J. Phys. Chem. Colloid Chem.*, **53**, 294 (1949) (through ref. 10).
17. D.M.C. MacEwan, *The X-Ray Identification and Crystal Structures of Clay Minerals* (Mineralogical Society, London, 1961), Chap. 4.
18. M.S. Stul and W.J. Mortier, *Clays and Clay Minerals*, **22**, 391 (1974).
19. A. Weiss, *Angew. Chem.*, **75**, 113 (1963).
20. M. Raupach, P.G. Slade, L. Janile and E.W. Radoslovich, *Clay and Clay Minerals*, **23**, 181 (1975).
21. D.M. Clementz, T.J. Pinnavaia and M.M. Mortland, *J. Phys. Chem.*, **77**, 196 (1973).
22. M.M. Mortland and T.J. Pinnavaia, *Nature*, **229**, 75 (1971).
23. D.V. Poel, P. Cloos, J. Helsen and E. Jannini, *Bull. Groupe Franc. Argiles*, **25**, 115 (1973).
24. Y. Soma, M. Soma and I. Harada, *J. Phys. Chem.*, **88**, 3034 (1984).

25. J.L. Burba III and J.L. McAtee, Jr., *Clay and Clay Minerals*, **25**, 113 (1977).
26. M.H. Koppelman and J.G. Dillard, *Clay and Clay Minerals*, **28**, 211 (1980).
27. D.R. Kosiur, *Clay and Clay Minerals*, **25**, 365 (1977).
28. U. Hoffman, A. Weiss, G. Koch, A. Mehler and A. Schultz, *Clay and Clay Minerals*, **4**, 273 (1956).
29. A. Yamagishi, unpublished results.
30. P.J. Ridler and B.R. Jennings, *Clay Minerals*, **15**, 121 (1980).
31. R.A. Dellagardia and J.K. Thomas, *J. Phys. Chem.*, **87**, 990 (1983).
32. R.A.S. Schoonheydt, P.De Pauw, D. Vliers and F.C. DeScrijver, *J. Phys. Chem.*, **85**, 5113 (1984).
33. P. Liebmman, G. Loew, S. Burt, J. Lewless and R.D. MacElroy, *Inorg. Chem.*, **21**, 1586 (1982).
34. V.E. Berkheiser and M.M. Mortland, *Clay and Clay Minerals*, **25**, 105 (1977).
35. R.H. Loeppert, Jr., M.M. Mortland and T.J. Pinnavaia, *Clay and Clay Minerals*, **27**, 201 (1979).
36. S.L. Swartzen-Allen and E. Matijevic, *J. Colloid and Interface Sci.*, **50**, 144 (1975).
37. P.K. Ghosh and A.J. Bard, *J. Phys. Chem.*, **88**, 5519 (1984).
38. J. Meering and R. Glaeser, *Bull. Groupe Franc. Argiles.*, **5**, 61 (1953).
39. R.M. Mortland and N. Barake, *Trans. 8th Int. Congr. Soil Sci.*, **3**, 433 (1964).
40. A. Yamagishi and M. Soma, *J. Am. Chem. Soc.*, **103**, 4640 (1981).
41. S.C. Bondy and M.E. Harrington, *Science*, **203**, 1243 (1979).
42. *IUPAC Informaton Bulletin*, No. 33, 68 (1968).
43. F.P. Dwyer and E.C. Gyarfazs, *J. Proc. Roy. Soc. N. S. Wales*, **83**, 232 (1949).
44. A. Yamagishi, *J. Phys. Chem.*, **86**, 2472 (1982).
45. This value is reported to be 14.8 Å in ref. 40. However, the later measurement revealed that the true value was twice of this.
46. A. Yamagishi and M. Soma, *J. Chem. Soc. Chem. Comm.*, 539 (1981).
47. A. Yamagishi, *Inorg. Chem.*, **24**, 1689 (1985).
48. P. Pfeiffer and K. Quehl, *Chem. Ber.*, **64**, 2667 (1931).
49. N.R. Davies and F.P. Dwyer, *Trans. Faraday Soc.*, **50**, 24 (1954).
50. A. Yamagishi, *J. Chem. Soc. Chem. Comm.*, 1128 (1981).
51. A. Yamagishi, K. Tanaka and I. Toyoshima, *J. Chem. Soc. Chem. Comm.*, 343 (1982).
52. A. Yamagishi, *Inorg. Chem.*, **21**, 1778 (1982).
53. A. Yamagishi and N. Fujita, *J. Colloid and Interface Sci.*, **100**, 136 (1983).
54. A. Yamagishi, *J. Phys. Chem.*, **86**, 233 (1982).
55. Y. Masuda and H. Yamatera, *Bull. Chem. Soc. Japan*, **57**, 58 (1984).
56. T. Tachibana, T. Yoshizumi and K. Hori, *Bull. Chem. Soc. Japan*, **52**, 34 (1979).
57. E.M. Arnett and O. Thompson, *J. Am. Chem. Soc.*, **103**, 968 (1981).
58. A. Collet, M.-J. Brienne and J. Jacques, *Chem. Rev.*, **80**, 215 (1980).
59. G. Blaschke, *Angew. Chem. Int. Ed. Engl.*, **19**, 13 (1980).
60. A. Yamagishi, M. Soma and R. Ohnishi, *Chem. Lett.*, **85** (1982).
61. A. Yamagishi, *Inorg. Chem.*, **21**, 3393 (1982).
62. R.C. Fay, A.Y. Girgis and U. Klabunde, *J. Am. Chem. Soc.*, **92**, 7056 (1970).
63. M. Yamamoto, E. Iwamoto, A. Kozawa, K. Takemoto, Y. Yamamoto and A. Tatehata, *Inorg. Nucl. Chem. Lett.*, **16**, 71 (1981).
64. A. Yamagishi, *J. Chem. Soc. Dalton Trans.*, 679 (1983).
65. S.H. Laurie, *Aust. J. Chem.*, **21**, 679 (1968).
66. A. Yamagishi and R. Ohnishi, *J. Chromatography*, **245**, 213 (1982).
67. A. Yamagishi, *J. Chromatography*, **262**, 41 (1983).
68. A.F. Wells, *Structural Inorganic Chemistry* (Oxford University Press, London, 1962), p. 983.
69. S.F. Mason, *Pure and Appl. Chem.*, **24**, 335 (1970).
70. G.C. Lalor, *J. Inorg. Nucl. Chem.*, **31**, 1783 (1969).
71. *IUPAC Nomenclature of Inorganic Chemistry*, 2nd Ed. (Butterworths, London, 1970).
72. F. Basolo and R.G. Pearson, *Mechanisms of Inorganic Reactions* (John Wiley and Sons, Inc., New York, 1958), Chaps. 3 and 4.
73. A. Yamagishi and R. Ohnishi, *Inorg. Chem.*, **21**, 4233 (1982).
74. A. Yamagishi, *Inorg. Chem.*, **25**, 55 (1986).
75. Ref. 72, p. 315.
76. A. Yamagishi and R. Ohnishi, *Angew. Chem. Int. Ed. Engl.*, **22**, 162 (1983).
77. D.W. Urray, *J. Am. Chem. Soc.*, **72**, 3035 (1968).
78. U. Mingelgrin and F. Tsvetkov, *Clays and Clay Minerals*, **33**, 285 (1985).
79. A. Yamagishi, *J. Am. Chem. Soc.*, **107**, 732 (1985).
80. A. Yamagishi, *Proc. of the 8th International Clay Conference* (in press), (1985); *Abstracts of the 1985 International Clay Conference*, p. 259 (1985).
81. A. Yamagishi, *J. Chromatography*, **319**, 299 (1985).
82. R. Noyori, I. Tomino and Y. Tanimoto, *J. Am. Chem. Soc.*, **101**, 3129 (1979).

83. Y. Okamoto, K. Suzuki, K. Ohta, K. Hatada and H. Yuki, *J. Am. Chem. Soc.*, **101**, 4769 (1979).
84. G.H. Posner, J.P. Mallamo and K. Miura, *J. Am. Chem. Soc.*, **103**, 2886 (1981).
85. J.A. Ballantine, M. Davies, H. Purnell, M. Rayanakorn, J.M. Thomas and K.J. Williams, *J. Chem. Soc. Chem. Comm.* 8 (1981).
86. J.M. Adams, A. Bylina and S.H. Graham, *Clay and Clay Minerals*, **75**, 190 (1982).
87. J.M. Adams, S.E. Davies, S.H. Graham and J.M. Thomas, *J. Catalysis*, **78**, 197 (1982).
88. M. Frenkel and S.D.H. Solomon, *Clays and Clay Minerals*, **25**, 463 (1977).
89. J.A. Ballantine, R.P. Galvin, R.M. O'Neil, H. Purnell, M. Rayanakorn and J.M. Thomas, *J. Chem. Soc. Chem. Comm.*, 695 (1981).
90. J.A. Ballantine, M. Davies, H. Purnell, M. Rayanakorn, J.M. Thomas and K.J. Williams, *J. Chem. Soc. Chem. Comm.*, 427 (1981).
91. T.A. Jackson, *Chemical Geology*, **7**, 295 (1971).
92. G. Natta, *J. Inorg. Nucl. Chem.*, **8**, 589 (1958).
93. J.J. Flores and W. Bonner, *J. Molec. Evol.*, **3**, 49 (1974).
94. T.D. Thompson and A. Tsunashima, *Clays and Clay Minerals*, **21**, 351 (1973).
95. S.W. Bailey, *The American Mineralogist*, **48**, 1196 (1963).
96. K-T. Liu and Y-C. Tong, *J. Org. Chem.*, **43**, 2717 (1978).
97. A. Cornelis and P. Laszlo, *Synthesis*, **162**, (1982).
98. A. Cornelis, P-Y. Herze and P. Laszlo, *Tetrahedron Letters*, **23**, 5035 (1982).
99. P. Laszlo and J. Lucchetti, *Tetrahedron Letters*, **25**, 1567 (1984).
100. T.J. Pinnavaia, R. Raythatha, J.G.S. Lee, L.J. Halloran and J.F. Hoffman, *J. Am. Chem. Soc.*, **101**, 6892 (1979).
101. M. Mazzei, W. Marconi and M. Riocci, *J. Molec. Catalysis*, **9**, 381 (1980).
102. T.J. Pinnavaia, *ACS Symposium Series*, **192**, 241 (1982).
103. A. Yamagishi, *J. Chem. Soc. Chem. Comm.*, 119 (1984).
104. A. Yamagishi, *J. Chem. Soc. Chem. Comm.*, 290 (1986).
105. F.A. Davis, R. Jenkins, Jr., S.Q.A. Rizvi and T.W. Panunto, *J. Chem. Soc. Chem. Comm.*, 402 (1979).
106. P. Pitchen, E. Dunach, M.N. Deshmukh and H.B. Kagan, *J. Am. Chem. Soc.*, **106**, 8188 (1984).
107. N.J. Leonard and C.R. Johnson, *J. Org. Chem.*, **27**, 2882 (1962).
108. P.K. Ghosh and A.J. Bard, *J. Am. Chem. Soc.*, **105**, 5691 (1983).
109. A. Yamagishi and A. Aramata, *J. Chem. Soc. Chem. Comm.*, 452 (1984).
110. A. Yamagishi and A. Aramata, *J. Electroanal. Chem.*, **191**, 449 (1985).
111. T. Komori and T. Nonaka, *J. Am. Chem. Soc.*, **106**, 2656 (1984).
112. D. Ege, P.K. Ghosh, J.R. White, J-F. Equey and A.J. Bard, *J. Am. Chem. Soc.*, **107**, 5644 (1985).
113. K. Harada, *The Origin of Life: Approach from Chemical Evolution* (Tokyo University Press, Tokyo, 1977), p. 25.
114. J.D. Bernal, *The Physical Basis of Life* (Routledge and Kegan Paul, London, 1951).
115. R. Buvet and C. Ponnampereuma, *Molecular Evolution vol. 1, Chemical Evolution and the Origin of Life* (North Holland Pub. Co., Amsterdam, 1971), (through ref. 115).
116. A. Weiss, *Angew. Chem. Int. Ed. Engl.*, **20**, 850 (1981).
117. A.M. Samii and G. Lagady, *Abstracts of the 8th International Clay Conference*, **204** (1985).
118. V.A. Otroshchenko, N.V. Vasilyeva and A.M. Kopilov, *Origins of Life*, **15**, 115 (1985).
119. A.G. Cairns-Smith, *Genetic Takeover* (Cambridge University Press, London, 1982), Chap. II.
120. A. G. Cairns-Smith, *Scientific American (No. 8)*, 74 (1985).
121. J.J. McCullough and R.M. Lemmon, *J. Molec. Evol.*, **3**, 57 (1974).
122. K.L. Stevenson and J.F. Verdick, *J. Am. Chem. Soc.*, **90**, 2974 (1969).
123. K. Yamanari, S. Naito and Y. Shimura, *Bull. Chem. Soc. Japan*, **54**, 3780 (1981).
124. H. Sigel, *Metal Ions in Biological Systems*, **8**, 125 (1979).